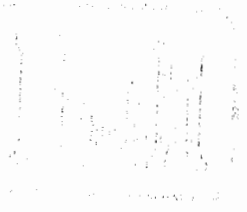


ADA084685



TECHNICAL REPORT GL-80.2

REVIEW

12



# ANALYTICAL AND GRAPHICAL METHODS FOR STABILITY ANALYSIS OF SLOPES IN ROCK MASSES

by

J. Hendron, Jr., E. J. Cording, and A. K. Aiyer  
Department of Civil Engineering  
University of Illinois, Urbana, Ill. 61801

March 1980

Reprint of NCG Technical Report No. 36

Approved For Public Release; Distribution Unlimited

Stamp: MAY 3 1980



U. S. Army Engineer Nuclear Cratering Group  
Livermore, Calif. 94550

Contract No. DACW39-67-C-0097

Ordered by Geotechnical Laboratory  
Army Engineer Waterways Experiment Station  
P.O. Box 631, Vicksburg, Miss. 39180

80 5 27 059

Destroy this report when no longer needed. Do not return  
it to the originator.

The findings in this report are not to be construed as an official  
Department of the Army position unless so designated  
by other authorized documents.

Unclassified

SECURITY CLASSIFICATION OF THIS PAGE (When Data Entered)

REPORT DOCUMENTATION PAGE		READ INSTRUCTIONS BEFORE COMPLETING FORM
1. REPORT NUMBER 9 Technical Report, GL-80-2	2. GOVT ACCESSION NO. AD-A084685	3. RECIPIENT'S CATALOG NUMBER
4. TITLE (and Subtitle) 6 ANALYTICAL AND GRAPHICAL METHODS FOR THE ANALYSIS OF SLOPES IN ROCK MASSES.	5. TYPE OF REPORT & PERIOD COVERED Reprint of NCG Technical Report No. 36	
10 Alfred Joseph Hendron, Jr. E. J. Cording and A. K. Aiyer		6. PERFORMING ORG. REPORT NUMBER
7. PERFORMING ORGANIZATION NAME AND ADDRESS Department of Civil Engineering University of Illinois, Urbana, Ill. 61801		8. CONTRACT OR GRANT NUMBER(s) Contract No. DACW 39-67-C-0097
11. CONTROLLING OFFICE NAME AND ADDRESS U. S. Army Engineer Nuclear Cratering Group Livermore, Calif. 94550		12. REPORT DATE 11 March 1980
14. MONITORING AGENCY NAME & ADDRESS (if different from Controlling Office) U. S. Army Engineer Waterways Experiment Station Geotechnical Laboratory P. O. Box 631, Vicksburg, Miss. 39180		10. PROGRAM ELEMENT, PROJECT, TASK AREA & WORK UNIT NUMBERS
16. DISTRIBUTION STATEMENT (of this Report) Approved for public release; distribution unlimited.		13. SECURITY CLASS. (of this report) Unclassified
17. DISTRIBUTION STATEMENT (of the abstract entered in Block 20, if different from report) 12 178		14. NUMBER OF PAGES 173
18. SUPPLEMENTARY NOTES 19 80-2, TR-36		15. SECURITY CLASS. (of this report) Unclassified
19. KEY WORDS (Continue on reverse side if necessary and identify by block number) 18 WES/TR-GL, NCG Dynamic slope stability      Slope stability Graphical methods              Stereonet Rock masses                      Vector analysis Rock mechanics		15a. DECLASSIFICATION/DOWNGRADING SCHEDULE
20. ABSTRACT (Continue on reverse side if necessary and identify by block number) In this report the methods of analyzing the static stability of rock slopes cut by a three-dimensional network of discontinuities are given. The general use of vector analysis to solve these problems analytically is described and a method utilizing stereonets to solve these problems graphically is also given. For both the graphical and analytical methods the general analysis of slopes cut by one, two, or three sets of discontinuities is presented which can take into account the porepressures acting on the (Continued)		

DD FORM 1 JAN 73 1473 EDITION OF 1 NOV 65 IS OBSOLETE

Unclassified  
SECURITY CLASSIFICATION OF THIS PAGE (When Data Entered)

176010

SW

Unclassified

SECURITY CLASSIFICATION OF THIS PAGE(When Data Entered)

20. ABSTRACT (Continued).

discontinuities and external forces acting on the slope. Detailed examples are given to illustrate both the graphical and vector methods of analysis.

The dynamic stability of slopes is also treated in this report. It is shown that the dynamic resistance of a three-dimensional rock slope can be calculated by either the graphic-stereonet method or the analytic vector analysis method. The dynamic resistance can then be used to estimate the movement of the slope under dynamic loading using a procedure given by Newmark (1965). A criterion is then given for determining if the calculated movement of the rock slope is acceptable or harmful.



Unclassified

SECURITY CLASSIFICATION OF THIS PAGE(When Data Entered)

**FOREWORD**

This study was performed by the Department of Civil Engineering, University of Illinois, under contract to the U. S. Army Engineer Waterways Experiment Station, Vicksburg, Mississippi (WES) for the U. S. Army Engineer Nuclear Cratering Group, Lawrence Radiation Laboratory, Livermore, California (NCG). The study was performed under Contract No. DACW 39-67-C-0097, "Evaluation of Analytical Methods of Determining the Stability of Rock Slopes," and was funded by NCG IAO 2-63, "Engineering Properties of Nuclear Craters." The contract was negotiated on 16 June 1967.

This report was prepared by Messrs. Hendron, Cording and Aiyer; and, was reviewed by Don C. Banks, Chief, Rock Mechanics Section, Soils Division, WES and by Major Richard H. Gates, C.E., Chief, Engineering Geology Division, NCG.

The contract was monitored by Don C. Banks, WES. The Contracting Officer at the time of publication was COL Ernest D. Peixotto, CE, Director of WES. Technical Director of WES was Mr. Fred R. Brown. The Director of NCG was LTC Robert L. LaFrenz, CE, and the Technical Director was Mr. Walter C. Day.

Accession For	
NTIS GPO/CI	<input checked="" type="checkbox"/>
DLC IAB	<input type="checkbox"/>
Unannounced	<input type="checkbox"/>
Publication	<input type="checkbox"/>
By	
Organization/	
Availability Codes	
Availability and/or special	
<b>A</b>	

## ABSTRACT

In this report the methods of analyzing the static stability of rock slopes cut by a three dimensional network of discontinuities are given. The general use of vector analysis to solve these problems analytically is described and a method utilizing stereonetts to solve these problems graphically is also given. For both the graphical and analytical methods the general analysis of slopes cut by one, two, or three sets of discontinuities is presented which can take into account the porepressures acting on the discontinuities and external forces acting on the slope. Detailed examples are given to illustrate both the graphical and vector methods of analysis.

The dynamic stability of slopes is also treated in this report. It is shown that the dynamic resistance of a three-dimensional rock slope can be calculated by either the graphic-stereonet method or the analytic vector analysis method. The dynamic resistance can then be used to estimate the movement of the slope under dynamic loading using a procedure given by Newmark (1965). A criterion is then given for determining if the calculated movement of the rock slope is acceptable or harmful.

**TABLE OF CONTENTS**

	<b>Page</b>
<b>FOREWORD</b> . . . . .	<b>i</b>
<b>ABSTRACT</b> . . . . .	<b>ii</b>
<b>LIST OF FIGURES</b> . . . . .	<b>vii</b>
<b>LIST OF TABLES</b> . . . . .	<b>xi</b>
<b>CHAPTER</b>	
<b>1. INTRODUCTION</b> . . . . .	<b>1</b>
<b>1.1 General</b> . . . . .	<b>1</b>
<b>1.2 Scope</b> . . . . .	<b>2</b>
<b>2. FUNDAMENTALS OF VECTOR ANALYSIS</b> . . . . .	<b>5</b>
<b>2.1 General</b> . . . . .	<b>5</b>
<b>2.2 Fundamental Vector Operations</b> . . . . .	<b>5</b>
<b>2.3 Vector Operations Used in Three Dimensional         Analysis of Slopes</b> . . . . .	<b>9</b>
<b>2.3.1 Unit Vectors Defining the Orientation of                 Joint Planes and the Line of Intersection                 of Joint Sets</b> . . . . .	<b>9</b>
<b>2.3.2 Resolution of Forces</b> . . . . .	<b>13</b>
<b>2.3.3 Line of Application of a Force and Point of                 Intersection of Two Forces</b> . . . . .	<b>15</b>
<b>2.3.4 Moment about an Axis</b> . . . . .	<b>19</b>
<b>2.3.5 Point of Intersection of a Force and a                 Joint Plane</b> . . . . .	<b>19</b>
<b>2.3.6 Geometry of a Triangle</b> . . . . .	<b>19</b>
<b>3. ANALYSIS OF ROCK SLOPES BY VECTOR METHODS</b> . . . . .	<b>22</b>
<b>3.1 General</b> . . . . .	<b>22</b>
<b>3.2 Stability Calculations by Vector Analysis for         Sliding on One Plane</b> . . . . .	<b>22</b>
<b>3.2.1 Calculation of Factor of Safety for                 Static Loads</b> . . . . .	<b>22</b>

TABLE OF CONTENTS (continued)

	Page
3.2.2 Calculation of Dynamic Resistance . . . . .	26
3.3 Example Problems of Sliding on One Plane by Vector Analysis . . . . .	30
3.4 Stability Calculations by Vector Analysis for Slopes Containing Two Sets of Joint Planes . . . . .	36
3.4.1 Calculation of Factor of Safety for Static Loads . . . . .	36
3.4.1.1 Description of Geometry and Loads . . . . .	36
3.4.1.2 Determination of the Mode of Sliding Failure . . . . .	38
3.1.4.3 Calculation of the Factor of Safety for Sliding . . . . .	41
3.1.4.4 Calculation of Static Factor of Safety for Rotations . . . . .	44
3.4.2 Calculation of Dynamic Resistance Against Sliding on Two Planes . . . . .	50
3.4.3 Example Problems for Slopes with Two Inter- secting Planes of Discontinuity Worked by Vector Analysis . . . . .	52
3.5 Analysis for Sliding on Two Planes by Engineering Graphics . . . . .	66
3.6 Method of Stability Analysis for Rock Slopes with Three Intersecting Joint Sets . . . . .	66
3.6.1 Determination of the Mode of Sliding Failure (Fig. 3.14) . . . . .	69
3.6.3 Calculation of the Factor of Safety for Sliding . . . . .	74
3.7 Computer Techniques . . . . .	80
4. GRAPHICAL SLOPE STABILITY ANALYSIS BY USE OF STEREOSETS .	83
4.1 Properties of Spherical Projections . . . . .	83
4.1.1 General . . . . .	83



**TABLE OF CONTENTS (continued)**

	Page
4.1.2 Equal Angle Projections . . . . .	85
4.2 Use of Stereonet to Evaluate Driving and Resisting Forces on a Potential Sliding Wedge of Rock . . . . .	90
4.3 Sliding on a Single Frictional Plane . . . . .	92
4.3.1 Orientation of reaction force on the plane of failure . . . . .	93
4.3.2 Stability of wedge of weight $\bar{W}$ with uplift force, $\bar{U}$ , acting on the failure plane . . . . .	93
4.3.3 Graphical procedure for determining the direction of resultant vector force . . . . .	95
4.3.4 Determination of direction of movement and factor of safety for case of resultant driving vector, $\bar{W} + \bar{U} + \bar{A}$ , acting on the wedge . . . . .	98
4.3.5 Minimum force $\bar{N}_W$ required to cause failure . . . . .	100
4.4 Sliding on Two Frictional Planes . . . . .	100
4.4.1 General . . . . .	100
4.4.2 Orientation of line of intersection of the two planes . . . . .	102
4.4.3 Reaction forces on the failure planes . . . . .	102
4.4.4 Method of locating boundary between stable and unstable zones . . . . .	102
4.4.5 Minimum force ( $\bar{N}_W$ ) required to cause sliding of the wedge . . . . .	107
4.4.6 Factor of safety and minimum forces required to stabilize the wedge . . . . .	109
4.5 Sliding of a Wedge Bounded by Three Planes . . . . .	112
4.6 Wedge Bounded by Three Planes but Daylighted by Cut Face . . . . .	115
4.7 Rotation of edge on Plane 3 . . . . .	117

TABLE OF CONTENTS (continued)

	Page
5. DYNAMIC STABILITY OF ROCK SLOPES . . . . .	122
5.1 Introduction . . . . .	122
5.2 Dynamic Analysis of Rock Slopes . . . . .	123
5.3 Permissible Movement of Rock Slopes . . . . .	129
6. SUMMARY AND CONCLUSIONS . . . . .	136
6.1 Static Stability of Rock Slopes . . . . .	136
6.2 Dynamic Stability . . . . .	142
REFERENCES . . . . .	148
APPENDIX A . . . . .	A-1
PROGRAM #1 . . . . .	A-2
PROGRAM #2 . . . . .	A-7

## LIST OF FIGURES

	Page
2.1 Scalar Product of Two Vectors . . . . .	7
2.2 Cross Product of Two Vectors . . . . .	8
2.3 Orientation of a Plane in Vector Notation. . . . .	10
2.4 Co-ordinate System for Describing Strikes and Dips . . . . .	12
2.5 Vector Description of the Orientation of Two Planes and Their Line of Intersection . . . . .	14
2.6 Resolution of Forces on a Plane into Normal and Tangential Components . . . . .	16
2.7 Equation of a Line in Vector Notation . . . . .	16
2.8 Moment Caused by Two Forces with Different Points of Application . . . . .	18
2.9 Moment of a Force about a Given Axis . . . . .	18
2.10 Intersection of the Line of Action of a Force on a Plane . . . . .	20
2.11 Geometry of a Triangle . . . . .	20
2.12 Geometry of a Tetrahedron . . . . .	20
3.1 Sliding on One Plane -- Strike of Plane Parallel to Strike of Slope Face . . . . .	23
3.2 Sliding on One Plane -- Strike of Plane not Parallel to Strike of Slope Face . . . . .	27
(a) Cutslope	
(b) Natural Slope -- Bedding Planes Dipping Toward Valley -- Sliding Block Isolated from Mass by Gully on Each Side	
3.3 Sliding on One Plane . . . . .	28
3.4 Failure of a Block Sliding on One Plane . . . . .	31
3.5 Stability of a Wedge Bounded by Two Joint Planes . . . . .	37
3.6 Sliding on Two Planes . . . . .	43
3.7 Rotational Stability of a Wedge Bounded by Two Joint Planes . . . . .	45

## LIST OF FIGURES

	Page
3.8 Stability of a Wedge Bounded by Two Joint Planes . . . . .	51
3.9 Stability of a Rock Wedge Bounded by Two Joint Planes. . .	53
3.10 Stability of a Rock Wedge Bounded by Two Joint Planes . .	58
3.11 Graphical Solution of Sliding Stability of a Rock Wedge Bounded by Two Joint Planes . . . . .	67
3.12 Forces on a Rock Wedge Bounded by Three Inter- secting Joint Planes . . . . .	68
3.13 Modes of Sliding Failure of a Rock Wedge Bounded by Three Intersecting Joint Sets . . . . .	70
3.14 Stability of a Rock Wedge Bounded by Three Inter- secting Joint Planes . . . . .	72
3.15 Flow Chart . . . . .	82
4.1 Projection of Plane and Lines on a Sphere . . . . .	84
4.2 Equal Angle Projection from Lower Hemisphere to Equatorial Plane of the Sphere . . . . .	86
4.3 Profile of Sphere Showing Method of Equal Angle, Lower Hemisphere Projection . . . . .	87
4.4 Stereonet (Wulff Net)(Equal Angle Projection) . . . . .	88
4.5 Determination of Line of Intersection of Two Planes . . .	91
4.6 Sliding on a Single Plane . . . . .	94
4.7 Graphical Summation of 3 Vectors . . . . .	96
4.8 Graphical Determination of Orientation of Resultant Vector, $\bar{W} + \bar{A} + \bar{U}$ . . . . .	97
4.9 Three Vectors on Single Plane . . . . .	99
4.10 Minimum Force Required to Cause Failure . . . . .	101
4.11 Sliding on Two Planes: Orientation of Line of Intersection . . . . .	103
4.12 Sliding on Two Planes: Block Diagram . . . . .	104
4.13 Sliding on Two Planes: Stereonet . . . . .	105

## LIST OF FIGURES

	Page
4.14 Sliding on Two Planes: Minimum Force Required to Cause Sliding . . . . .	108
4.15 Minimum Forces Required to Stabilize the Wedge . . . . .	110
4.16 Wedge Bounded by Three Planes: Block Diagram . . . . .	113
4.17 Wedge Bounded by Three Planes: Stereonet . . . . .	114
4.18 Wedge Bounded by Three Planes: Plane 3 Daylighted at Edge of Block . . . . .	116
4.19 Rotation of Wedge on Plane 3 . . . . .	118
5.1 El Centro, California, Earthquake of May 18, 1940, N-S Component . . . . .	125
5.2 Rigid Block on a Moving Support . . . . .	127
5.3 Rectangular Block Acceleration Pulse . . . . .	127
5.4 Velocity Response to Rectangular Block Acceleration . . . . .	127
5.5 Standardized Displacement for Normalized Earthquakes (Unsymmetrical Resistance) . . . . .	130
5.6 Relationship Between Peak Shear Strength and the Component of Strength Due to Surface Roughness . . . . .	132
5.7 An Example of a Discontinuity Illustrating First and Second-Order Irregularities . . . . .	134
6.1 Friction Angle Required for Stability of Wedge Weight, $W$ , for $C_1 = C_2$ . . . . .	139
6.2 $\tan \phi_{\text{Required}}$ for Stability of a Wedge of Weight, $W$ for Various Values of $\beta$ , $\gamma$ , and $\alpha$ . . . . .	141
6.3 Wedge Acting under own Weight Case 1: Single Plane, $\beta = 180^\circ$ . . . . .	143
6.4 Wedge Acting under own Weight Case 2: $C_1 = 0$ , and $C_2 = \text{any value}$ (Single Plane Case) . . . . .	144
6.5 Wedge Acting under own Weight Case 3: $\beta = 0$ ; Any $C_1, C_2, \alpha$ . . . . .	145

LIST OF FIGURES

	Page
6.6 Wedge Acting under own Weight	
Case 4: $C_1 = C_2 \neq 0, \beta \neq 0$ . . . . .	146
6.7 Wedge Acting under own Weight	
Case 5: $C_1 \neq C_2, \beta \neq 0$ . . . . .	147

LIST OF TABLES

	Page
3.1 Range of Angles for which a rotation is kinematically impossible . . . . .	48
6.1 Cases . . . . .	140

## CHAPTER ONE

### INTRODUCTION

#### 1.1 General

The design and analysis of rock slopes is somewhat different than the design and analysis of slopes in soil because of the patterns of discontinuities in the rock mass. The spatial orientation of these discontinuities and the shearing resistance along them govern the stability of rock slopes. Thus the method of analysis used must take into account the three dimensional intersection of the joint sets with each other and intersection of these discontinuities with the face or surface of the rock slope. Limit equilibrium methods of analysis have recently been developed to analyze these problems in three dimensions which will be explained and illustrated in this report.

In all methods of limit equilibrium analysis the shape of the potential failure is assumed at the outset. In the limit equilibrium methods used for soil slopes, sections of log spirals or circles are normally chosen to represent the failure surface. Although displacements are ignored in limit equilibrium methods, it must be kinematically possible for the displacements to take place in the direction assumed along the failure surface chosen. Surfaces composed of sections of circles or log spirals pose no kinematic difficulties. In rock slopes the potential system of failure surfaces already exist in the mass but the kinematics of sliding must be checked to delineate the possible directions and surfaces on which it is physically possible for sliding to take place.



After the potential failure surface is assumed in either the rock or soil slope stability analysis, the next step in the limit equilibrium method is to calculate the shearing resistance required along the potential failure surface to keep the potential sliding mass in equilibrium. This portion of the analysis is basically an exercise in statics.

After the shearing resistance required for equilibrium has been found, it is compared with the available shearing resistance. This comparison is usually expressed in terms of a factor of safety, which must be defined very carefully. Finally the slip surface giving the lowest factor of safety is found. In soils this is usually an iterative process with failure surfaces of the same shape but with different sizes and orientations. But in rock slopes there may only be several potential failure wedges to consider, each having a different shape governed by various intersections of the sets of discontinuities.

## 1.2 Scope

In this report the methods of analyzing the static stability of rock slopes in three dimensions are given and a method is suggested for assessing the dynamic stability of rock slopes. The methods of static analysis for three dimensional wedges are based primarily on the work of Wittke (1964, 1965a, 1965b, 1966), and Londe (1965). Since vector analysis is used in the analyses of Wittke and Londe, a review of vector operations commonly used in slope stability calculations is given in Chapter 2. The notation used for expressing strikes, dips, etc. in terms of vectors is also given in Chapter 2.

In Chapter 3 various combinations of the vector analyses of Wittke and Londe are presented for determining the static factor of safety

of rock slopes. The cases treated include slopes in rock masses containing one, two, or three sets of joints. Example calculations are given for determining the factor of safety of several typical problems by these methods. The concept of the dynamic resistance of rock slopes is also introduced in Chapter 3. The method given in Chapter 3 for computing the dynamic resistance of a rock slope in three dimensions is original with this report. The dynamic resistance can be used for predicting dynamic displacements due to earthquake motions in the method of dynamic analysis given by Newmark (1965).

In Chapter 4 procedures are given for performing graphical solutions of three dimensional rock slope stability problems by the use of stereonets. The principles of the equal angle and equal area projections are reviewed in this chapter and the equal angle projection is used in this report for the three dimensional analysis of rock slopes. The methods for analyzing rock wedges bounded by one, two, and three joint planes are similar to those given by John (1968) and example problems are illustrated. In cases where the static factor of safety is greater than unity a method is also shown for computing the magnitude and direction of the limiting dynamic resistance of a rock slope in three dimensions by the use of stereonets. In cases where the factor of safety is either less than unity or less than the desired value a method is also shown for determining the optimum direction and magnitude of rock anchor or rock bolting forces required to achieve the desired factor of safety.

In Chapter 5 procedures are given for estimating the dynamic displacement of rock slopes by utilizing the method proposed by

Newmark (1965). The minimum dynamic resistance for rock slopes as developed in Chapter 3 is used in these calculations. Guidelines are also given for determining if the dynamic displacement calculated is harmful to the stability of the slope.

In Chapter 6 a summary and conclusions are given.

CHAPTER TWO  
FUNDAMENTALS OF VECTOR ANALYSIS

2.1 General

In this chapter the elements of vector analysis used in three dimensional slope stability analyses are reviewed to serve as a ready reference for the reader. Then the system used in this report for describing the three-dimensional orientation of joint planes, the line of intersection of different joint sets, and the resolution of forces, is introduced in terms of vector notation.

2.2 Fundamental Vector Operations

A vector is a quantity which possesses both a magnitude and a direction. Velocity, force, and momentum are examples of vector quantities. Vectors of unit length may also be used to describe certain reference directions such as a normal to a plane or the direction of any line with respect to a set of orthogonal axes. A vector  $\bar{A}$  may be described by the set of its directional components ( $A_x, A_y, A_z$ ) parallel to the rectangular Cartesian axes ( $x, y, z$ ). Thus,

$$\bar{A} = (A_x, A_y, A_z) \quad (2.1)$$

A vector may also be expressed in terms of its components. For example,

$$\bar{A} = \bar{i}A_x + \bar{j}A_y + \bar{k}A_z \quad (2.2)$$

where  $\bar{i}$ ,  $\bar{j}$ , and  $\bar{k}$  are unit vectors directed along positive ( $x, y, z$ ) axes respectively.

The magnitude of a vector  $\bar{A}$  is given by its absolute value denoted by

$$A = (A_x^2 + A_y^2 + A_z^2)^{1/2} \quad (2.3)$$

Vectors may be added simply by summing the components in the x, y, and z directions. Thus if  $\vec{C}(C_x, C_y, C_z)$  represents the sum of two vectors  $\vec{A}(A_x, A_y, A_z)$  and  $\vec{B}(B_x, B_y, B_z)$ , then it follows that

$$\begin{aligned}\vec{C} &= (\vec{i}A_x + \vec{j}A_y + \vec{k}A_z) + (\vec{i}B_x + \vec{j}B_y + \vec{k}B_z) \\ &= \vec{i}(A_x + B_x) + \vec{j}(A_y + B_y) + \vec{k}(A_z + B_z) \\ &= \vec{i}C_x + \vec{j}C_y + \vec{k}C_z\end{aligned}\quad (2.4)$$

Equating the components in the x, y, and z directions,

$$C_x = A_x + B_x, \quad C_y = A_y + B_y, \quad C_z = A_z + B_z \quad (2.5)$$

The scalar product or the dot product of two vectors  $\vec{A}$  and  $\vec{B}$  is denoted in the form  $\vec{A} \cdot \vec{B}$  and has a magnitude given by

$$\vec{A} \cdot \vec{B} = A_x B_x + A_y B_y + A_z B_z \quad (2.6)$$

$$= AB \cos \theta \quad (2.7)$$

where  $\theta$  denotes the angle formed by the vectors A and B (Fig. 2.1). The scalar product is frequently used to obtain the component of a vector in a given direction. For example, if  $\vec{i}$  is a unit vector in the x direction,  $\vec{A} \cdot \vec{i}$  yields  $A_x = A \cos \alpha'$  where  $\alpha'$  is the direction angle between the vector  $\vec{A}$  and the positive x axis. Similarly,  $A_y = A \cos \beta'$ ,  $A_z = A \cos \gamma'$  where  $\beta'$ , and  $\gamma'$  denote direction angles between the vector  $\vec{A}$  and the positive y and z axes respectively. Substitution of these expressions into Eq. (2.3) yields

$$\cos^2 \alpha' + \cos^2 \beta' + \cos^2 \gamma' = 1 \quad (2.8)$$

Thus the cosines of the direction angles (direction cosines) of vector  $\vec{A}$  are not independent; they must satisfy Eq. (2.8)

A vector product or cross product of two vectors  $\vec{A}$  and  $\vec{B}$  is defined

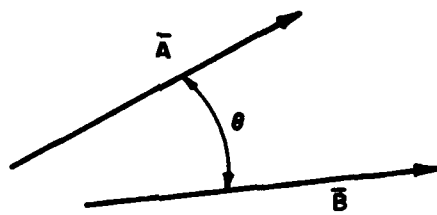


FIG. 2.1 SCALAR PRODUCT OF TWO VECTORS

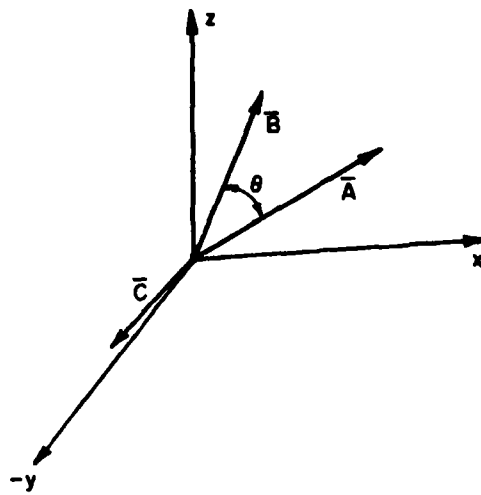


FIG. 2.2 CROSS PRODUCT OF TWO VECTORS

to be a third vector  $\vec{C}$  whose magnitude is given by the relation

$$C = AB \sin \theta \quad (2.9)$$

where  $\theta$  denotes the angle between vectors  $\vec{A}$  and  $\vec{B}$ . The direction of  $\vec{C}$  is perpendicular to the plane formed by vectors  $\vec{A}$  and  $\vec{B}$  as shown in Fig.

2.2. The vector product of  $\vec{A}$  and  $\vec{B}$  is denoted in the form

$$\vec{C} = \vec{A} \times \vec{B} \quad (2.10)$$

where  $\times$  denotes vector product or cross product. The sense of  $\vec{C}$  is such that it is in the direction a right hand threaded screw perpendicular to the plane formed by  $\vec{A}$  and  $\vec{B}$  would move if  $\vec{A}$  were rotated into  $\vec{B}$ .

In determinant notation the vector product is given as

$$\vec{C} = \vec{A} \times \vec{B} = \begin{vmatrix} \vec{i} & \vec{j} & \vec{k} \\ A_x & A_y & A_z \\ B_x & B_y & B_z \end{vmatrix} \quad (2.11)$$

It should be noted that

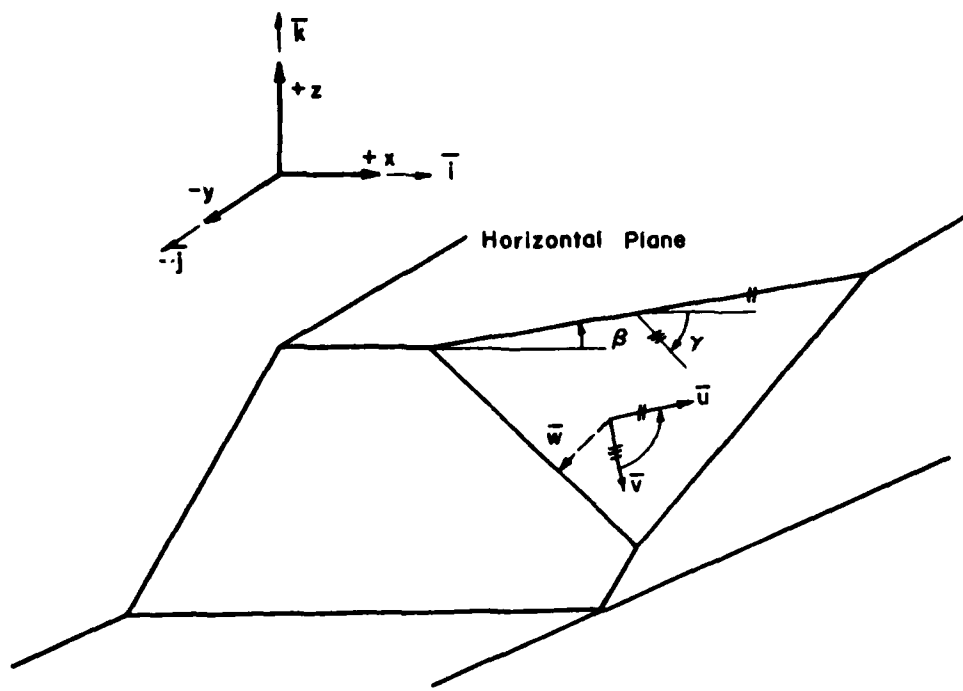
$$\vec{A} \times \vec{B} = -\vec{B} \times \vec{A} \quad (2.12)$$

### 2.3 Vector Operations Used in Three Dimensional Analysis of Slopes

#### 2.3.1 Unit Vectors Defining the Orientation of Joint Planes and the Line of Intersection of Joint Sets

The orientation of joints and planes of weakness are normally reported by the field geologist in terms of strike and dip. In this report, the system given by Wittke (1954) will be used to describe the orientation of the discontinuities in relation to the slope face being investigated. According to this system, as shown in Fig. 2.3, the x axis is parallel to the strike of the slope surface, the positive z axis is upward and the positive y axis is directed toward the slope. The strike of a plane of weakness is given by the angle  $\beta$  measured in





$$\bar{u} = \cos \beta \bar{i} + \sin \beta \bar{j}$$

$$\bar{v} = \cos \gamma \sin \beta \bar{i} - \cos \gamma \cos \beta \bar{j} - \sin \gamma \bar{k}$$

$$\bar{w} = \bar{u} \times \bar{v} = \begin{vmatrix} \bar{i} & \bar{j} & \bar{k} \\ u_x & u_y & u_z \\ v_x & v_y & v_z \end{vmatrix}$$

FIG. 2.3 ORIENTATION OF A PLANE IN VECTOR NOTATION

a horizontal plane in a counterclockwise direction from the positive x-axis as shown in Fig. 2.3. The value of  $\beta$  can range between 0 and 180 degrees. The dip of a plane with the horizontal is denoted by the angle  $\gamma$  in a direction at 90 degrees to the strike. The dip,  $\gamma$ , can range from 0 to 180 degrees and is measured downward from a horizontal line directed at an angle,  $\beta$ , equal to  $\beta - 90^\circ$  to the positive x axis. An example of the use of this notation to describe the orientation of two planes is shown in Fig. 2.4. The strike and dip are described by the unit vectors  $\bar{u}$  and  $\bar{v}$  respectively, and are written in terms of the angles  $\beta$  and  $\gamma$  as shown in Fig. 2.3, i.e.,

$$\bar{u} = \cos \beta \bar{i} + \sin \beta \bar{j}$$

and

$$\bar{v} = \cos \gamma \sin \beta \bar{i} - \cos \gamma \cos \beta \bar{j} - \sin \gamma \bar{k}$$

or

$$\bar{u} = (\cos \beta, \sin \beta, 0) \quad (2.13)$$

$$\bar{v} = (\cos \gamma \sin \beta, -\cos \gamma \cos \beta, -\sin \gamma) \quad (2.14)$$

Since the strike and dip are at 90 degrees, the scalar product  $\bar{u} \cdot \bar{v}$  should be zero.  $\bar{u} \cdot \bar{v} = \cos \beta \cos \gamma \sin \beta - \sin \beta \cos \gamma \cos \beta = 0$ . Thus Eqs. (2.13) and (2.14) satisfy the orthogonal relationship required for the unit vectors describing the strike and dip.

The cross product of  $\bar{u}$  and  $\bar{v}$  gives a unit vector  $\bar{w}$  which is perpendicular to both  $\bar{u}$  and  $\bar{v}$  and thus directed normal to the plane described by  $\bar{u}$  and  $\bar{v}$ . The vector  $\bar{w}$  is obtained by expanding the determinant given in Eq. (2.15).

$$\bar{w} = \bar{u} \times \bar{v} = \begin{vmatrix} \bar{i} & \bar{j} & \bar{k} \\ u_x & u_y & u_z \\ v_x & v_y & v_z \end{vmatrix} \quad (2.15)$$

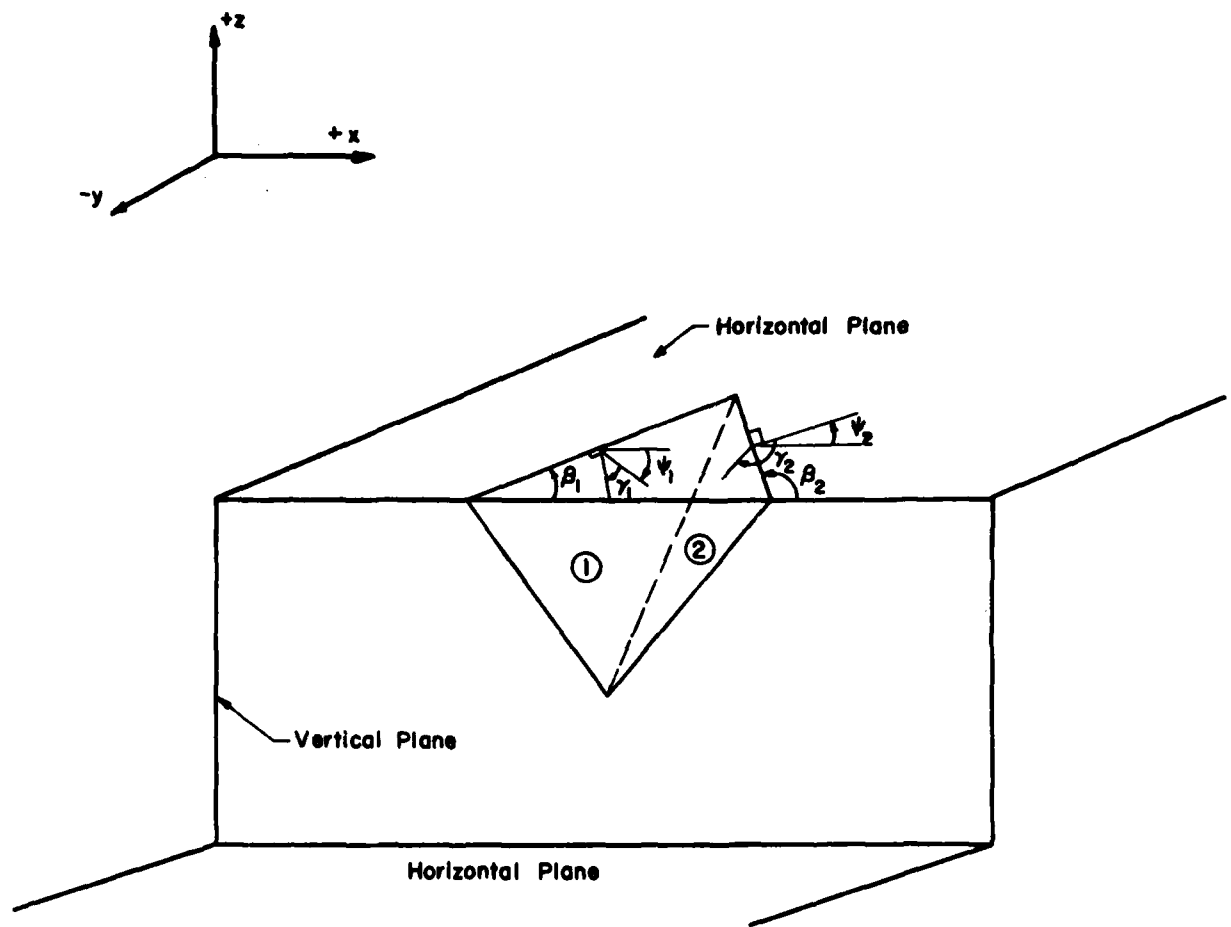


FIG. 2.4 CO-ORDINATE SYSTEM FOR DESCRIBING STRIKES AND DIPS

The direction of  $\bar{w}$  is normal to the plane of  $\bar{u}$  and  $\bar{v}$  in the direction of advance of a right hand screw in turning from  $\bar{u}$  to  $\bar{v}$  through the smallest angle between these vectors ( $< 180^\circ$ ). The magnitude of  $\bar{w}$  is equal to the quantity  $uv \sin \theta$  which assumes the value of unity because  $\theta = 90^\circ$  and  $\bar{u}$  and  $\bar{v}$  are unit vectors. The sense of  $\bar{w}$  for the two planes shown in Fig. 2.4 is shown in Fig. 2.5. Note that for plane 1 the direction of  $\bar{w}_1$  is normal to plane 1 and directed downward into the slope and  $\bar{w}_2$  is normal to plane 2 directed upward out of the slope. The specification of the unit vector  $\bar{w}$  normal to a plane is sufficient to completely describe the orientation of that plane.

The direction of the line of intersection of two joint planes (planes 1 and 2) is given by a vector  $\bar{x}_{12}$  having the direction of the cross product of the normal unit vectors to the two planes. Thus for planes 1 and 2 shown in Fig. 2.5 a vector  $\bar{x}_{12}$  along the line of intersection is given by

$$\bar{x}_{12} = \bar{w}_2 \times \bar{w}_1 \quad (2.16)$$

where  $\bar{x}_{12}$  is directed downward along the line of intersection as shown in Fig. 2.5.

### 2.3.2 Resolution of Forces

The component of a force  $\bar{R}$  in the direction given by a unit vector  $\bar{n}$  is given by

$$\bar{R} \cdot \bar{n} = R \cos \theta \quad (2.17)$$

where  $\theta$  is the angle between  $\bar{R}$  and  $\bar{n}$ . Thus, for example, the component of a force  $\bar{R}$  normal to a plane is given by  $\bar{R} \cdot \bar{w}$  and is given by

$$R_N = \bar{R} \cdot \bar{w} = R_x w_x + R_y w_y + R_z w_z \quad (2.18)$$

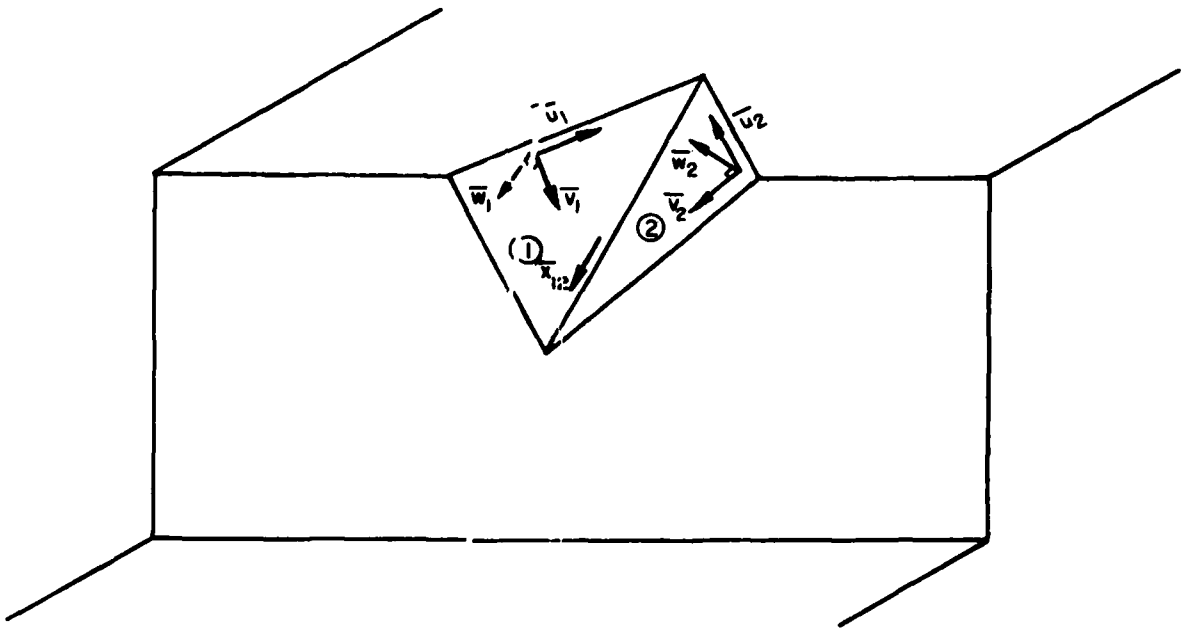


FIG. 2.5 VECTOR DESCRIPTION OF THE ORIENTATION OF TWO PLANES AND THEIR LINE OF INTERSECTION

Similarly the component of  $\vec{R}$  in the direction of the line of intersection of two planes is  $\vec{R} \frac{x_{12}}{x_{12}}$ .

The obliquity of a force  $\vec{R}$  on a given plane is the angle  $\phi'$ , which the force  $\vec{R}$  makes with the normal to the plane  $\vec{w}$  as shown in Fig. 2.6.

$$\tan \phi' = R_T / R_N$$

where  $R_N$  and  $R_T$  are the components of  $R$  normal and tangential to the plane, respectively. Note that  $R_N = \vec{R} \cdot \vec{w} = R_x w_x + R_y w_y + R_z w_z = R \cos \phi'$  and

$$\begin{aligned} R_T &= |\vec{R} \times \vec{w}| = R \sin \phi' \\ &= [(R_y w_z - R_z w_y)^2 + (R_z w_x - R_x w_z)^2 + (R_x w_y - R_y w_x)^2]^{1/2} \end{aligned} \quad (2.19)$$

Therefore the obliquity of a force on a plane is given by

$$\tan \phi' = \frac{R_T}{R_N} = \frac{[(R_y w_z - R_z w_y)^2 + (R_z w_x - R_x w_z)^2 + (R_x w_y - R_y w_x)^2]^{1/2}}{(R_x w_x + R_y w_y + R_z w_z)} \quad (2.20)$$

The vector  $\vec{R}_T$  may also be given by  $\vec{R} - R_N \vec{w}$  which is given by

$$\vec{R}_T = (R_x - R_N w_x) \vec{i} + (R_y - R_N w_y) \vec{j} + (R_z - R_N w_z) \vec{k}$$

since  $R_N \vec{w} = R_N w_x \vec{i} + R_N w_y \vec{j} + R_N w_z \vec{k}$ . Thus the obliquity may also be given as

$$\tan \phi' = \frac{[(R_x - R_N w_x)^2 + (R_y - R_N w_y)^2 + (R_z - R_N w_z)^2]^{1/2}}{R_x w_x + R_y w_y + R_z w_z} \quad (2.21)$$

### 2.3.3 Line of Application of a Force and Point of Intersection of Two Forces

In order to analyze rotational stability, the point of application of a force and its direction must be known. If the vector  $\vec{OS}$  from the selected origin of coordinates  $O$  to a point  $S$ , on the line of action of the force  $\vec{W}$  is known, the line of action of  $\vec{W}$  may be expressed as the line joining the tips of the set of radius vectors given by

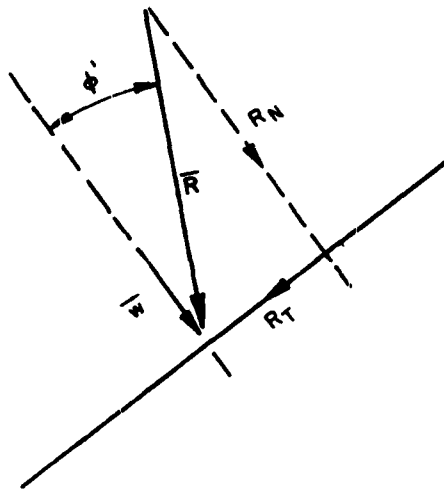


FIG. 2.6 RESOLUTION OF FORCES ON A PLANE INTO NORMAL AND TANGENTIAL COMPONENTS

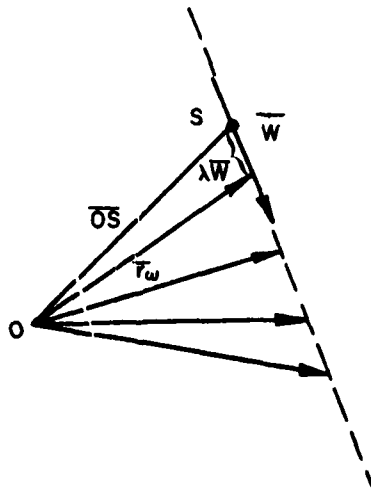


FIG. 2.7 EQUATION OF A LINE IN VECTOR NOTATION

$$\bar{r}_w = \overline{OS} + \lambda \bar{W} \quad (2.22)$$

and shown in Fig. 2.7.

In a three-dimensional problem the set of applied forces will not in general intersect, and the moment of each force about a particular axis of rotation may be considered separately, or the forces may be moved parallel to the axis of rotation about which moments are being summed until the forces intersect. For example, in analyzing the rotation of a wedge as shown in Fig. 2.8 around the axis defined by the unit vector  $\bar{d}$ , for the external force  $\bar{P}$  applied at point N and the weight  $\bar{W}$  applied through the center of gravity S, either of these forces may be shifted any distance K parallel to  $\bar{d}$  without changing the moment about  $\bar{d}$ . Thus the forces may be moved in this manner until their lines of action intersect. If the line of action of  $\bar{W}$  is defined by

$$\bar{r}_w = \overline{OS} + \lambda \bar{W} \quad (\lambda = \text{constant}) \quad (2.23)$$

and the line of action of  $\bar{P}$  is defined by

$$\bar{r}_p = \overline{ON} + \delta \bar{P} \quad (\delta = \text{constant}) \quad (2.24)$$

the resultant  $\bar{R}$  of  $\bar{P}$  and  $\bar{W}$  can be considered to act at a point of intersection I by setting

$$\bar{r}_w = \bar{r}_p + K \cdot \bar{d} \quad (2.25)$$

Substitution of Eqs. (2.23) and (2.24) in Eq. (2.25) yields

$$\overline{OS} + \lambda \bar{W} = \overline{ON} + \delta \bar{P} + K \bar{d} \quad (2.26)$$

If three equations are written from Eq. (2.26) in terms of the x, y, and z components of  $\bar{P}$  and  $\bar{W}$  they can be solved simultaneously for

$$\lambda = \lambda_1, \delta = \delta_1 \text{ and } K = K_1$$

which locate the point of intersection I. The vector from the origin O,



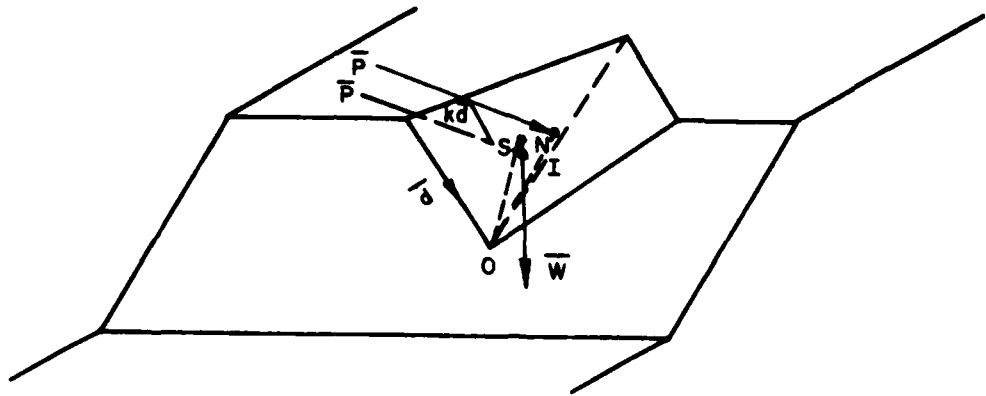


FIG. 2.8 MOMENT CAUSED BY TWO FORCES WITH DIFFERENT POINTS OF APPLICATION

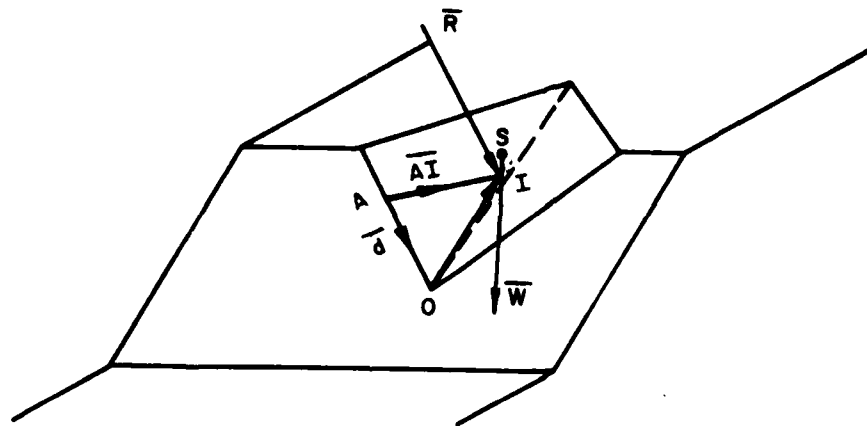


FIG. 2.9 MOMENT OF A FORCE ABOUT A GIVEN AXIS

to I, the point of application of  $\vec{R}$ , is thus

$$\vec{OI} = \vec{OS} + \lambda_1 \vec{w} \quad (2.27)$$

#### 2.3.4 Moment about an Axis

The magnitude of the moment about axis  $\vec{d}$  through point A as shown in Fig. 2.9 caused by the force  $\vec{R}$  acting at point I is

$$M_d = (\vec{AI} \times \vec{R}) \cdot \vec{d} \quad (2.28)$$

where

$$\vec{AI} = \vec{AO} + \vec{OI}$$

#### 2.3.5 Point of Intersection of a Force and a Joint Plane

The point of intersection of a force and a joint plane is found by equating the line of action of the force and the equation of a plane.

The equation of a plane is given by

$$\vec{r}_p \cdot \vec{w} = \text{constant} \quad (2.29)$$

where  $\vec{r}_p$  is a radius vector from the origin to a point in the plane, and  $\vec{w}$  the unit vector normal to the plane. If the vector  $\vec{OF}$  from the origin to any point F in the plane is known, then the constant is determined and the equation of the plane is:

$$\vec{r}_p \cdot \vec{w} = (\vec{OF} \cdot \vec{w})$$

The point where the force P intersects the plane is thus given by solving simultaneously the equation for the line of action of the force and the equation of the plane giving

$$(\vec{ON} + \delta \vec{P}) \cdot \vec{w} = (\vec{OF} \cdot \vec{w}) \quad (2.30)$$

The solution yields  $\delta_Q$ , the value of  $\delta$  defining the piercing point Q of the force  $\vec{P}$  on the plane p as shown in Fig. 2.10.

#### 2.3.6 Geometry of a Triangle

The area of the triangle OKL shown in Fig. 2.11 is given by

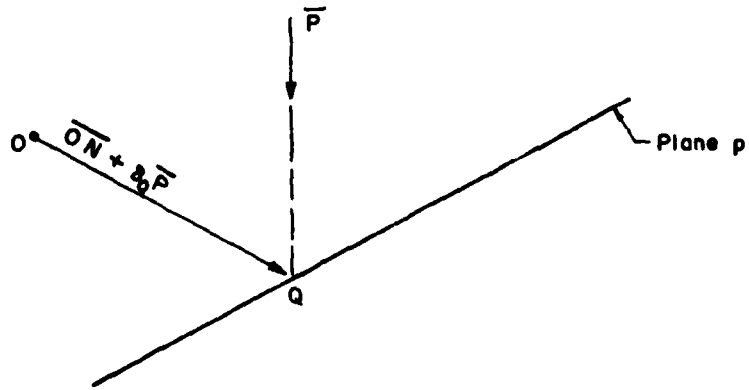


FIG. 2.10 INTERSECTION OF THE LINE OF ACTION OF A FORCE ON A PLANE

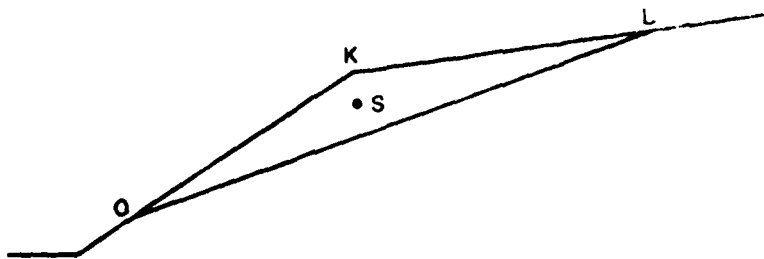


FIG. 2.11 GEOMETRY OF A TRIANGLE

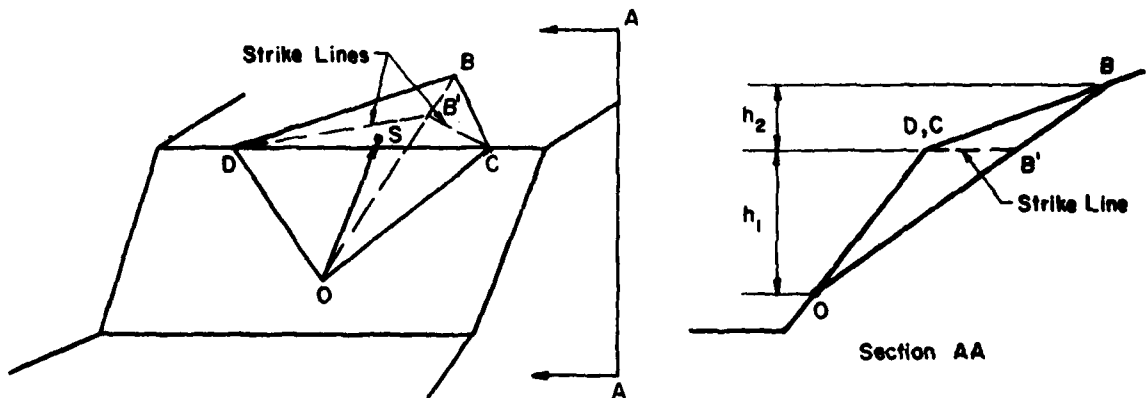


FIG. 2.12 GEOMETRY OF A TETRAHEDRON

$$A = 1/2 |\overline{OK} \times \overline{OL}| \quad (2.31)$$

and the vector from 0 to the centroid, S, is given by

$$\overline{OS} = 1/3 (\overline{OK} + \overline{OL}) \quad (2.32)$$

### 2.3.7 Geometry of a Tetrahedron

The volume of a tetrahedron as shown in Fig. 2.12 is given by

$$V = 1/6 |\overline{DB'} \times \overline{DC}| (h_1 + h_2) \quad (2.33)$$

The centroid at point S may be described by the vector from the origin,  $\overline{OS}$ , given by

$$\overline{OS} = 1/4 (\overline{OD} + \overline{OC} + \overline{OB}) \quad (2.34)$$

The components of  $\overline{OS}$  are thus the coordinates of the centroid.

CHAPTER THREE  
ANALYSIS OF ROCK SLOPES BY VECOTR METHODS

3.1 General

In this chapter analytical methods are presented for determining the static factor of safety of rock slopes. The cases covered include rock slopes cut by one, two, or three joint sets. Example problems are given where various combinations of the vector analyses of Wittke and Londe are utilized. A typical example problem is also worked by common engineering graphics. The notion of dynamic resistance is also introduced in this chapter for rock slopes and example calculations of the minimum dynamic resistance are illustrated. The methods given in this chapter for computing the dynamic resistance of a rock slope in three dimensions is original with this report and is intended to be used for predicting dynamic motions under earthquake loadings in conjunction with Newmark's method of analysis for the dynamic stability of slopes.

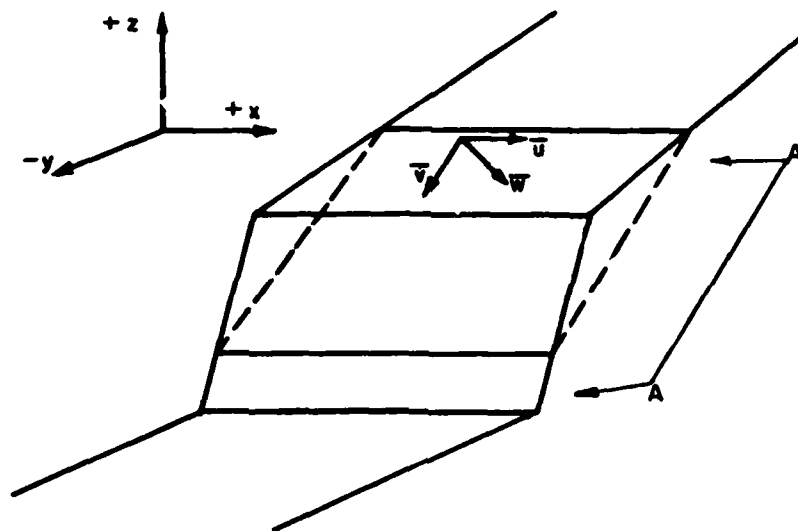
3.2 Stability Calculations by Vector Analysis for Sliding on One Plane

3.2.1 Calculation of Factor of Safety for Static Loads

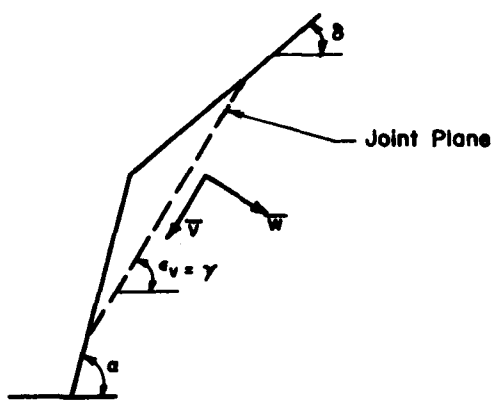
The simplest special case of a rock slope stability problem is where the strike of one of the planes of weakness is parallel to the strike of the slope face as shown in Fig. 3.1. For the coordinate system adopted in Chapter 2, this condition can be expressed when the unit vector  $\bar{u}$  in the direction of the strike has components of zero in the y and z directions i.e.,

$$\bar{u} = (u_x, u_y, u_z) = (1, 0, 0).$$

Then the unit vector  $\bar{v}$  in the direction of the dip has its x component equal to zero, i.e.,



(a)



(b)  
Section A-A

FIG. 3.1 SLIDING ON ONE PLANE — STRIKE OF PLANE PARALLEL TO STRIKE OF SLOPE FACE

$$\bar{v} = (v_x, v_y, v_z) = (0, v_y, v_z)$$

The inclination of the line of fall of the plane,  $\epsilon_v$ , will determine the kinematic possibility of sliding. The angle of fall  $\epsilon_v$  is given by

$$\tan \epsilon_v = \frac{v_z}{v_y} = \tan(\gamma) \quad (3.1)$$

where  $\gamma$  is the angle of dip of the plane. In order for sliding to be kinematically possible,  $\epsilon_v$  must be smaller than  $\alpha$  if  $0 < \alpha < \pi$  as shown in Fig. 3.1(b). If  $\alpha = \pi$ , then  $\epsilon_v$  must be smaller than  $\pi$  for the sliding to be possible.

For a slope acted upon only by gravity and the plane of weakness striking parallel to the slope face, the sliding will occur parallel to the unit vector  $\bar{v}$  in the direction of the dip. The magnitude of the component  $T$  of the weight  $\bar{W}$  acting parallel to  $\bar{v}$  may be obtained from

$$T = \bar{W} \cdot \bar{v} \quad (3.2)$$

where  $\bar{W} = (0, 0, -W)$ . The vector  $\bar{T}$  is given by

$$\bar{T} = T\bar{v} \quad (3.3)$$

The magnitude of the component of  $\bar{W}$  normal to the direction of sliding is

$$N = \bar{W} \cdot \bar{w}$$

where  $\bar{w}$  is the unit vector normal to the plane of sliding as given by  $\bar{u} \times \bar{v}$ . The magnitude of the available resisting force is given by  $N \tan \phi$  where  $\phi$  is the angle of shearing resistance between the joint surfaces in the direction of sliding. The factor of safety against sliding is the quotient of the resisting and the driving force in the direction of sliding and is given by

$$F.S. = \frac{N \tan \phi}{T} = \frac{(\bar{W} \cdot \bar{w}) \tan \phi}{(\bar{W} \cdot \bar{v})} \quad (3.4)$$

For the case shown in Fig. 3.1, the unit vector in the direction of the strike is given by  $\bar{u} = \bar{i} u_x = \bar{i}$  and the dip is given by  $\bar{v} = \bar{j} v_y + \bar{k} v_z$ . The unit vector  $\bar{w}$  normal to the plane of weakness is given by

$$\bar{w} = \bar{u} \times \bar{v} = \begin{vmatrix} \bar{i} & \bar{j} & \bar{k} \\ 1 & 0 & 0 \\ 0 & v_y & v_z \end{vmatrix} = -\bar{j} v_z + \bar{k} v_y$$

Thus the magnitude of the component of the weight in the direction of sliding is given by

$$T = \bar{W} \cdot \bar{v} = -W v_z \quad (3.5)$$

and the component of the weight normal to the plane of weakness is

$$N = \bar{W} \cdot \bar{w} = -W v_y \quad (3.6)$$

Thus the factor of safety according to Eq. (3.4) is:

$$F.S. = \frac{-W v_y \tan \phi}{-W v_z} = \frac{v_y}{v_z} \tan \phi = \frac{\tan \phi}{\tan \gamma} \quad (3.7)$$

which is a well known expression for the factor of safety of slopes potentially free to slide down the dip angle  $\gamma$  under gravity loading only.

If a slope is loaded by its own weight  $\bar{W}$ , and a pore water force  $\bar{U}$  acting on the potential failure plane in the direction of the unit vector  $-\bar{w}$ , then the factor of safety is given by

$$F.S. = \frac{(\bar{W} \cdot \bar{w}) - U}{(\bar{W} \cdot \bar{v})} \tan \phi \quad (3.8)$$

When the magnitude of the porewater force  $U$  is given by  $KW$ , Eq. (3.8) reduces to

$$F.S. = \frac{(-W v_y - KW)}{-W v_z} \tan \phi$$



$$F.S. = \frac{\tan \phi}{\tan \gamma} + K \frac{\tan \phi}{v_z} = \frac{\tan \phi}{\tan \gamma} - K \frac{\tan \phi}{\sin \gamma} \quad (3.9)$$

where  $\gamma$  is the dip of the potential failure plane and  $v_z = -\sin \gamma$ .

The case may also be considered where sliding can take place on one joint or bedding plane as shown in Fig. 3.2(a) or 3.2(b). In the general case the potential sliding wedge can be acted on by its weight  $\bar{W}$ , the porewater force  $\bar{U}$  acting on the plane of sliding, and an external force  $\bar{Q}$  which may be applied by a structure, such as a dam. In many cases where we are concerned with large slopes, however, the weight  $\bar{W}$  will be large compared with  $\bar{Q}$ . In the analysis of sliding on one plane with the forces  $\bar{W}$ ,  $\bar{U}$  and  $\bar{Q}$  acting on the wedge, the forces are added vectorially into a resultant  $\bar{R}$  which is given by

$$\bar{R} = \bar{W} + \bar{U} + \bar{Q} \quad (3.10)$$

The resisting reaction in plane a b c as shown in Fig. 3.3 is  $\bar{R}'$  and is equal and opposite to  $\bar{R}$ . Thus the direction of sliding is in the direction of the projection of  $\bar{R}$  on plane a b c and not necessarily in the direction of the dip. The angle of friction mobilized,  $\phi'$ , by the force  $\bar{R}$  is given by Eq. 2.20 for sliding on one plane as

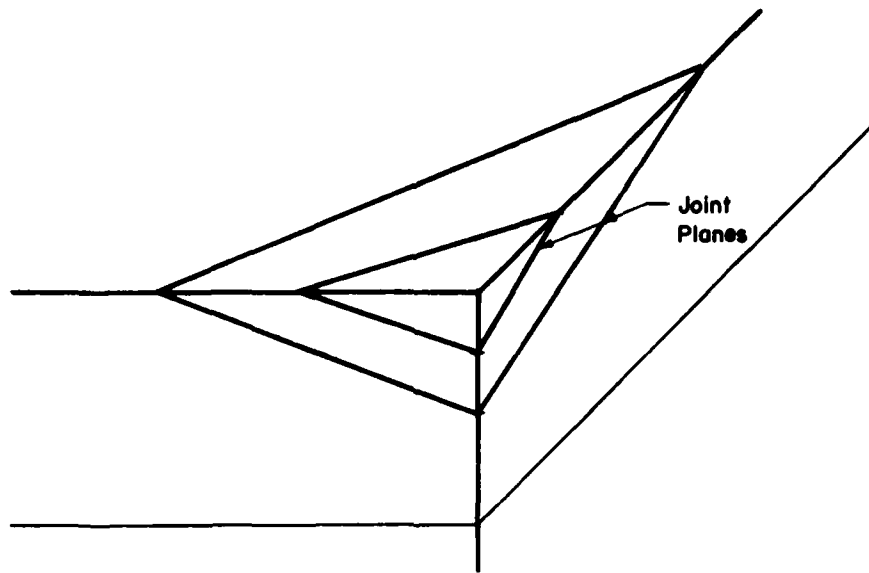
$$\tan \phi' = \frac{[(R_{yz} - R_{zy})^2 + (R_{zx} - R_{xz})^2 + (R_{xy} - R_{yx})^2]^{1/2}}{R_{xx} + R_{yy} + R_{zz}} \quad (3.11)$$

Thus the factor of safety for this case is given by

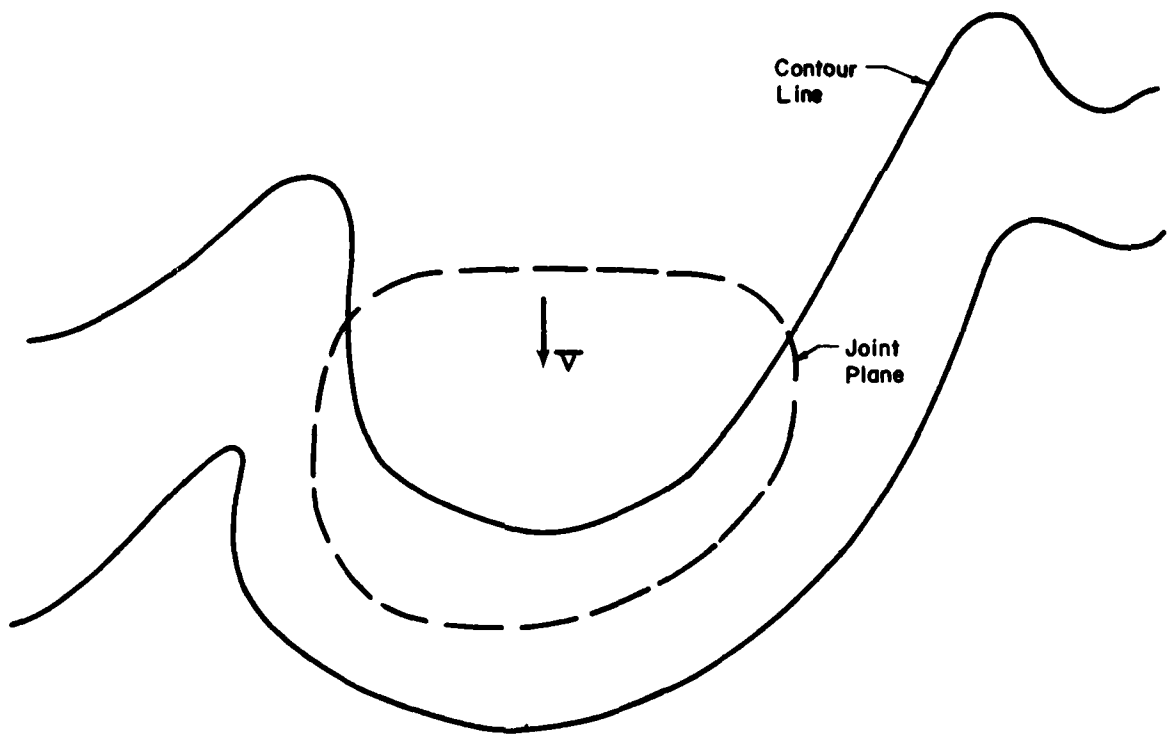
$$F.S. = \frac{\tan \phi}{\tan \phi'} \quad (3.12)$$

### 3.2.2 Calculation of Dynamic Resistance

It should also be noted that Wittke (1965) has treated an earthquake loading as an equivalent static load applied in a horizontal plane and parallel to the projection of the unit vector in a direction of the dip,



(a) Cutslope



(b) Natural Slope — Bedding Planes Dipping Toward Valley — Sliding Block Isolated from Mass by Gully on Each Side

FIG. 3.2 SLIDING ON ONE PLANE — STRIKE OF PLANE NOT PARALLEL TO STRIKE OF SLOPE FACE

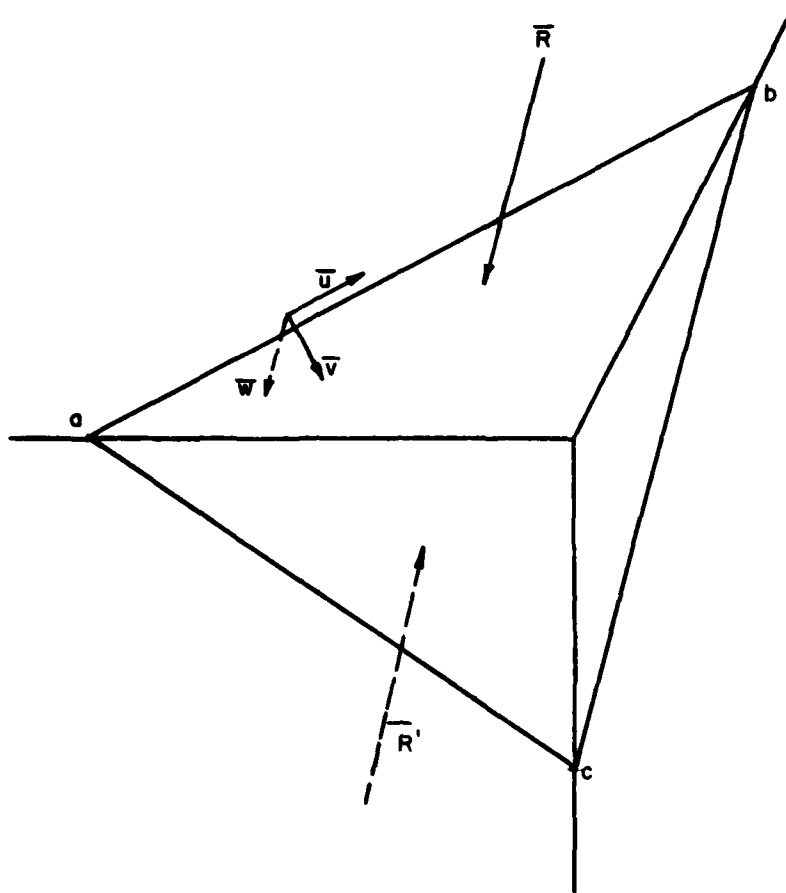


FIG. 3.3 SLIDING ON ONE PLANE

$\bar{v}$ , in a horizontal plane. Thus, according to the analysis of Wittke (1965) for earthquake loading, the problem is simply analyzed as for the general case presented above where

$$\bar{R} = \bar{W} + \bar{U} + \bar{Q} + \bar{H}$$

where

$$\bar{H} = \bar{i} \frac{v_x}{(v_x^2 + v_y^2)^{\frac{1}{2}}} \frac{1}{2} k_1 W + \bar{j} \frac{v_y}{(v_x^2 + v_y^2)^{\frac{1}{2}}} \frac{1}{2} k_1 W$$

The seismic coefficient  $k_1$  is taken between 0 and 0.2 depending on the intensity of the earthquake motion expected, and the force  $\bar{H}$  is in a horizontal plane and parallel to the projection of the unit vector in a direction of the dip,  $\bar{v}$ , in a horizontal plane. The factor of safety is as given by Eq. 3.12. This approach, however, is not recommended by the authors since it is considered as being an unduly conservative approach to earthquake stability. The approach proposed in this report for assessing the dynamic stability of rock slopes will essentially follow the concepts proposed by Newmark (1965), which are presented in Chapter 5. In order to use the Newmark method of analysis, however, it is necessary to establish the resistance available to resist dynamic loads. This dynamic resistance is the resistance which is available in addition to the resistance required for static stability. The dynamic resistance is denoted by  $\bar{N}W$  where  $\bar{W}$  is the weight of the potential sliding block and  $N$  is a coefficient to be determined in the following manner. The force  $\bar{N}W$  is that force applied to the potential sliding block which is necessary to just make the block slide (i.e. F.S. = 1). Depending on the direction in which  $\bar{N}W$  is applied, its magnitude will vary. The magnitude of  $\bar{N}W$  appropriate for design or analysis is the magnitude of  $\bar{N}W$  applied in such a direction as to make  $\bar{N}W$

a minimum. For a potential failure of a block sliding on one plane as shown in Fig. 3.4(a)  $\overline{NW}$  should be applied in a direction  $\theta$  to the horizontal which will give the minimum value of  $\overline{NW}$  to just cause the block to slide. The direction and magnitude of the minimum value of  $\overline{NW}$  can be determined as shown in Fig. 3.4(b). The direction and magnitude of the weight  $\overline{W}$  is known and the direction of a resultant  $\overline{R}$  is known and is inclined at  $\phi$  to the normal of the plane of sliding when sliding begins to take place. Then the magnitude of the vector  $\overline{NW}$  is minimum when it joins the tip of the weight vector  $\overline{W}$  in a direction which makes an angle of  $90^\circ$  with the resultant  $\overline{R}$ . Thus from geometry, the minimum magnitude of  $\overline{NW}$  is given by

$$NW = W \sin (\phi - \gamma)$$

or

$$N = \sin (\phi - \gamma) \quad (3.13)$$

where  $\phi$  is the angle of shearing resistance and  $\gamma$  is the dip. Thus the minimum value of  $N$  occurs when  $\overline{NW}$  is in the same direction of the horizontal projection of the dip but is inclined upward from the horizontal at an angle of  $\theta = (\phi - \gamma)$  and  $N$  has a magnitude of  $\sin (\phi - \gamma)$  for the case of sliding on one plane. Using this minimum value of  $\overline{NW}$  as the dynamic resistance is a conservative estimate because it is assumed that the earthquake motions are in the most unfavorable orientation for the slope being investigated.

### 3.3 Example Problems of Sliding on One Plane by Vector Analysis

Slope stability calculations by vector analysis are performed in this section for several cases involving sliding on one plane. In some of these cases the same answer could be arrived at quickly by means of

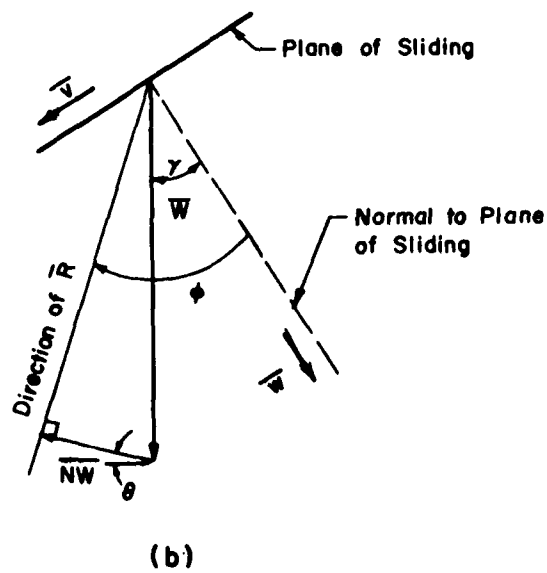
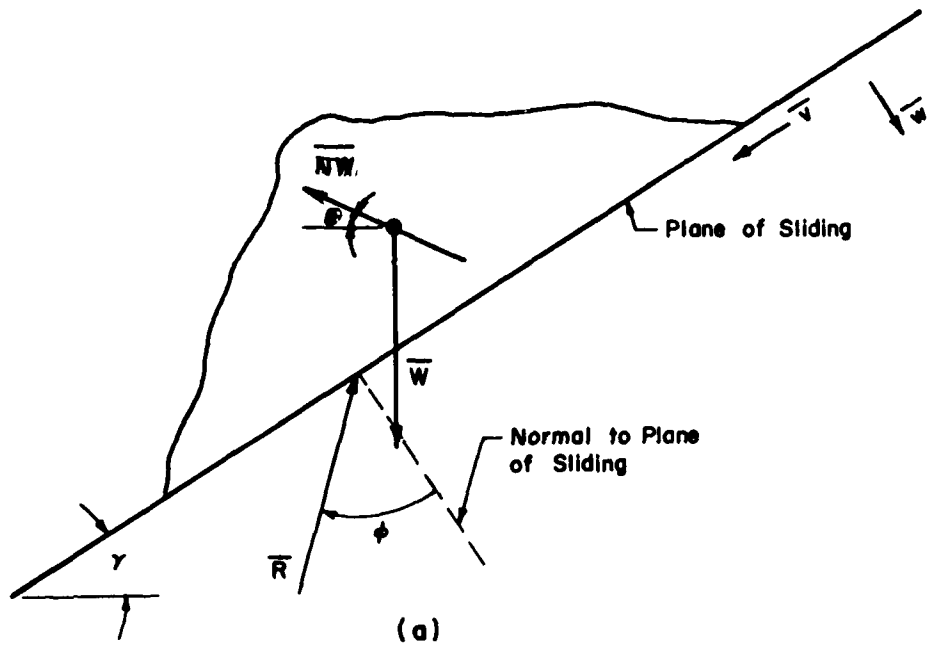


FIG. 3.4 FAILURE OF A BLOCK SLIDING ON ONE PLANE

conventional analysis, in others it would be more difficult to do by conventional means.

For example, consider a wedge of rock sliding on a plane which strikes East-West and dips  $30^\circ$  South and which has a friction angle of  $40^\circ$ .

Consider the positive x direction to be East, the positive y direction to be North and the positive z direction to be upwards. The unit vector in the direction of the strike is given by

$$\bar{u} = (1, 0, 0)$$

The unit vector in the dip direction is given by

$$\bar{v} = (0, -0.866, -0.500)$$

and the unit vector normal to the plane is

$$\bar{w} = \bar{u} \times \bar{v} = (0, 0.500, -0.866)$$

and  $\bar{w}$  is directed downward normal to the plane.

#### Case I

First consider the factor of safety of the block acted on by its own weight only. In this case the resultant force  $\bar{R}$  acting on the block is equal to the weight  $\bar{W}$  given by

$$\bar{R} = \bar{W} = (0, 0, -W)$$

The magnitude of the component of  $\bar{R}$  normal to the plane is given by

$$N = \bar{R} \cdot \bar{w} = 0.866 W$$

then  $\bar{N} = 0.866 W \bar{w} = (0, 0.433W, -0.750W)$

the tangential component of  $\bar{R}$  on the plane of sliding is

$$\bar{T} = \bar{R} - \bar{N} = (0, -0.433W, -0.25W)$$

the magnitude of  $\bar{T}$  is given by

$$T = W [(-0.433)^2 + (-0.25)^2]^{1/2} = 0.50W$$

$$\text{then F.S.} = \frac{N \tan \phi}{T} = \frac{0.866W \tan 40^\circ}{0.50W} = 1.455$$

Check: By Eq. 3.7

$$\text{F.S.} = \frac{\tan 40^\circ}{\tan 30^\circ} = 1.455$$

### Case II

Consider now that a force  $\bar{A}$  acts on the wedge in addition to the weight of the wedge  $\bar{W}$ . The force  $\bar{A}$  acts parallel to the strike (East) and has a magnitude of  $0.20W$ .

$$\text{Thus} \quad \bar{R} = \bar{A} + \bar{W} = (0.20W, 0, -W)$$

$$\text{and} \quad N = \bar{R} \cdot \bar{w} = 0.866W$$

$$\text{and} \quad \bar{N} = N\bar{w} = (0, 0.433W, -0.75W)$$

The component of  $\bar{R}$  tangential to the plane is

$$\bar{T} = \bar{R} - \bar{N} = (0.200W, -0.433W, -0.250W) \text{ and } T = 0.540W.$$

$$\therefore \text{F.S.} = \frac{N \tan \phi}{T} = \frac{0.866W \tan 40^\circ}{0.54W} = 1.35$$

Note that in this case sliding does not take place down the dip but in the direction of the vector  $\bar{T}$ .

### Case III

Consider now that the wedge is acted on by its own weight and a force  $\bar{A}$  having a magnitude of  $0.20W$  and acting in a direction parallel to the unit vector in the direction of the dip. In this case the normal component is still given by  $N = \bar{W} \cdot \bar{w} = 0.866W$  as given in Case I. The magnitude of the driving tangential force  $\bar{T}$  is the sum of the magnitudes of  $\bar{A}$  and the tangential component of the weight on the plane. The factor of safety is therefore given by



$$F.S. = \frac{0.866W \tan 40^\circ}{0.50W + 0.20W} = 1.05$$

#### Case IV

Now consider that the plane under the wedge of weight  $\bar{W}$  as in Case I is acted upon by a porewater force,  $\bar{U}$ , which increases until the factor of safety decreases from 1.455 to 1.0. The porewater force does not change the driving force  $\bar{T}$ . Therefore, as in Case I,

$$T = 0.50W$$

The magnitude of the normal force  $N$  as given in Case I is reduced by the magnitude of the porewater force,  $U$ . That is

$$N = 0.866W - U$$

$$\text{and } F.S. = 1.0 = \frac{0.866W - U}{0.50W} \tan 40^\circ$$

and solving for  $U$

$$U = 0.271W$$

Check: By Eq. 3.9

$$F.S. = 1.0 = \frac{\tan \phi}{\tan \gamma} - \frac{K \tan \phi}{\sin \gamma} = \frac{\tan 40^\circ}{\tan 30^\circ} - K \frac{\tan 40^\circ}{\sin 30^\circ}$$

Solving  $K = 0.271$

$$\therefore U = 0.271W$$

#### Case V

Consider the same wedge to be acted on by its own weight  $\bar{W}$ , a porewater force  $\bar{U}$  of magnitude  $0.44W$  acting normal to and on the plane of sliding, and a force  $\bar{A}$  having a magnitude  $A = 0.60W$  and acting in a direction  $S 45^\circ W$  at a dip of  $10^\circ$ . Then

$$\bar{W} = (0, 0, -W)$$

$$\bar{U} = 0.44W(-\bar{w}) = (0, -0.22W, 0.371W)$$

The unit vector,  $\bar{a}$ , in the direction of force  $\bar{A}$  is given by Eq. 2.14 with  $\gamma = 170^\circ$  and  $\beta = 135^\circ$ , thus,

$$\begin{aligned}\bar{a} &= [-\cos 10^\circ \sin 45^\circ, -(-\cos 10^\circ)(-\cos 45^\circ), -\sin 10^\circ] \\ \bar{a} &= (-0.696, -0.696, -0.174)\end{aligned}$$

Thus

$$\bar{A} = A\bar{a} = (-0.418W, -0.418W, -0.105W)$$

and

$$\bar{R} = \bar{W} + \bar{U} + \bar{A} = (-0.418W, -0.638W, -0.734W)$$

The magnitude of the component of  $R$  normal to the plane of sliding is given by

$$N = R \cdot w = 0.316W$$

∴

$$\bar{N} = N\bar{w} = (0, 0.158W, -0.274W)$$

The component of  $\bar{R}$  tangential to the plane of sliding is

$$\bar{T} = \bar{R} - \bar{N} = (-0.418W, -0.796W, -0.460W)$$

∴

$$T = 1.009W$$

$$\begin{aligned}\text{F.S.} &= \frac{N \tan 40^\circ}{T} = \frac{0.316W \tan 40^\circ}{1.009W} \\ &= 0.262\end{aligned}$$

#### Case VI

Consider the slope acted on by only its own weight as in Case I.

It is desired to calculate the magnitude of the minimum dynamic resistance  $\overline{NW}$ .

This is simply given by Eq. 3.13 as

$$NW = W \sin (\phi - \gamma) = W \sin 10^\circ$$

or

$$N = \sin 10^\circ = 0.174$$

### 3.4 Stability Calculations by Vector Analysis for Slopes Containing Two Sets of Joint Planes.

#### 3.4.1 Calculation of Factor of Safety for Static Loads

##### 3.4.1.1 Description of Geometry and Loads

The general case of two systems of joint planes is as shown in Fig. 3.5 where planes 1 and 2 denote the joint planes, planes 3 and 4 denote the planes defining the faces of the slope,  $\gamma_1$  and  $\gamma_2$  denote the dip angles of planes 1 and 2,  $\beta_1$  and  $\beta_2$  denote the strike angles of planes 1 and 2 measured counterclockwise from the positive x direction and  $\alpha$  and  $\delta$  denote the inclination of planes 3 and 4 with the horizontal. The unit vectors in the direction of the strike planes 1 and 2 are given by Eq. 2.13:

$$\bar{u}_1 = (\cos \beta_1, \sin \beta_1, 0) \quad \bar{u}_2 = (\cos \beta_2, \sin \beta_2, 0)$$

and the unit vectors in the direction of the dip for planes 1 and 2 are given by Eq. 2.14:

$$\bar{v}_1 = (\cos \gamma_1 \sin \beta_1, -\cos \gamma_1 \cos \beta_1, -\sin \gamma_1)$$

$$\bar{v}_2 = (\cos \gamma_2 \sin \beta_2, -\cos \gamma_2 \cos \beta_2, -\sin \gamma_2)$$

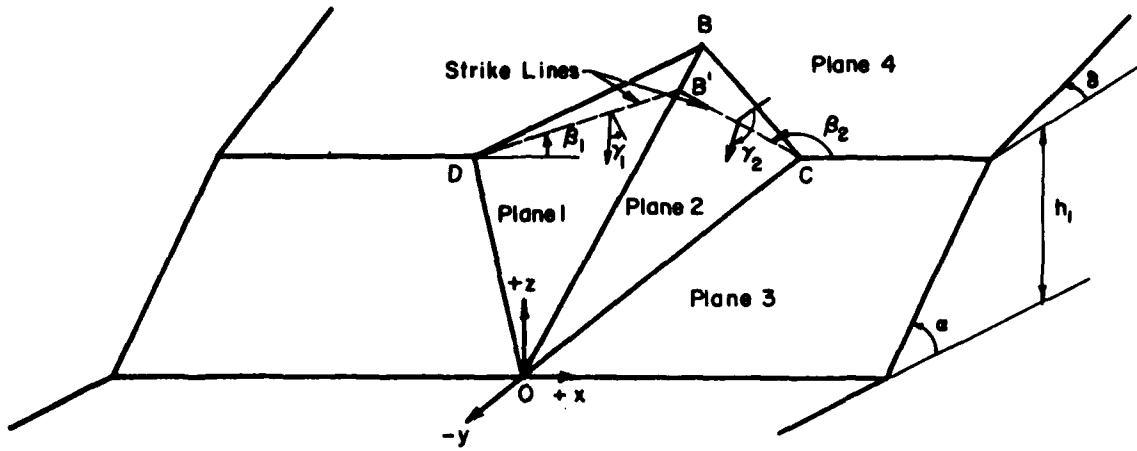
The unit vectors normal to each plane are given by

$$\bar{w}_1 = \bar{u}_1 \times \bar{v}_1$$

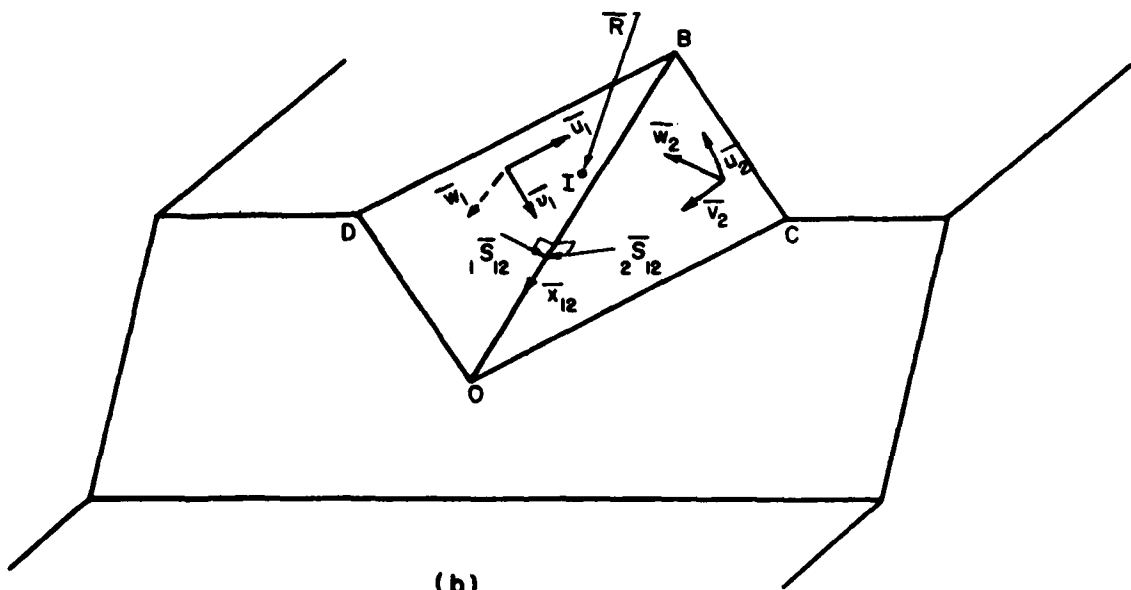
and

$$\bar{w}_2 = \bar{u}_2 \times \bar{v}_2$$

Note on Fig. 3.5 that  $\bar{w}_1$  is directed downward into plane 1 and  $\bar{w}_2$  is directed outward from plane 2 when the normals are defined in this manner. Also note that the plane designated as plane 1 is the one with the lowest value of  $\beta$ . In the case where the strikes of two planes are the same the plane designated as plane 1 is the one with the smallest value of  $\gamma$ . This convention is necessary to maintain the proper sign convention for the following vector operations.



(a)



(b)

FIG. 3.5 STABILITY OF A WEDGE BOUNDED BY TWO JOINT PLANES

The loading of the slope consists of (1) dead load  $\bar{W}$  acting at the center of gravity of the mass considered, (2) live load  $\bar{Q}$  applied at any point, (3) porewater forces  $\bar{U}_1$  and  $\bar{U}_2$  acting on planes 1 and 2 respectively and (4) dynamic loads induced by ground motions from earthquakes or nuclear detonations. The resultant  $\bar{R}$  of the loads in any given case can be determined, and let the point of application of the resultant be at point I.

#### 3.4.1.2 Determination of the Mode of Sliding Failure

For the case of a tetrahedron bounded by two base planes which may be intersecting joint sets, failure may occur by sliding along the line of intersection of the two planes or by sliding on either one of the two planes.

The first step in determining the mode of failure is to check if the disturbing forces tend to lift the tetrahedron from either or both of the supporting planes. Thus considering the rock wedge OBCD (Fig. 3.5), the resultant force  $\bar{R}$  tends to break the contact between the tetrahedron and planes 1 and 2 respectively if

$$\bar{R} \cdot \bar{w}_1 < 0 \quad (3.14)$$

and

$$\bar{R} \cdot \bar{w}_2 > 0$$

If Eqs. 3.14 show that the resultant force  $\bar{R}$  tends to lift the tetrahedron off of both supports, then equilibrium is not possible unless the joints can take tension or rock bolts are added to take the computed tension. Normally this will not happen for large slopes acted on by their own weight and porepressures, but could occur for small tetrahedrons near the surface of steep or overhanging slopes. If Eqs. 3.14 show that lifting occurs off of one of the supporting planes then we can definitely say that sliding cannot occur on that plane.

If Eqs. 3.14 show that lifting off of the wedge from the supporting planes does not occur, i.e.

$$\begin{aligned}\bar{R} \cdot \bar{w}_1 &> 0 \\ \bar{R} \cdot \bar{w}_2 &< 0\end{aligned}\tag{3.14a}$$

then we must make further kinematic tests to see whether sliding takes place on plane 1 only or plane 2 only or along the line of intersection of planes 1 and 2.

In order to evaluate the mode of sliding it is necessary to define two new vectors  ${}_1\bar{s}_{12}$  and  ${}_2\bar{s}_{12}$  which are given by

$$\begin{aligned}{}_1\bar{s}_{12} &= \bar{x}_{12} \times \bar{w}_1 \\ {}_2\bar{s}_{12} &= \bar{x}_{12} \times \bar{w}_2\end{aligned}\tag{3.15}$$

and are as shown in Fig. 3.5(b). The vector  ${}_1\bar{s}_{12}$  is in plane 1 perpendicular to the line of intersection  $\bar{x}_{12}$  and the vector  ${}_2\bar{s}_{12}$  is in plane 2 perpendicular to the line of intersection  $\bar{x}_{12}$ .

If sliding is to occur along the line of intersection  $\bar{x}_{12}$ , then Eqs. 3.16, 3.17 and 3.18 must be satisfied simultaneously.

$$\bar{R} \cdot {}_1\bar{s}_{12} > 0\tag{3.16}$$

$$\bar{R} \cdot {}_2\bar{s}_{12} > 0\tag{3.17}$$

$$\epsilon_x < \alpha \text{ if } 0 < \alpha < \pi \text{ and } \epsilon_x < \delta \text{ if } \alpha = \pi\tag{3.18}$$

where

$$\epsilon_x = \tan^{-1} \left( \frac{x_{12z}}{x_{12y}} \right)\tag{3.19}$$

and  $x_{12y}$ ,  $x_{12z}$  = y and z components of vector  $\bar{x}_{12}$ . The vector  $\bar{x}_{12}$  along the line of intersection is defined in Chapter 2 and is given by Eq. 2.16 as

$$\bar{x}_{12} = \bar{w}_2 \times \bar{w}_1$$

If sliding is to occur on plane 1 only, then both the following equations must be satisfied:

$$\bar{R} \cdot \bar{w}_1 > 0 \quad (3.20)$$

and 
$$\bar{R} \cdot {}_1\bar{s}_{12} < 0 \quad (3.21)$$

Similarly if sliding is to occur on plane 2 only, then Eqs. 3.22 and 3.23 must be satisfied.

$$\bar{R} \cdot \bar{w}_2 < 0 \quad (3.22)$$

$$\bar{R} \cdot {}_2\bar{s}_{12} < 0 \quad (3.23)$$

The physical interpretation of Eqs. 3.16 - 3.23 may be made as follows. Eq. 3.16 is satisfied only if the resultant force  $\bar{R}$  has a component which tends to push the wedge on plane 1 toward the line of intersection  $\bar{x}_{12}$ . Similarly Eq. 3.17 is satisfied only if the resultant force  $\bar{R}$  has a component pushing the wedge on plane 2 toward the line of intersection  $\bar{x}_{12}$ . Thus Eqs. 3.16 and 3.17 ensure that the resultant force  $\bar{R}$  wedges the tetrahedron between the two plane so that sliding can only take place on both the planes along the line of intersection. In order for sliding along the line of intersection to be kinematically possible, it should also be ensured that the line of intersection does not plunge into the rock slope and this check is provided by Eq. 3.18. Thus when all the three kinematic conditions specified by Eqs. 3.16 through 3.18 are satisfied simultaneously sliding can occur along the line of intersection. The tendency to slide will be downhill if  $\bar{R} \cdot \bar{x}_{12} > 0$  and uphill if  $\bar{R} \cdot \bar{x}_{12} < 0$  (Fig. 3.5).

Eq. 3.21 indicates a component of  $\bar{R}$  on plane 1 tending to move the block away from plane 2 by sliding on plane 1 and Eq. 3.20 establishes the condition for contact on plane 1. Thus Eqs. 3.20 and 3.21 are suf-

efficient and necessary conditions for sliding to occur on plane 1. Similarly Eqs. 3.22 and 3.23 specify the conditions for sliding on plane 2.

### 3.4.1.3 Calculation of the Factor of Safety for Sliding

If the kinematic tests discussed above show that sliding takes place on only plane 1 or on only plane 2, then the factor of safety can be computed from Eq. 3.4 for sliding on one plane. Thus for sliding on plane 1 the factor of safety may be computed as

$$F.S. = \frac{N_1 \tan \phi_1}{T_1} = \frac{(\bar{R} \cdot \bar{w}_1) \tan \phi_1}{T_1} \quad (3.24)$$

where

$$\bar{T}_1 = \bar{R} - (\bar{R} \cdot \bar{w}_1) \bar{w}_1 = T_{1x} \bar{i} + T_{1y} \bar{j} + T_{1z} \bar{k}$$

Thus Eq. 3.24 becomes

$$F.S. = \frac{(\bar{R} \cdot \bar{w}_1) \tan \phi_1}{[T_{1x}^2 + T_{1y}^2 + T_{1z}^2]^{1/2}} \quad (3.25)$$

which may be written as:

$$F.S. = \frac{\tan \phi_1 [R_x w_{1x} + R_y w_{1y} + R_z w_{1z}]}{[(R_y w_{1z} - R_z w_{1y})^2 + (R_z w_{1x} - R_x w_{1z})^2 + (R_x w_{1y} - R_y w_{1x})^2]^{1/2}} \quad (3.26)$$

For sliding on plane 2 only, the factor of safety is given as

$$F.S. = \frac{N_2 \tan \phi_2}{T_2} = \frac{-(\bar{R} \cdot \bar{w}_2) \tan \phi_2}{T_2} \quad (3.27)$$

The minus sign appearing in Eq. 3.27 is due to the direction of the unit normal  $\bar{w}_2$  as shown in Fig. 3.5.

Eq. 3.27 can be expanded to yield

$$F.S. = \frac{\tan \phi_2 [(-R_x w_{2x} - R_y w_{2y} - R_z w_{2z})]}{[(R_y w_{2z} - R_z w_{2y})^2 + (R_z w_{2x} - R_x w_{2z})^2 + (R_x w_{2y} - R_y w_{2x})^2]^{1/2}} \quad (3.28)$$



If the kinematic tests of Eqs. 3.16, 3.17 and 3.18 are satisfied and sliding takes place on both planes 1 and 2 along the line of intersection  $\bar{x}_{12}$ , then the factor of safety may be computed in the following manner.

The first step is to compute the magnitude of the driving force,  $T_{12}$ , shown in Fig. 3.6, in the direction of sliding. This is simply given by

$$T_{12} = \frac{\bar{R} \cdot \bar{x}_{12}}{x_{12}} \quad (3.29)$$

where  $x_{12}$  represents the magnitude of the vector  $\bar{x}_{12}$ . The vector  $\bar{T}_{12}$  is in the same direction as  $\bar{x}_{12}$  and is given by

$$\bar{T}_{12} = \frac{T_{12} \bar{x}_{12}}{x_{12}} \quad (3.30)$$

It is convenient to define the vector  $\bar{N}_{12}$ , normal to the line of intersection which is given by

$$\bar{N}_{12} = \bar{R} - \bar{T}_{12} \quad (3.31)$$

In order to evaluate the frictional resistances on planes 1 and 2, it is necessary to determine the components  $\bar{N}_1$  and  $\bar{N}_2$  of  $\bar{N}_{12}$  acting normal to planes 1 and 2 respectively. The relationship of the vectors  $\bar{R}$ ,  $\bar{T}_{12}$ ,  $\bar{N}_{12}$ ,  $\bar{N}_1$  and  $\bar{N}_2$  are shown in Sections AA and BB of Fig. 3.6. From Fig. 3.6 it is obvious that

$$N_1 \bar{w}_1 + N_2 (-\bar{w}_2) = \bar{N}_{12} \quad (3.32)$$

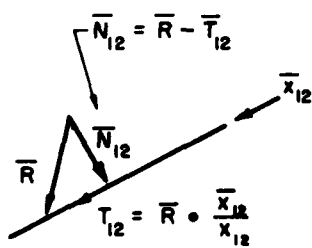
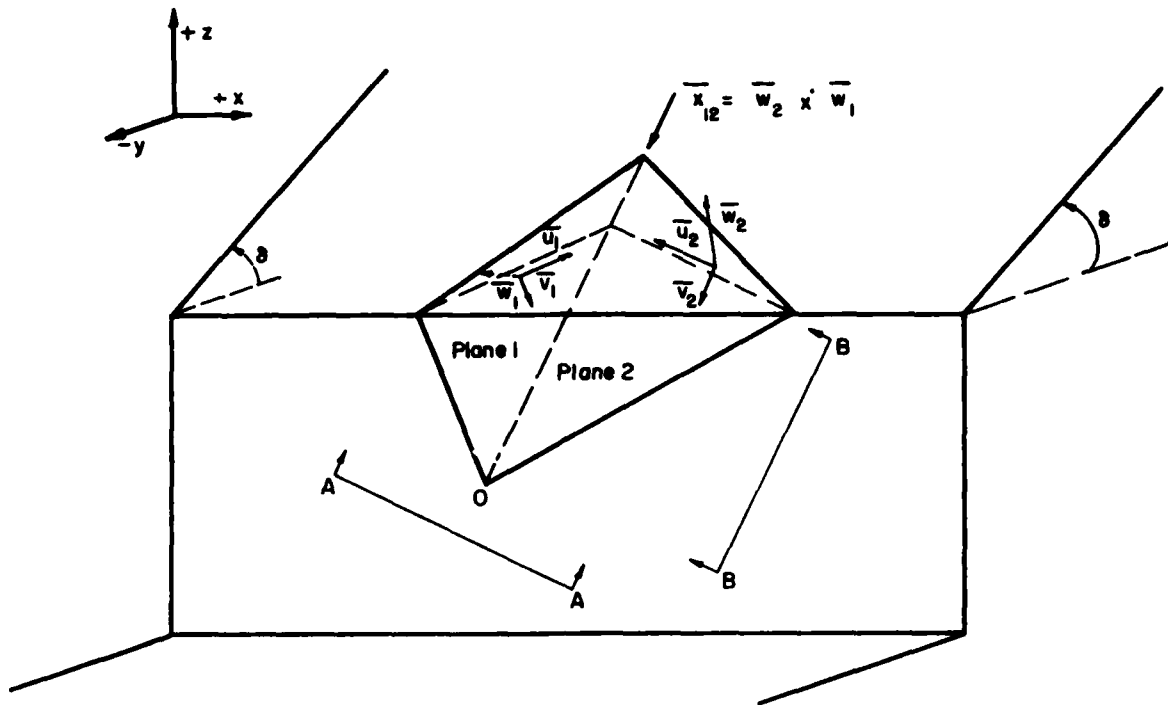
where  $N_1$  and  $N_2$  represent the magnitudes of the two component vectors  $\bar{N}_1$  and  $\bar{N}_2$  respectively.

Thus

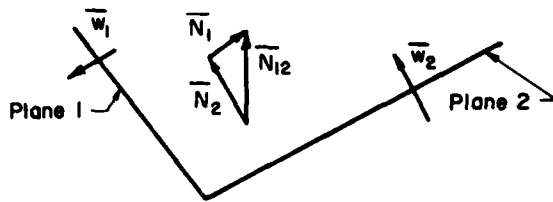
$$N_1 w_{1x} - N_2 w_{2x} = N_{12x} \quad (3.33)$$

$$N_1 w_{1y} - N_2 w_{2y} = N_{12y} \quad (3.34)$$

$$N_1 w_{1z} - N_2 w_{2z} = N_{12z} \quad (3.35)$$



Section B-B



Section A-A

**FIG. 3.6 SLIDING ON TWO PLANES**

Any two of Eqs. 3.33, 3.34, and 3.35 can be used to determine  $N_1$  and  $N_2$  and the third equation can be used to check the numerical values of  $N_1$  and  $N_2$ . After  $N_1$  and  $N_2$  are obtained the factor of safety for sliding on both planes may be determined from the equation

$$\text{F.S.} = \frac{N_1 \tan \phi_1 + N_2 \tan \phi_2}{T_{12}} \quad (3.36)$$

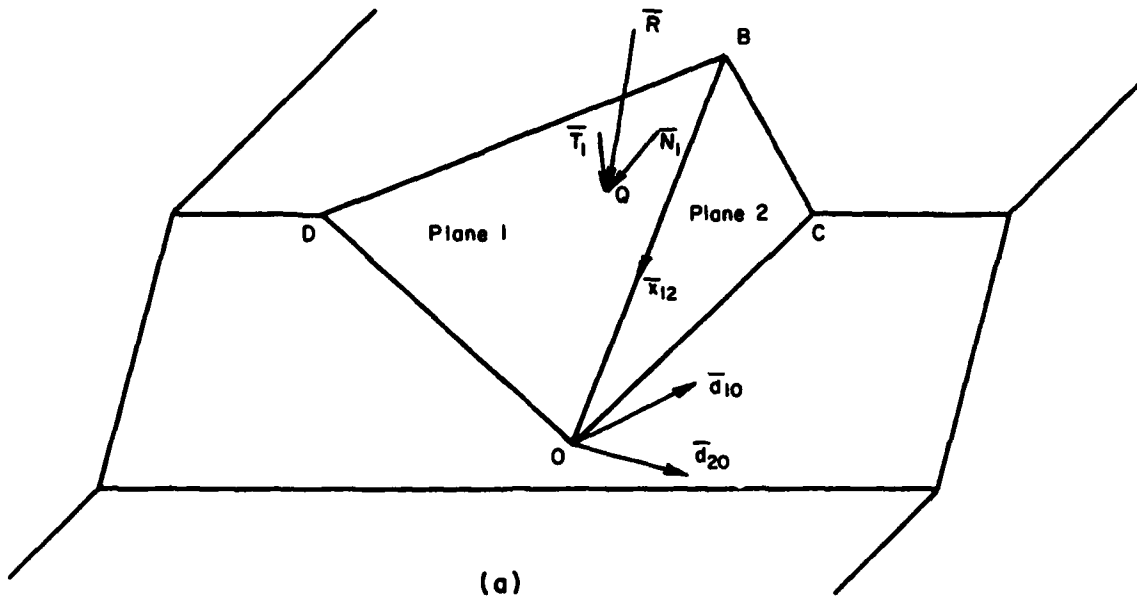
#### 3.4.1.4 Calculation of Static Factor of Safety for Rotations

In addition to the previously investigated sliding movements which endanger stability, the rock wedge OBCD may rotate about the support edges, OC or OD, or about the axes at point O perpendicular to planes 1 and 2, when the resultant load exerts an overturning moment about these axes (Fig. 3.7). Even though all the above modes of failure by rotation are conceivable, under normal conditions the most probably axes of rotation are  $\bar{d}_{10}$  and  $\bar{d}_{20}$  (Fig. 3.7) and therefore consideration is given only to rotations about these two axes in this section. The treatment of rotation about  $\overline{OC}$ ,  $\overline{OD}$ ,  $\bar{d}_{1B}$  or  $\bar{d}_{2B}$  is similar and is not developed in this report. The axes of rotation  $\bar{d}_{10}$  and  $\bar{d}_{20}$  pass through O and are perpendicular to planes 1 and 2 respectively. In a rotation, say about the  $\bar{d}_{10}$  axis, all points of the wedge in the region of the area ODB move tangential to plane 1 while the surface OCB of the rock wedge separates from plane 2. The equations of the  $\bar{d}_{10}$  and  $\bar{d}_{20}$  axes are obtained as follows:

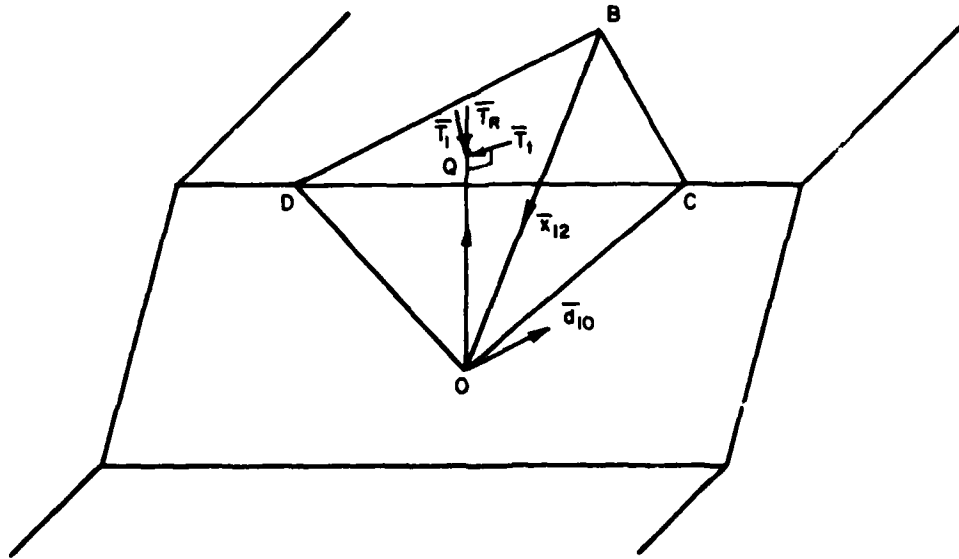
$$\bar{d}_{10} = -\bar{w}_1 \quad (3.37)$$

$$\bar{d}_{20} = -\bar{w}_2 \quad (3.38)$$

In the analysis for rotations, it is necessary to know the points of application of the various forces acting on the rock wedge OBCD so



(a)



(b)

FIG. 3.7 ROTATIONAL STABILITY OF A WEDGE BOUNDED BY TWO JOINT PLANES

that the point of application I (Fig. 2.8) of the resultant force  $\bar{R}$  can be determined. The weight  $\bar{W}$  acts vertically downwards at the center of gravity S of the rock wedge as shown in Fig. 2.8. The vector  $\overline{OS}$  as shown in Fig. 2.8 can be obtained from geometrical considerations as

$$\overline{OS} = 1/4(\overline{OD} + \overline{OC} + \overline{OB}) \quad (3.39)$$

(also Eq. 2.34)

where the vectors  $\overline{OD}$ ,  $\overline{OC}$  and  $\overline{OB}$  are given by the following equations:

$$\overline{OD} = \left( \frac{h_1}{\tan \alpha \tan \beta_1} - \frac{h_1}{\tan \gamma_1 \sin \beta_1}, \frac{h_1}{\tan \alpha}, h_1 \right) \quad (3.40)$$

$$\overline{OC} = \left( \frac{h_1}{\tan \alpha \tan \beta_2} - \frac{h_1}{\tan \gamma_2 \sin \beta_2}, \frac{h_1}{\tan \alpha}, h_1 \right) \quad (3.41)$$

$$\overline{OB} = \frac{\bar{x}_{12}}{x_{12z}} (h_1 + h_2) \quad (3.42)$$

$$h_2 = \frac{\tan \alpha - \tan \epsilon_x}{\tan \epsilon_x - \tan \delta} \cdot \frac{\tan \delta}{\tan \alpha} \cdot h_1 \quad (3.43)$$

where  $h_1$ ,  $h_2$ ,  $\alpha$ ,  $\delta$ ,  $\gamma_1$ ,  $\beta_1$ ,  $\gamma_2$ , and  $\beta_2$  are defined in Fig. 3.9.

The weight of the rock wedge can be determined from its volume V which is given by:

$$V = \frac{1}{6} |DB' \times DC| (h_1 + h_2) \quad (3.44)$$

(also Eq. 2.33)

where

$$\overline{DC} = \overline{OC} - \overline{OD} \quad (3.45)$$

$$\overline{DB'} = \overline{OB'} - \overline{OD} \quad (3.46)$$

$$\overline{OB'} = \frac{\bar{x}_{12}}{x_{12z}} h_1 \quad (3.47)$$

The point of application, I, of the resultant force  $\bar{R}$  is determined from the known magnitudes and lines of action of the component forces by using Eq. (2.27) and the principles of vector analysis as explained in Chapter 2.

For a rotation to be possible about the  $\bar{d}_{10}$  axis, the resultant force  $\bar{R}$  must have a positive scalar component of moment about the  $\bar{x}_{12}$  and  $\bar{d}_{10}$  axes as evaluated by Eq. (2.28); i.e.,

$$M_x = \text{moment of } \bar{R} \text{ about } \bar{x}_{12} = \bar{x}_{12} \cdot (\overline{OI} \times \bar{R}) > 0 \quad (3.48)$$

and 
$$M_{d10} = \text{moment of } \bar{R} \text{ about } \bar{d}_{10} = \bar{d}_{10} \cdot (\overline{OI} \times \bar{R}) > 0 \quad (3.49)$$

Similarly the moments of  $\bar{R}$  about the  $\bar{x}_{12}$  and  $\bar{d}_{20}$  axes have to satisfy Eqs. (3.50) and (3.51) if a rotation is to occur about the  $\bar{d}_{20}$  axis.

$$M_x = \bar{x}_{12} \cdot (\overline{OI} \times \bar{R}) < 0 \quad (3.50)$$

and 
$$M_{d20} = \bar{d}_{20} \cdot (\overline{OI} \times \bar{R}) > 0 \quad (3.51)$$

In addition a few kinematic tests must also be satisfied and these tests are dependent on the magnitude of the angles  $\eta$ ,  $k_{10}$  and  $k_{20}$  which are defined as follows:

$$\begin{aligned} \eta &= \text{wedge angle between planes 1 and 2} \\ &= \cos^{-1} (\bar{w}_1 \cdot \bar{w}_2) \quad 0 < \eta < \pi \end{aligned} \quad (3.52)$$

$$k_{10} = \text{DOB} = \cos^{-1} \frac{\overline{OD} \cdot \overline{OB}}{(\overline{OD})(\overline{OB})} \quad 0 < k_{10} < \pi \quad (3.53)$$

$$k_{20} = \text{COB} = \cos^{-1} \frac{\overline{OC} \cdot \overline{OB}}{(\overline{OC})(\overline{OB})} \quad 0 < k_{20} < \pi \quad (3.54)$$

The range of angles  $\eta$ ,  $k_{10}$  and  $k_{20}$  for which a rotation about the  $\bar{d}_{10}$  and  $\bar{d}_{20}$  axes is kinematically impossible, is given in Table 3.1.

The analyses for determining the static factor of safety for rotations about  $\bar{d}_{10}$  and  $\bar{d}_{20}$  axes are similar in principle and therefore the details of the analysis will be given only for the case of rotation about the  $\bar{d}_{10}$  axis.

The resultant  $\bar{R}$  is first resolved into components  $\bar{N}_1$  and  $\bar{T}_1$  at its point of intersection, Q, with plane 1, as shown in Fig. 3.7(a). Thus

Axis of Rotation:  $\bar{d}_{10}$

$\eta$	$k_{10}$	$k_{20}$	Supplementary Condition
$0 < \eta < \pi$	$> \pi/2$	$> \pi/2$	-
$0 < \eta < \pi$	$< \pi/2$	$> \pi/2$	-
$< \pi/2$	$> \pi/2$	$< \pi/2$	$\frac{\tan k_{20}}{\tan(\pi - k_{10})} > \sec(\pi - \eta)$

Axis of Rotation:  $\bar{d}_{20}$

$\eta$	$k_{10}$	$k_{20}$	Supplementary Condition
$0 < \eta < \pi$	$> \pi/2$	$> \pi/2$	-
$0 < \eta < \pi$	$> \pi/2$	$< \pi/2$	-
$< \pi/2$	$< \pi/2$	$> \pi/2$	$\frac{\tan k_{10}}{\tan(\pi - k_{20})} > \sec(\pi - \eta)$

Table 3.1 Range of Angles for which a rotation is kinematically impossible.

$$\bar{N}_1 = (\bar{R} \cdot \bar{w}_1) \bar{w}_1 \quad (3.55)$$

and

$$\bar{T}_1 = \bar{R} - \bar{N}_1 \quad (3.56)$$

The component  $\bar{T}_1$  tangential to plane 1 is now resolved into components  $\bar{T}_r$  and  $\bar{T}_t$  [Fig. 3.7(b)]. The force  $\bar{T}_r$  has the direction of the vector  $\overline{OQ}$  and the force  $\bar{T}_t$  has the direction of the tangent to the rotation which Q executes in the case of a rotation about  $\bar{d}_{10}$ . The force  $\bar{T}_t$  is thus the only component of the loading which exerts an overturning moment about the  $\bar{d}_{10}$  axis. The resolution of force  $\bar{T}_1$  into its components  $\bar{T}_t$  is done as follows:

$$\bar{T}_1 = \bar{T}_r + \bar{T}_t = c_1(-\overline{OQ}) + c_2(\overline{OQ} \times \bar{w}_1) \quad (3.57)$$

In Eq. 3.57,  $-\overline{OQ}$  and  $\overline{OQ} \times \bar{w}_1$  are vectors in the direction of  $\bar{T}_r$  and  $\bar{T}_t$ . By equating the x, y and z components of  $\bar{T}_1$  as given by Eqs. 3.56 and 3.57, the values of the two coefficients  $c_1$  and  $c_2$  may be determined. Eqs. 3.56 and 3.57 give three equations for the two unknowns  $c_1$  and  $c_2$  and therefore one of these equations can be used to check the calculations for  $c_1$  and  $c_2$ . With  $c_1$  and  $c_2$  known,  $\bar{T}_r$  and  $\bar{T}_t$  are obtained as follows:

$$\bar{T}_r = -c_1 \overline{OQ} \quad (3.58)$$

$$\bar{T}_t = c_2(\overline{OQ} \times \bar{w}_1) \quad (3.59)$$

The magnitude of the overturning moment  $M_{d10}$  can be obtained by the relation:

$$M_{d10} = T_t OQ \quad (3.60)$$

The magnitude of the restoring moment of the frictional force on plane 1 due to the normal component  $\bar{N}_1$  is obtained as

$$M_{rd10} = N_1 \tan \phi_1 OQ \quad (3.61)$$



The factor of safety against rotation can now be obtained as the ratio of the restoring moment to the overturning moment

$$\text{F.S. (against rotation)} = \frac{N_1 \tan \phi_1 \cdot OQ}{T_t \cdot OQ} = N_1 \tan \phi_1 / T_t \quad (3.62)$$

The factor of safety against rotation about the  $\bar{d}_{20}$  axis can also be determined in a similar manner. Moments  $M_{d10}$  and  $M_{d20}$  are very often negative and in these cases only the sliding stability need be analyzed.

### 3.4.2 Calculation of Dynamic Resistance Against Sliding on Two Planes

The direction and magnitude of the minimum dynamic resistance  $\bar{NW}$  which is necessary to just make the potential block slide on the two base planes may be found by the following procedure.

A unit vector  $\bar{r}_1$  is first defined in the direction of the resultant reaction  $\bar{R}_1$  on plane 1 (Fig. 3.8). In the limiting state of equilibrium  $\bar{R}_1$  is inclined at an angle  $\phi_1$  to the upward normal  $\bar{w}_1$  to plane 1 and tends to oppose the downward movement along the line of intersection  $\bar{x}_{12}$ . Therefore,

$$\bar{r}_1 = -\bar{w}_1 \cos \phi_1 - \bar{x}_{12} \sin \phi_1 / x_{12} \quad (3.63)$$

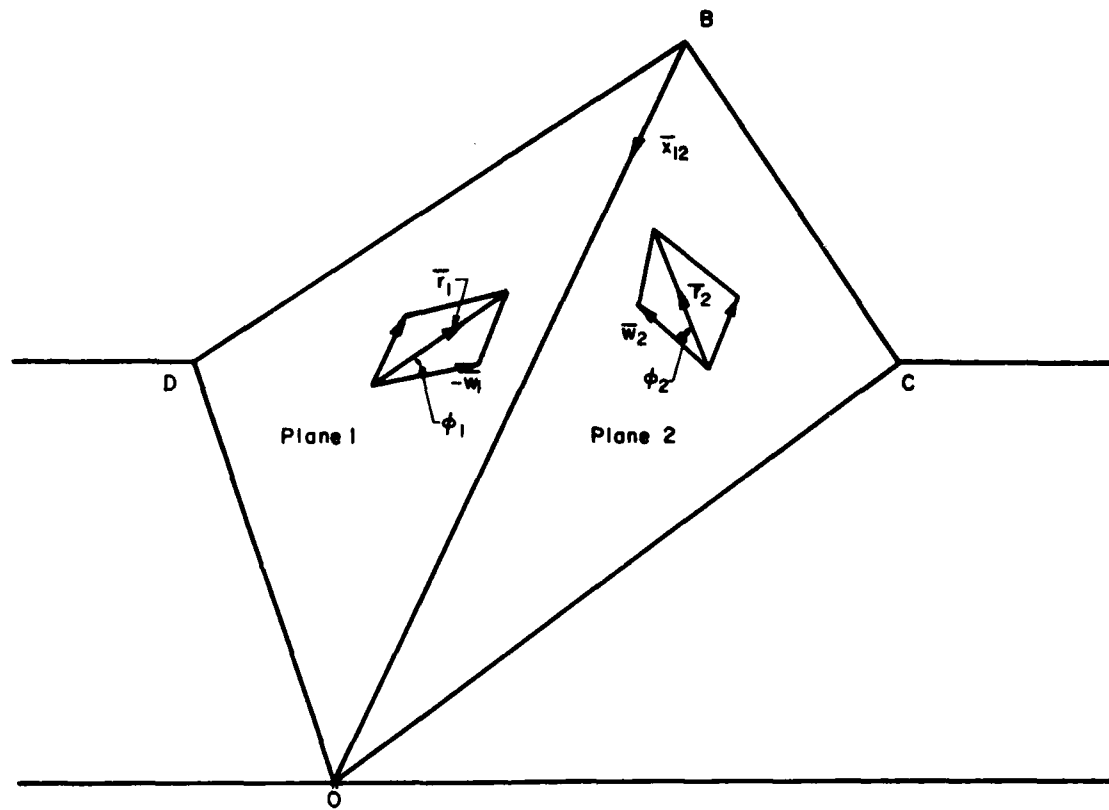
Similarly a unit vector  $\bar{r}_2$  is defined in the direction of the resultant reaction  $\bar{R}_2$  on plane 2. From Fig. 3.8 it can be seen that

$$\bar{r}_2 = \bar{w}_2 \cos \phi_2 - \bar{x}_{12} \sin \phi_2 / x_{12} \quad (3.64)$$

where  $\phi_2$  is the angle of friction on plane 2.

The magnitude of the dynamic resistance vector  $\bar{NW}$  will be a minimum when the vector  $\bar{NW}$  is normal to the plane containing  $\bar{R}_1$  and  $\bar{R}_2$ . Therefore a unit vector  $\bar{n}$  in the direction of  $\bar{NW}$  may be obtained by the equation:

$$\bar{n} = (\bar{r}_1 \times \bar{r}_2) / |\bar{r}_1 \times \bar{r}_2| \quad (3.65)$$



$$|\bar{r}_1| = 1$$

$$\bar{r}_1 = -\bar{w}_1 \cdot \cos \phi_1 - \frac{\bar{x}_{12}}{|\bar{x}_{12}|} \sin \phi_1$$

$$|\bar{r}_2| = 1$$

$$\bar{r}_2 = \bar{w}_2 \cdot \cos \phi_2 - \frac{\bar{x}_{12}}{|\bar{x}_{12}|} \sin \phi_2$$

FIG. 3.8 STABILITY OF A WEDGE BOUNDED BY TWO JOINT PLANES

where  $|\bar{r}_1 \times \bar{r}_2|$  represents the magnitude of the vector  $(\bar{r}_1 \times \bar{r}_2)$ .

The magnitude of the minimum dynamic resistance, NW, may now be determined by the equation

$$NW = \bar{R} \cdot \bar{n} \quad (3.66)$$

where  $\bar{R}$  is the resultant of all static loads acting on the sliding rock wedge. From Eq. 3.66 it follows that

$$N = \frac{\bar{R} \cdot \bar{n}}{W} \quad (3.67)$$

### 3.4.3 Example Problems for Slopes with Two Intersecting Planes of Discontinuity Worked by Vector Analysis.

#### Problem 1

Determine the factor of safety of the rock wedge OBCD shown in Fig. 3.9. Also estimate the direction and magnitude of the minimum dynamic resistance  $\overline{NW}$  which is necessary to just make the potential block OBCD slide.

<u>Plane 1</u>	<u>Plane 2</u>
$\beta_1 = 36^\circ$	$\beta_2 = 94^\circ$
$\gamma_1 = 62^\circ$	$\gamma_2 = 121^\circ$
$\phi_1 = 20^\circ$	$\phi_2 = 40^\circ$
$\alpha = 70^\circ$	$\delta = 20^\circ$

#### Solution

Static Factor of safety against sliding

According to Eqs. 2.13, 2.14 and 2.15, for plane 1,

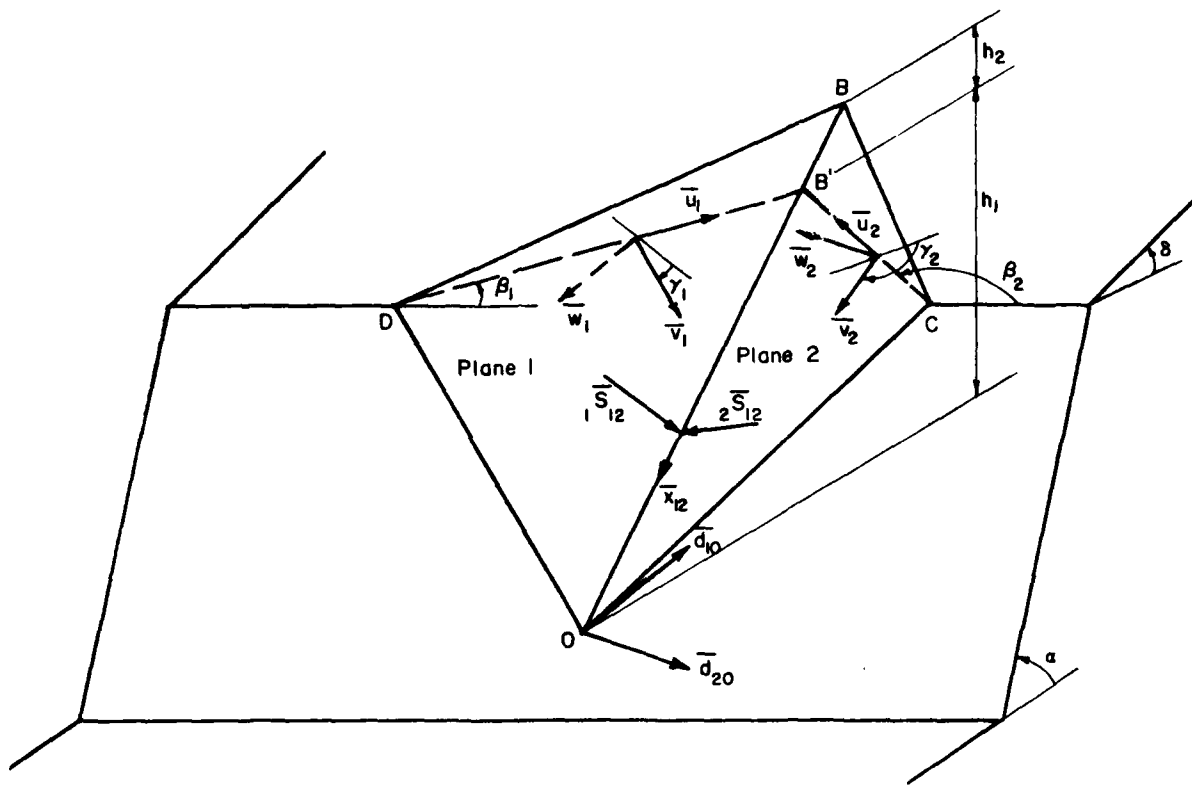


FIG. 3.9 STABILITY OF A ROCK WEDGE BOUNDED BY TWO JOINT PLANES

$$\bar{u}_1 = (0.809, 0.588, 0.000) \quad (2.13)$$

$$\bar{v}_1 = (0.276, -0.380, -0.883) \quad (2.14)$$

$$\bar{w}_1 = (-0.519, 0.714, -0.469) \quad (2.15)$$

and for plane 2,

$$\bar{u}_2 = (-0.070, 0.998, 0.000) \quad (2.13)$$

$$\bar{v}_2 = (-0.514, -0.036, -0.857) \quad (2.14)$$

$$\bar{w}_2 = (-0.855, -0.060, 0.515) \quad (2.15)$$

The only load that enters the calculation in this problem is the weight  $W$  of the rock wedge OBCD acting vertically downwards in the  $-z$  direction.

Therefore the resultant load  $\bar{R}$  may be expressed as

$$\bar{R} = (0, 0, -W)$$

$$\bar{R} \cdot \bar{w}_1 = 0.469W > 0$$

and  $\bar{R} \cdot \bar{w}_2 = -0.515W < 0 \quad (3.14a)$

Therefore lifting off of the rock wedge from the support planes does not occur.

$$\begin{aligned} \bar{x}_{12} &= \bar{w}_2 \times \bar{w}_1 \\ &= (-0.340, -0.669, -0.642) \end{aligned} \quad (2.16)$$

and  $x_{12} = 0.987$

$$\begin{aligned} {}_1\bar{s}_{12} &= \bar{x}_{12} \times \bar{w}_1 \\ &= (0.722, 0.172, -0.590) \end{aligned} \quad (3.15)$$

and  ${}_2\bar{s}_{12} = \bar{x}_{12} \times \bar{w}_2 \quad (3.15)$

$$= (-0.383, 0.725, -0.551)$$

$$\bar{R} \cdot {}_1\bar{s}_{12} = 0.590W > 0 \quad (3.16)$$

$$\bar{R} \cdot {}_2\bar{s}_{12} = 0.551W > 0 \quad (3.17)$$

$$\begin{aligned}\epsilon_x &= \tan^{-1} \left( \frac{x_{12z}}{x_{12y}} \right) \\ &= \tan^{-1} \left( \frac{-0.642}{-0.669} \right) = 43.8^\circ\end{aligned}\quad (3.19)$$

$$\dots \delta < \epsilon_x < \alpha \quad (3.18)$$

Thus according to Eqs. 3.16, 3.17, and 3.18, sliding is kinematically possible only along the line of intersection  $\bar{x}_{12}$ . Since  $\bar{R} \cdot \bar{x}_{12} = 0.642W > 0$  sliding tends to occur down the line of intersection.

$$\begin{aligned}T_{12} &= \bar{R} \cdot \bar{x}_{12}/x_{12} = 0.642W/0.987 \\ &= 0.650W\end{aligned}\quad (3.29)$$

and

$$\bar{T}_{12} = 0.650W \frac{\bar{x}_{12}}{x_{12}} = (-0.223W, -0.440W, -0.420W) \quad (3.30)$$

$$\bar{N}_{12} = \bar{R} - \bar{T}_{12} = (0.223W, 0.440W, -0.580W) \quad (3.31)$$

$$\begin{aligned}&= N_1 \bar{w}_1 + N_2 (-\bar{w}_2) \\ &= N_1 (-0.519, 0.714, -0.469) + \\ &\quad N_2 (0.855, 0.060, -0.515)\end{aligned}\quad (3.32)$$

Solving

$$N_1 = 0.565W, \quad N_2 = 0.605W$$

$$F.S. = \frac{N_1 \tan \phi_1 + N_2 \tan \phi_2}{T_{12}} \quad (3.36)$$

$$= \frac{0.565W \tan 20^\circ + 0.605W \tan 40^\circ}{0.650W}$$

$$= 1.10$$

Stability against rotation.

According to Eqs. 3.39 through 3.43

$$\overline{OD} = (-0.404h_1, 0.346h_1, h_1) \quad (3.40)$$

$$OD = 1.138h_1$$

$$\overline{OC} = (0.602h_1, 0.364h_1, h_1) \quad (3.41)$$

$$OC = 1.220h_1$$

$$\overline{OB} = (0.741h_1, 1.460h_1, 1.398h_1) \quad (3.42)$$

$$OB = 2.155h_1$$

$$\overline{OS} = (0.235h_1, 0.547h_1, 0.850h_1) \quad (3.39)$$

In order to apply the kinematic tests for rotation, it is necessary to establish the values of the angles  $k_{10}$ ,  $k_{20}$  and  $\eta$ .

$$k_{10} = \cos^{-1} \frac{\overline{OD} \cdot \overline{OB}}{(\overline{OD})(\overline{OB})} = 48.1^\circ < \pi/2 \quad (3.53)$$

$$k_{20} = \cos^{-1} \frac{\overline{OC} \cdot \overline{OB}}{(\overline{OC})(\overline{OB})} = 25.3^\circ < \pi/2 \quad (3.54)$$

$$\eta = \cos^{-1}(\bar{w}_1 \cdot \bar{w}_2) = 80.9^\circ < \pi/2 \quad (3.52)$$

$$M_x = \bar{x}_{12} \cdot (\overline{OI} \times \bar{R}) \quad (3.48)$$

$$= \bar{x}_{12} \cdot (\overline{OS} \times \bar{R}) = 0.03Wh_1 > 0$$

For these values of  $\eta$ ,  $k_{10}$ ,  $k_{20}$  and  $M_x$ , a rotation about axis  $\bar{d}_{10}$  is kinematically possible. However the rotation can occur only if  $M_{d10} > 0$ .

$$\bar{d}_{10} = -\bar{w}_1 = (0.519, -0.714, 0.469) \quad (3.37)$$

$$\overline{OI} = \overline{OS} = (0.235h_1, 0.547h_1, 0.850h_1)$$

$$M_{d10} = \bar{d}_{10} \cdot (\overline{OI} \times \bar{R}) \quad (3.49)$$

$$= -0.452Wh_1 < 0$$

Therefore rotation about  $\bar{d}_{10}$  axis does not occur.

#### Minimum Dynamic Resistance

The unit vector  $\bar{r}_1$  in the direction of the resultant reaction on plane 1 is given by Eq. 3.63 as

$$\bar{r}_1 = (0.607, -0.439, 0.663) \quad (3.63)$$

The unit vector  $\bar{r}_2$  in the direction of the resultant reaction on plane 2 can be obtained in a similar manner from Eq. 3.64

$$\bar{r}_2 = (-0.434, 0.388, 0.810) \quad (3.64)$$

The unit vector in the direction of the minimum dynamic resistance vector  $\overline{NW}$  is then given by

$$n = \frac{\bar{r}_1 \times \bar{r}_2}{|\bar{r}_1 \times \bar{r}_2|} = (-0.616, -0.785, 0.046) \quad (3.65)$$

The magnitude of the minimum dynamic resistance is now obtained as

$$NW = |\bar{R} \cdot \bar{n}| = 0.046W \quad (3.66)$$

or

$$N = 0.046 \quad (3.67)$$

### Problem 2

Determine the factor of safety of the rock wedge OBCD shown in Fig.

3.10 when (a)  $P = 0$  and (b)  $P = 10$  tons in the positive  $y$  direction.

<u>Plane 1</u>	<u>Plane 2</u>
$\phi_1 = 30^\circ$	$\phi_2 = 30^\circ$
$\beta_1 = 17^\circ$	$\beta_2 = 63^\circ$
$\gamma = 60^\circ$	$\gamma_2 = 80^\circ$
$\alpha = 90^\circ$	$\delta = 0^\circ$

Point of application of  $P$  is  $S$  such that  $\overline{OS} = (-6.1, 2.0, 9.0)$ . The dimensions are in feet units.

### Solution

Case (a)  $P = 0$

Static Factor of Safety against sliding

For plane 1,

$$\bar{u}_1 = (0.955, 0.292, 0.000) \quad (2.13)$$



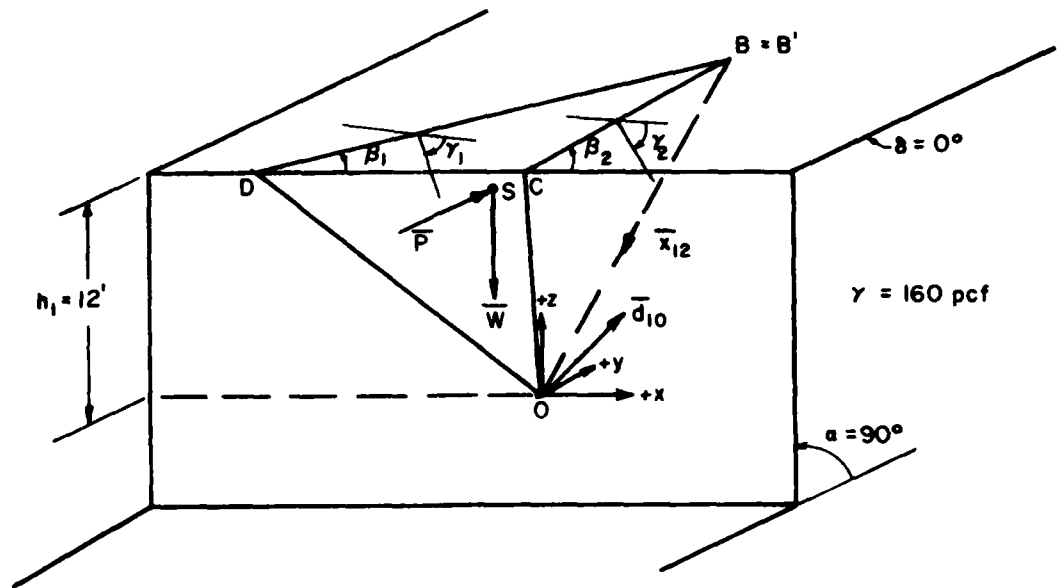


FIG. 3.10 STABILITY OF A ROCK WEDGE BOUNDED BY TWO JOINT PLANES

$$\bar{v}_1 = (0.146, -0.478, -0.866) \quad (2.14)$$

$$\bar{w}_1 = (-0.253, 0.827, -0.499) \quad (2.15)$$

For plane 2,

$$\bar{u}_2 = (0.454, 0.890, 0.000) \quad (2.13)$$

$$\bar{v}_2 = (0.155, -0.079, -0.985) \quad (2.14)$$

$$\bar{w}_2 = (-0.877, 0.447, -0.174) \quad (2.15)$$

When  $\bar{P} = 0$

$$\bar{R} = (0, 0, -W)$$

where  $W$  = weight of the rock wedge OBCD

$$\bar{x}_{12} = \bar{w}_2 \times \bar{w}_1 \quad (2.16)$$

$$= (-0.079, -0.394, -0.594)$$

$$x_{12} = 0.717$$

$${}_1\bar{S}_{12} = \bar{x}_{12} \times \bar{w}_1 \quad (3.15)$$

$$= (0.688, 0.110, -0.165)$$

$${}_2\bar{S}_{12} = \bar{x}_{12} \times \bar{w}_2 \quad (3.15)$$

$$= (0.334, 0.507, -0.381)$$

$$\bar{R} \cdot {}_1\bar{S}_{12} = 0.165W > 0 \text{ and} \quad (3.16)$$

$$\bar{R} \cdot {}_2\bar{S}_{12} = 0.381W > 0 \quad (3.17)$$

$$\epsilon_x = \tan^{-1} \left( \frac{x_{12z}}{x_{12y}} \right) = \tan^{-1} \left( \frac{-0.594}{-0.394} \right) \quad (3.19)$$

$$= 56.4^\circ$$

$$\therefore \delta < \epsilon_x < \alpha \quad (3.18)$$

Thus according to Eqs. 3.16, 3.17 and 3.18, sliding is kinematically possible only along the line of intersection  $\bar{x}_{12}$ .

Since  $\bar{R} \cdot \bar{x}_{12} = 0.594W > 0$ , sliding tends to occur down the line of intersection.

$$\begin{aligned} T_{12} &= \bar{R} \cdot \bar{x}_{12} / x_{12} = 0.549W / 0.717 \\ &= 0.828W \end{aligned} \quad (3.29)$$

$$\begin{aligned} \bar{T}_{12} &= 0.828W \frac{\bar{x}_{12}}{x_{12}} \\ &= (-0.091W, -0.455W, -0.696W) \end{aligned} \quad (3.30)$$

$$\begin{aligned} \bar{N}_{12} &= \bar{R} - \bar{T}_{12} \\ &= (0.091W, 0.455W, -0.314W) \end{aligned} \quad (3.31)$$

$$\begin{aligned} &= N_1 \bar{w}_1 + N_2 (-\bar{w}_2) \\ &= N_1 (-0.253, 0.827, -0.499) + \\ &\quad N_2 (0.877, -0.477, 0.174) \end{aligned}$$

Solving

$$N_1 = 0.733W, \quad N_2 = 0.314W$$

$$\begin{aligned} F.S. &= \frac{0.733 \tan 30^\circ + 0.314W \tan 30^\circ}{0.828W} \\ &= 0.73 < 1 \end{aligned}$$

Stability against Rotation.

$$\overline{OD} = (-23.70, 0, 12.00) \quad (3.40)$$

$$OD = 26.60$$

$$\overline{OC} = (-2.40, 0, 12.00) \quad (3.41)$$

$$OC = 12.25$$

$$\begin{aligned} \overline{OB} &= \frac{12}{-0.594} (-0.079, -0.394, -0.594) \\ &= (1.60, 8.00, 12.00) \end{aligned} \quad (3.42)$$

$$OB = 14.50$$

$$\overline{OS} = \frac{1}{4} (\overline{OB} + \overline{OC} + \overline{OD}) \quad (3.39)$$

$$= (-6.10, 2.00, 9.00)$$

$$k_{10} = \cos^{-1} \left( \frac{\overline{OD} \cdot \overline{OB}}{\overline{OD} \cdot \overline{OB}} \right) = 74^\circ < \pi/2 \quad (3.53)$$

$$k_{20} = \cos^{-1} \left( \frac{\overline{OC} \cdot \overline{OB}}{\overline{OC} \cdot \overline{OB}} \right) = 38^\circ < \pi/2 \quad (3.54)$$

$$n = \cos^{-1} (\bar{w}_1 \cdot \bar{w}_2) = 47.4^\circ < \pi/2 \quad (3.52)$$

$$M_x = \bar{x}_{12} \cdot (\overline{OS} \times \bar{R}) \quad (3.48)$$

$$= 2.561W > 0 \text{ indicating thereby that the resultant}$$

$\bar{R}$  intersects plane 1. For these values of  $n$ ,  $k_{10}$ ,  $k_{20}$ , and  $M_x$  a rotation about axis  $\bar{d}_{10}$  is kinematically possible.

$$\bar{d}_{10} = -\bar{w}_1 = (0.253, -0.827, 0.499) \quad (3.37)$$

$$M_{d10} = \bar{d}_{10} \cdot (\overline{OS} \times \bar{R}) \quad (3.49)$$

$$= 4.539W > 0$$

Therefore a rotation can occur about the  $\bar{d}_{10}$  axis and the factor of safety against rotation can be determined as follows:

$$N_1 = \bar{R} \cdot \bar{w}_1 = 0.499W$$

$$\bar{N}_1 = (\bar{R} \cdot \bar{w}_1) \bar{w}_1 = (-0.126W, 0.413W, -0.250W) \quad (3.55)$$

$$\bar{T}_1 = \bar{R} - \bar{N}_1 = (0.126W, -0.413W, -0.750W) \quad (3.56)$$

$$= c_1 (-\overline{OQ}) + c_2 (\overline{OQ} \times \bar{w}_1) \quad (3.57)$$

$$\overline{OQ} = \overline{OI} + \psi \bar{R} = \overline{OS} + \psi \bar{R}$$

$$= [-6.1, 2.0, (9.0 - \psi W)]$$

Since  $\overline{OQ}$  and  $\bar{w}_1$  are mutually perpendicular,  $\overline{OQ} \cdot \bar{w}_1 = 0$

$$\therefore (6.1 \times 0.253) + (2.0 \times 0.827) - 0.499 (9.0 - \psi W) = 0$$

$$\therefore (9.0 - \psi W) = 6.40$$

$$\therefore \overline{OQ} = (-6.10, 2.00, 6.40)$$

$$\overline{OQ} \times \bar{w}_1 = (-6.29, -4.67, -4.54)$$

$$\therefore \bar{T}_1 = (0.126W, -0.413W, -0.750W)$$

$$= c_1(6.10, -2.00, -6.40) + c_2(-6.29, -4.67, -4.54)$$

Solving  $c_1 = 0.078W$ ;  $c_2 = 0.055W$

$$\bar{T}_t = c_2(\overline{OQ} \times \bar{w}_1) \quad (3.59)$$

$$= (-0.346W, -0.257W, -0.250W)$$

$$T_t = 0.498W$$

$$F.S. = \frac{N_1 \tan \phi_1}{T_t} = \frac{0.499W \times \tan 30^\circ}{0.498W} = 0.58 \quad (3.62)$$

Note: It may be noted that all the lengths in the above case are expressed in feet-units.

Case (b)  $\bar{P} = (0, 10, 0)$

In Case (a) the only force in the system is the weight  $\bar{W}$  of the rock wedge and it is not necessary to know the magnitude of  $\bar{W}$  for estimating the factor of safety of the rock wedge. But in Case (b) there is an additional external force  $\bar{P}$  of magnitude 10 tons acting in the positive y-direction through the center of gravity, S, of the rock wedge and therefore it becomes necessary, in the present case, to compute the magnitude of  $\bar{W}$ .

$$h_2 = 0 \quad (3.43)$$

$$\overline{DC} = \overline{OC} - \overline{OD} \quad (3.45)$$

$$= (21.30, 0, 0)$$

$$\overline{OB}' = \frac{\bar{x}_{12}}{x_{12z}} h_1 \quad (3.47)$$

$$= (1.60, 7.96, 12.00)$$

$$\overline{DB}' = \overline{OB}' - \overline{OD} \quad (3.46)$$

$$= (25.30, 7.96, 0) \quad (3.46)$$

$$V = \frac{1}{6} |\overline{DB}' \times \overline{DC}| (h_1 + h_2) \quad (3.44)$$

$$= 339.1 \text{ ft}^3$$

$$W = \frac{339.1 \times 160}{2000} = 27.13 \text{ tons}$$

$$\bar{W} = (0, 0, -27.13)$$

$$\bar{P} = (0, 10, 0)$$

$$\bar{R} = \bar{W} + \bar{P} = (0, 10, -27.13)$$

$$\bar{R} \cdot {}_1\bar{S}_{12} = 5.58 > 0 \quad (3.16)$$

$$\bar{R} \cdot {}_2\bar{S}_{12} = 15.41 > 0 \quad (3.17)$$

$$\delta < \epsilon_x < \alpha$$

The above values show that sliding is kinematically possible only along the line of intersection of planes 1 and 2. Since  $\bar{R} \cdot \bar{x}_{12} = 12.48 > 0$ , sliding tends to occur down the line of intersection.

$$T_{12} = \bar{R} \cdot \bar{x}_{12}/x_{12} = 12.48/0.717 = 17.41 \quad (3.29)$$

$$\bar{T}_{12} = 17.41 \bar{x}_{12}/x_{12} = (-1.918, -9.567, -14.423) \quad (3.30)$$

$$\bar{N}_{12} = \bar{R} - \bar{T}_{12} = (1.918, 19.567, -12.707) \quad (3.31)$$

$$= N_1(-0.253, 0.827, -0.499) +$$

$$N_2(0.877, -0.447, 0.174)$$

Solving  $N_1 = 29.4$  tons  $N_2 = 10.7$  tons

$$F.S. = \frac{29.4 \tan 30^\circ + 10.7 \tan 30^\circ}{17.41}$$

$$= 1.33$$

Stability against Rotation.

$$M_x = \bar{x}_{12} \cdot (\overline{OS} \times \bar{R})$$

$$= 112.84 > 0$$

∴ The resultant  $\bar{R}$  intersects plane 1 as in Case (a).

$$n = 47.4^\circ < \pi/2$$

$$k_{10} = 74^\circ < \pi/2$$

$$k_{20} = 38^\circ < \pi/2$$

For these values of  $n$ ,  $k_{10}$ ,  $k_{20}$ , and  $M_x$ , a rotation about  $d_{10}$  is kinematically possible.

$$d_{10} = -\bar{w}_1 = (0.253, -0.827, 0.499) \quad (3.37)$$

$$M_{d10} = \bar{d}_{10} \cdot (\overline{OS} \times \bar{R})$$

$$= 70.0 > 0$$

Therefore a rotation tends to occur about the  $\bar{d}_{10}$  axis. The factor of safety against rotation can be determined as follows.

$$N_1 = \bar{R} \cdot \bar{w}_1 = 21.83$$

$$\bar{N}_1 = N_1 \bar{w}_1 = (-5.523, 18.053, -10.893) \quad (3.55)$$

$$\bar{T}_1 = \bar{R} - \bar{N}_1 = (5.523, -8.053, -16.237) \quad (3.56)$$

$$= c_1(-\bar{OQ}) + c_2(\bar{OQ} \times \bar{w}_1) \quad (3.57)$$

$$\begin{aligned} \bar{OQ} &= \bar{OI} + \psi \bar{R} = \bar{OS} + \psi \bar{R} \\ &= [-6.1, (2.0 + 10\psi), (9.0 - 27.13\psi)] \end{aligned}$$

$\bar{OQ}$  and  $\bar{w}_1$  are mutually perpendicular

$$\therefore \bar{OQ} \cdot \bar{w}_1 = 0$$

$$\therefore (6.1 \times 0.253) + (2.0 + 10\psi) 0.827 - 0.499(9.0 - 27.13\psi) = 0$$

Solving  $\psi = 0.0593$

$$\therefore \bar{OQ} = (-6.10, 2.59, 7.39)$$

$$\bar{OQ} \times \bar{w}_1 = (-7.41, -4.91, -4.39)$$

$$\begin{aligned} \bar{T}_1 &= (5.523, -8.053, -16.237) \\ &= c_1(6.10, -2.59, -7.39) + \\ &\quad c_2(-7.41, -4.91, -4.39) \end{aligned}$$

Solving  $c_1 = 1.77$   $c_2 = 0.71$

$$T_t = c_2(\bar{OQ} \times \bar{w}_1) \quad (3.59)$$

$$\begin{aligned} &= 0.71(-7.41, -4.91, -4.39) \\ &= (-5.261, -3.496, -3.117) \end{aligned}$$

$$T_t = 7.04 \text{ tons}$$

$$F.S. = \frac{N_1 \tan \phi_1}{T_t} = \frac{21.83 \tan 30^\circ}{7.04}$$

$$= 1.79$$

Thus the provision of the lateral force P increases the stability of the wedge OBCD against both sliding and rotation.

Note: In case (b) all the forces are in ton-units and all the lengths are in feet-units.



### 3.5 Analysis for Sliding on Two Planes by Engineering Graphics

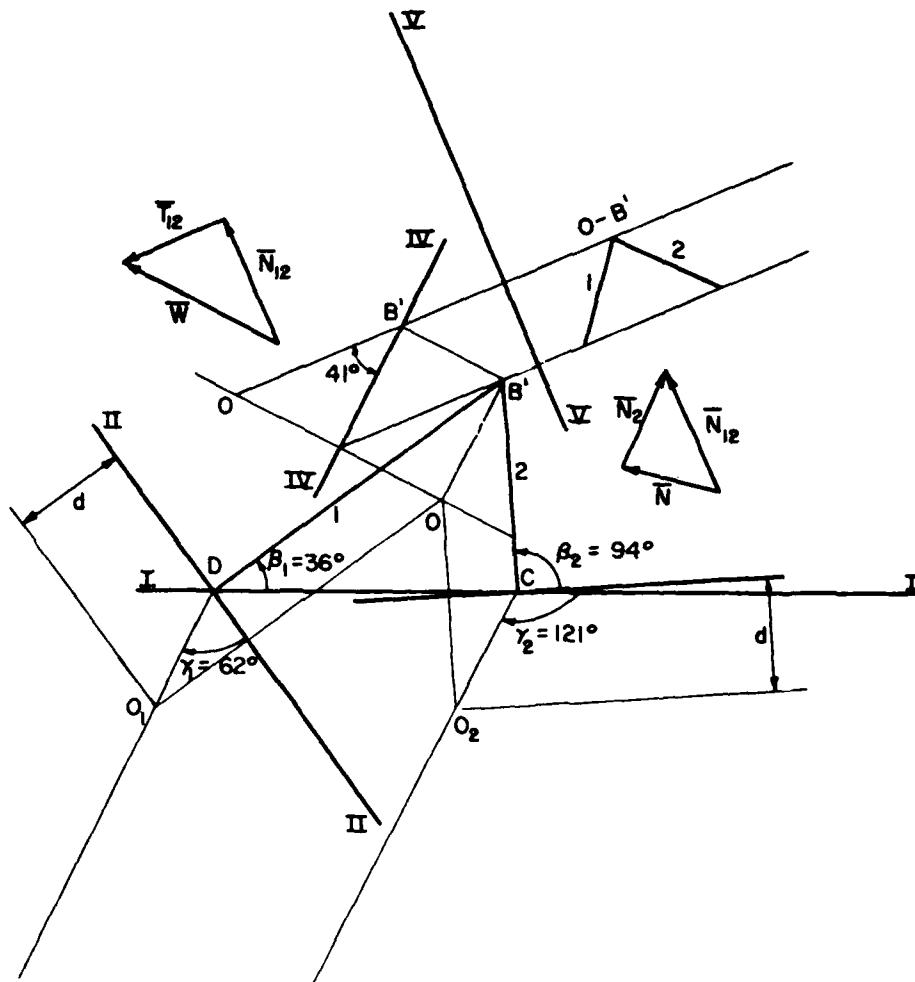
The factor of safety of a rock wedge sliding on the two base planes can also be determined graphically by using the principles of engineering descriptive geometry. To illustrate the procedure, Problem 1 of section 3.4.3 will be solved using this method. The details of this graphical solution are shown in Fig. 3.11.

The lines  $DB'$  and  $CB'$  represent the strikes of planes 1 and 2 inclined at angles  $\beta_1$  and  $\beta_2$  with the front of the slope, I-I. An edge view of each plane is drawn as an auxiliary elevation to locate the position of a point O common to both the planes situated at any depth,  $d$ , below the horizontal plane  $DCB'$ . Since  $B'$  is also a point common to both the planes,  $B'O$  represents the line of intersection of planes 1 and 2. A side elevation parallel to  $B'O$  gives the true dip of the line of intersection  $B'O$ . The weight vector  $\bar{W}$  is then resolved into components  $\bar{N}_{12}$  and  $\bar{T}_{12}$ , respectively normal and parallel to the line of intersection  $B'O$  as shown in Fig. 3.11. An auxiliary elevation of the two planes looking in the direction  $OB'$  is obtained and the components  $\bar{N}_1$  and  $\bar{N}_2$  of  $\bar{N}_{12}$  normal to planes 1 and 2 respectively are then determined. Once the magnitudes of  $\bar{N}_1$  and  $\bar{N}_2$  are known, the factor of safety is computed using the relationship

$$F.S. = \frac{N_1 \tan \phi_1 + N_2 \tan \phi_2}{T_{12}} \quad (3.36)$$

### 3.6 Method of Stability Analysis for Rock Slopes with Three Intersecting Joint Sets.

In this section, the stability against sliding of a tetrahedral volume of rock, ABCD bounded by three planes 1, 2 and 3 and an exterior surface ABD, is investigated by using Londe's method of analysis (Fig. 3.12).



Units	Scale for Forces	1" = 60 Units
$W = 66$		
$T_{12} = 42$		
$N_1 = 38$	$\tan 20^\circ = .364$	$38 \times .364 = 13.8$
$N_2 = 40$	$\tan 40^\circ = .840$	$40 \times .840 = \frac{33.6}{47.4}$
	$F.S. = \frac{47.4}{42.0} = 1.12$	

FIG. 3.11 GRAPHICAL SOLUTION OF SLIDING STABILITY OF A ROCK WEDGE BOUNDED BY TWO JOINT PLANES

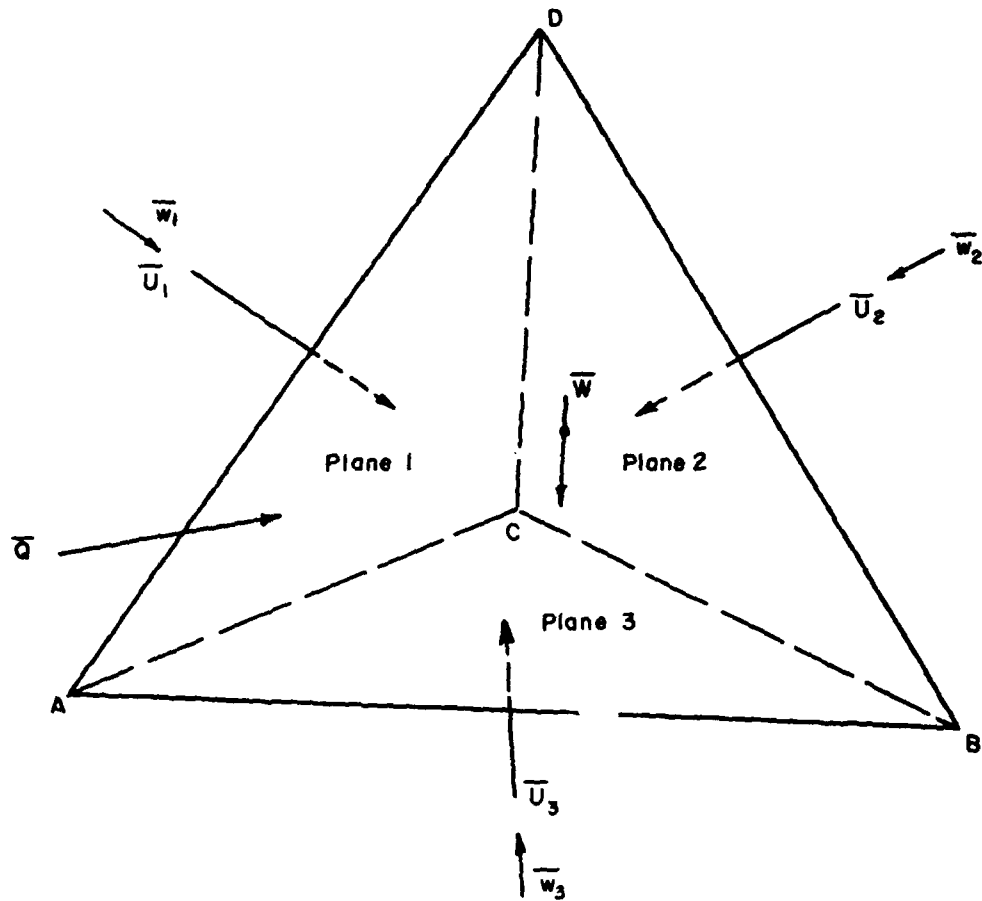


FIG. 3.12 FORCES ON A ROCK WEDGE BOUNDED BY THREE INTERSECTING JOINT PLANES

Sliding failure of the tetrahedral rock mass ABCD, can occur by separation from one or two of the three bounding planes. There are thus six possible modes of sliding failure as shown in Fig. 3.13. The mode of failure in a given case will depend on the geometry of the problem and the magnitude and direction of the resultant of the applied forces,  $\bar{R}$ , as defined by the equation:

$$\bar{R} = \bar{W} + \bar{Q} + \bar{U}_1 + \bar{U}_2 + \bar{U}_3 \quad (3.68)$$

Where  $\bar{W} = (W_x, W_y, W_z)$  = total weight vector of the tetrahedral volume of rock

$\bar{Q} = (Q_x, Q_y, Q_z)$  = any externally applied force on the rock wedge

$\bar{U}_1, \bar{U}_2, \bar{U}_3$  = hydrostatic uplift or porewater forces that act on planes 1, 2 and 3 respectively

The first step in the stability analysis of the rock wedge ABCD, is to determine the mode of sliding failure for a given set of input conditions. This can be done as explained in the following section.

### 3.6.1 Determination of the Mode of Sliding Failure (Fig. 3.14)

Let  $\bar{w}_1, \bar{w}_2$  and  $\bar{w}_3$  represent unit vectors normal to planes 1, 2 and 3 respectively, directed towards the inside of the rock volume. The resultant force  $\bar{R}$  lifts the tetrahedron from all three contact faces if all the three following equations are satisfied simultaneously

$$\bar{R} \cdot \bar{w}_1 > 0 \quad (3.69)$$

$$\bar{R} \cdot \bar{w}_2 > 0 \quad (3.70)$$

$$\bar{R} \cdot \bar{w}_3 > 0 \quad (3.71)$$

In such a case equilibrium is not possible unless the joints can take tension or rock bolts are provided to resist the tensile forces across the faces.

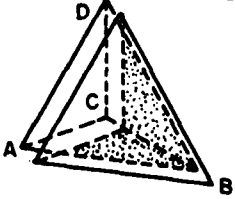
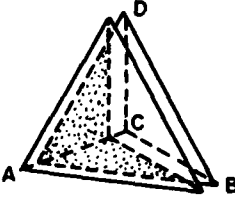
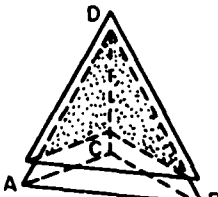
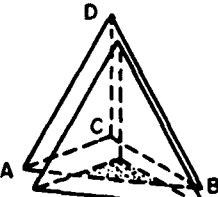
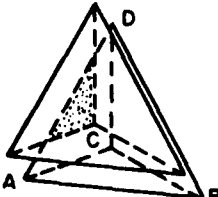
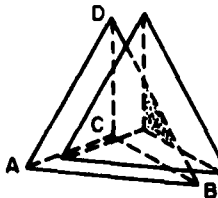
NATURE OF SLIDING	CONTACT FACES	OPEN FACES	DIAGRAM
Direction CB	2 and 3	1	
Direction CA	3 and 1	2	
Direction CD	1 and 2	3	
In Plane 3. Direction Between CB and CA	3	1 and 2	
in Plane 1 Direction Between CA and CB	1	2 and 3	
In Plane 2 Direction Between CD and CB	2	3 and 1	

FIG. 3.13 MODES OF SLIDING FAILURE OF A ROCK WEDGE BOUNDED BY THREE INTERSECTING JOINT SETS

If Eqs. 3.69 through 3.71 show that lifting off of the wedge from the support planes does not occur, then further kinematic tests must be made to determine the mode of sliding failure.

The vectors  $\bar{x}_{12}$ ,  $\bar{x}_{23}$  and  $\bar{x}_{31}$  along the lines of intersection CD, CB and CA are given by the following equations:

$$\bar{x}_{12} = \bar{w}_2 \times \bar{w}_1 \quad (3.72)$$

$$\bar{x}_{23} = \bar{w}_3 \times \bar{w}_2 \quad (3.73)$$

$$\bar{x}_{31} = \bar{w}_1 \times \bar{w}_3 \quad (3.74)$$

Let us now define two new vectors,  ${}_1\bar{s}_{12}$  and  ${}_2\bar{s}_{12}$  orthogonal to  $\bar{x}_{12}$  and lying in planes 1 and 2 respectively as follows:

$${}_1\bar{s}_{12} = \bar{x}_{12} \times \bar{w}_1 \quad (3.75)$$

$${}_2\bar{s}_{12} = \bar{w}_2 \times \bar{x}_{12} \quad (3.76)$$

Similarly the vectors  ${}_2\bar{s}_{23}$  and  ${}_3\bar{s}_{23}$  normal to  $\bar{x}_{23}$  and lying in planes 2 and 3 respectively are given by

$${}_2\bar{s}_{23} = \bar{x}_{23} \times \bar{w}_2 \quad (3.77)$$

$${}_3\bar{s}_{23} = \bar{w}_3 \times \bar{x}_{23} \quad (3.78)$$

The vectors  ${}_1\bar{s}_{31}$  and  ${}_3\bar{s}_{31}$  normal to  $\bar{x}_{31}$  and lying in planes 1 and 3 respectively are similarly given by

$${}_3\bar{s}_{31} = \bar{x}_{31} \times \bar{w}_3 \quad (3.79)$$

$${}_1\bar{s}_{31} = \bar{w}_1 \times \bar{x}_{31} \quad (3.80)$$

The orientations of all the vectors defined by Eqs. 3.72 through 3.80 are shown in Fig. 3.14.

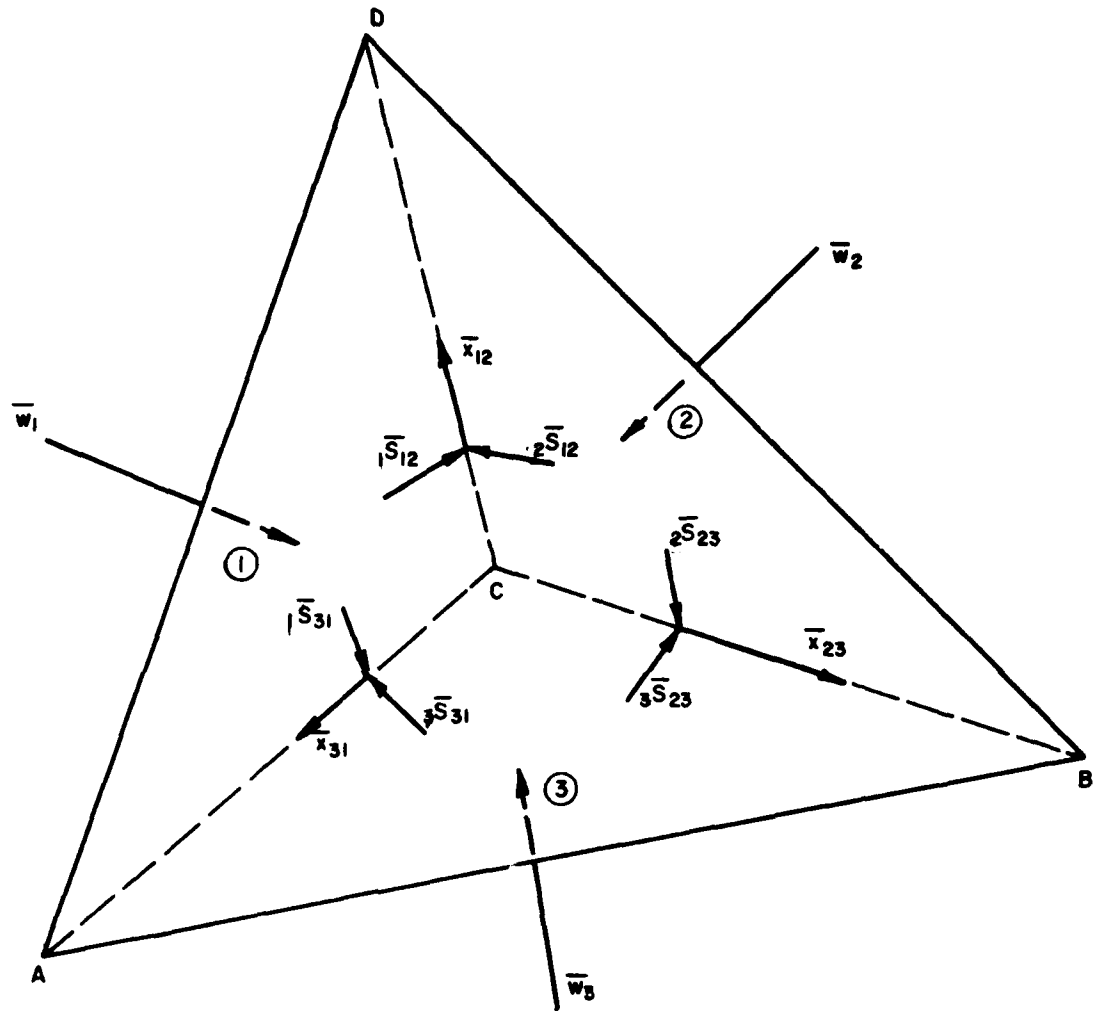


FIG. 3.14 STABILITY OF A ROCK WEDGE BOUNDED BY THREE INTERSECTING JOINT PLANES

If sliding is to occur along the line of intersection  $\bar{x}_{12}$ , the resultant  $\bar{R}$  of the applied forces must have a component along  $\bar{x}_{12}$  which tends to open up plane 3. This condition can be represented vectorially by the equation

$$\bar{R} \cdot \bar{x}_{12} \geq 0 \quad (3.81)$$

In addition the components of  $\bar{R}$  on plane 1 and 2 along vectors  ${}_1\bar{s}_{12}$  and  ${}_2\bar{s}_{12}$  must be directed towards the line of intersection  $\bar{x}_{12}$ . In other words,

$$\bar{R} \cdot {}_1\bar{s}_{12} \geq 0 \quad (3.82)$$

$$\bar{R} \cdot {}_2\bar{s}_{12} \geq 0 \quad (3.83)$$

Eqs. 3.81 through 3.83 must be satisfied simultaneously if the rock wedge ABCD is to slide along  $\bar{x}_{12}$  with face 3 open. The conditions to be satisfied for sliding to occur along  $\bar{x}_{23}$  and  $\bar{x}_{31}$  can be obtained in a similar manner.

They are:

$$\text{For sliding along } \bar{x}_{23}, \bar{R} \cdot \bar{x}_{23} \geq 0 \quad (3.84)$$

$$\bar{R} \cdot {}_2\bar{s}_{23} \geq 0 \quad (3.85)$$

$$\bar{R} \cdot {}_3\bar{s}_{23} \geq 0 \quad (3.86)$$

$$\text{For sliding along } \bar{x}_{31}, \bar{R} \cdot \bar{x}_{31} \geq 0 \quad (3.87)$$

$$\bar{R} \cdot {}_1\bar{s}_{31} \geq 0 \quad (3.88)$$

$$\bar{R} \cdot {}_3\bar{s}_{31} \geq 0 \quad (3.89)$$

If sliding is to occur on any one plane only, say on plane 1, then  $\bar{R}$  must have a component normal to plane 1 directed towards the outside of the rock wedge ABCD. In other words

$$\bar{R} \cdot \bar{w}_1 \leq 0 \quad (3.90)$$



In addition the components of  $\bar{R}$  on plane 1 along  ${}_1\bar{S}_{12}$  and  ${}_1\bar{S}_{31}$  must be directed away from  $\bar{x}_{12}$  and  $\bar{x}_{31}$ . In other words

$$\bar{R} \cdot {}_1\bar{S}_{12} \leq 0 \quad (3.91)$$

$$\bar{R} \cdot {}_1\bar{S}_{31} \leq 0 \quad (3.92)$$

The corresponding equations for cases of sliding on planes 2 and 3 are as follows.

For sliding on plane 2 only:

$$\bar{R} \cdot \bar{w}_2 \leq 0 \quad (3.93)$$

$$\bar{R} \cdot {}_2\bar{S}_{12} \leq 0 \quad (3.94)$$

$$\bar{R} \cdot {}_2\bar{S}_{23} \leq 0 \quad (3.95)$$

For sliding on plane 3 only:

$$\bar{R} \cdot \bar{w}_3 \leq 0 \quad (3.96)$$

$$\bar{R} \cdot {}_3\bar{S}_{23} \leq 0 \quad (3.97)$$

$$\bar{R} \cdot {}_3\bar{S}_{31} \leq 0 \quad (3.98)$$

### 3.6.2 Calculation of the Factor of Safety for Sliding

After deciding on the mode of sliding failure based on the kinematic tests mentioned above, the next step is to estimate the factor of safety against sliding under the given conditions. The procedure for estimating the factor of safety is basically the same as that explained in Section 3.4.1.3 of this chapter for the case of a rock wedge bounded by two joint planes. Three example problems have been added to illustrate the method of analysis.

In the preceding analysis, of Section 3.6.1, however, it has been tacitly assumed that the critical rock wedge is bounded by all the three joint planes and the exterior slope face as shown in Fig. 3.12. When the field conditions

are such that this assumption is valid, the method of stability analysis presented above is directly applicable. But in a majority of cases, it is likely that the critical rock wedge is bounded by two (rather than by all the three) joint planes. Under these conditions the stability analysis has to be performed as explained in Section 3.4.1.3.

### 3.6.3 Example Problems for Slopes with Three Intersecting Planes of Discontinuity Worked by Vector Analysis

#### Problem 1

Determine the factor of safety against sliding of the rock wedge ABCD shown in Fig. 3.12. Also estimate the direction and magnitude of the minimum dynamic resistance  $\bar{N}$  which is necessary to just make the potential block ABCD slide.

$$\bar{w}_1 = (0.00, 0.72, 0.69)$$

$$\bar{w}_2 = (0.63, -0.12, 0.77)$$

$$\bar{w}_3 = (0.00, 0.00, 1.00)$$

$$\bar{W} = (0, 0, -36.5 \text{ tons}) \quad \bar{Q} = (0, 0, 0)$$

$$U_1 = 23.6 \text{ tons} \quad U_2 = 8.0 \text{ tons} \quad U_3 = 5.7 \text{ tons}$$

$$\phi_1 = 40^\circ \quad \phi_2 = 40^\circ \quad \phi_3 = 40^\circ$$

#### Solution

$$\bar{R} = \bar{W} + \bar{Q} + \bar{U}_1 + \bar{U}_2 + \bar{U}_3 \quad (3.68)$$

$$= \bar{W} + \bar{Q} + U_1 \bar{w}_1 + U_2 \bar{w}_2 + U_3 \bar{w}_3$$

$$= (5.05, 16.04, -8.34) \quad \text{all in ton-units}$$

$$R = 18.8 \text{ tons}$$

$$\bar{x}_{12} = (-0.638, -0.435, 0.454) \quad (3.72)$$

$$x_{12} = 0.895$$

$$\bar{x}_{23} = (0.120, 0.630, 0) \quad (3.73)$$

$$x_{23} = 0.640$$

$$\bar{x}_{31} = (0.720, 0, 0) \quad (3.74)$$

$$x_{31} = 0.720$$

$${}_1\bar{s}_{12} = (-0.626, 0.440, -0.459) \quad (3.75)$$

$${}_2\bar{s}_{12} = (0.280, -0.777, -0.351) \quad (3.76)$$

$${}_2\bar{s}_{23} = (0.485, -0.093, -0.410) \quad (3.77)$$

$${}_3\bar{s}_{23} = (-0.630, 0.120, 0) \quad (3.78)$$

$${}_3\bar{s}_{31} = (0, -0.720, 0) \quad (3.79)$$

$$\bar{s}_{131} = (0, 0.497, -0.518) \quad (3.80)$$

$$\bar{R} \cdot \bar{w}_3 = -8.34 < 0 \quad (3.96)$$

Thus plane 3 is closed and a failure by lifting from the base planes does not occur.

$$\bar{R} \cdot {}_3\bar{s}_{23} = -1.25 < 0 \quad (3.97)$$

$$\bar{R} \cdot {}_3\bar{s}_{31} = -11.55 < 0 \quad (3.98)$$

Eqs. 3.96 through 3.98 thus indicate that sliding can occur only on plane 3.

$$N_3 = \bar{R} \cdot (-\bar{w}_3) = 8.34 \text{ tons}$$

$$\bar{N}_3 = N_3(-\bar{w}_3) = (0, 0, -8.34)$$

$$\bar{T}_3 = \bar{R} - \bar{N}_3 = (5.05, 16.04, 0)$$

$$T_3 = 16.8 \text{ tons}$$

$$\text{F.S.} = \frac{N_3 \tan \phi_3}{T_3} = \frac{8.34 \tan 40^\circ}{16.8}$$

$$= 0.42$$

Problem 2

Work out Problem 1 with the following changes:

$$U_1 = 12.0 \text{ tons} \quad U_2 = 2.0 \text{ tons} \quad U_3 = 2.0 \text{ tons}$$

Solution

$$\bar{R} = \bar{W} + \bar{Q} + \bar{U}_1 + \bar{U}_2 + \bar{U}_3 \quad (3.68)$$

$$= \bar{W} + \bar{Q} + U_1 \bar{w}_1 + U_2 \bar{w}_2 + U_3 \bar{w}_3$$

$$= (1.26, 8.40, -24.68)$$

$$\bar{R} \cdot \bar{w}_3 = -24.68 < 0 \quad (3.71)$$

and therefore lifting off of the rock wedge from all the base planes is not possible.

$$\bar{R} \cdot \bar{x}_{23} = 5.45 > 0 \quad (3.84)$$

$$\bar{R} \cdot {}_2\bar{s}_{23} = 9.94 > 0 \quad (3.85)$$

$$\bar{R} \cdot {}_2\bar{s}_{23} = 0.22 > 0 \quad (3.86)$$

The above equations show that sliding can occur only along the line of intersection  $\bar{x}_{23}$ .

$$T_{23} = \bar{R} \cdot \bar{x}_{23} / x_{23} = 8.50 \text{ tons}$$

$$\bar{T}_{23} = T_{23} \cdot \frac{\bar{x}_{23}}{x_{23}} = (1.60, 8.35, 0)$$

$$\bar{N}_{23} = \bar{R} - \bar{T}_{23} = (-0.34, -.05, -24.68)$$

$$= N_2(-\bar{w}_2) + N_3(-\bar{w}_3)$$

$$= N_2(-0.63, 0.12, -0.77) +$$

$$N_3(0, 0, -1.00)$$

Solving  $N_2 = 0.54$  tons     $N_3 = 24.26$  tons

$$\begin{aligned} \text{F.S.} &= \frac{0.54 \tan 40^\circ + 24.26 \tan 40^\circ}{8.50} \\ &= 2.44 \end{aligned}$$

### Problem 3

A rock cut slope runs East-West and the three major joint sets intersecting the slope have the following orientations:

<u>Joint Plane</u>	<u>Strike</u>	<u>Dip</u>
1	N47°E	44°SE
2	N20°W	83°SW
3	N69°W	16°SW

The angle of shearing resistance on all the three joint planes is estimated to be  $20^\circ$ . Determine the factor of safety of the slope against a sliding failure.

### Solution

Consider the positive x direction to be East, the positive y direction to be North and the positive z direction to be upwards. Then the three joint planes have the following strike and dip angles.

Plane 1	$\beta_1 = 47^\circ$	$\gamma_1 = 44^\circ$
Plane 2	$\beta_2 = 110^\circ$	$\gamma_2 = 97^\circ$
Plane 3	$\beta_3 = 159^\circ$	$\gamma_3 = 164^\circ$

The unit normals to planes 1, 2 and 3 can be defined by Eqs. 2.13, 2.14 and 2.15. When these normals are oriented such that they are directed toward the interior of the rock wedge they are defined by the following equations:

$$\bar{w}_1 = (0.474, -0.508, 0.719)$$

$$\bar{w}_2 = (-0.933, -0.339, 0.122)$$

$$\bar{w}_3 = (-0.099, -0.257, 0.961)$$

$$\bar{x}_{12} = (-0.182, 0.729, 0.635) \quad (3.72)$$

$$x_{12} = 0.983$$

$$\bar{x}_{23} = (0.295, -0.885, -0.206) \quad (3.73)$$

$$x_{23} = 0.955$$

$$\bar{x}_{31} = (-0.303, -0.526, -0.172) \quad (3.74)$$

$$x_{31} = 0.631$$

$${}_1\bar{s}_{12} = (0.847, 0.432, -0.253) \quad (3.75)$$

$${}_2\bar{s}_{12} = (-0.304, 0.570, -0.741) \quad (3.76)$$

$${}_2\bar{s}_{23} = (-0.178, -0.157, -0.925) \quad (3.77)$$

$${}_3\bar{s}_{23} = (0.903, 0.263, 0.163) \quad (3.78)$$

$${}_3\bar{s}_{31} = (-0.550, 0.309, 0.026) \quad (3.79)$$

$${}_1\bar{s}_{31} = (0.466, -0.137, -0.403) \quad (3.80)$$

$$\bar{R} = (0, 0, -W)$$

$$\bar{R} \cdot \bar{w}_1 = -0.719W < 0$$

$$\bar{R} \cdot \bar{w}_2 = -0.122W < 0$$

$$\bar{R} \cdot \bar{w}_3 = -0.961W < 0$$

Therefore failure by lifting off of all the base planes is not possible as shown by comparison of the above three equations with Eqs. 3.69, 3.70, 3.71. It can easily be verified that all kinematic tests are satisfied only for sliding on plane 3. In other words

$$\bar{R} \cdot \bar{w}_3 = -0.961W < 0 \quad (3.96)$$

$$\bar{R} \cdot {}_3\bar{S}_{23} = -0.163W < 0 \quad (3.97)$$

$$\bar{R} \cdot {}_3\bar{S}_{31} = -0.026W < 0 \quad (3.98)$$

$$N_3 = \bar{R} \cdot (-\bar{w}_3) = 0.961 W$$

$$\bar{N}_3 = N_3(-\bar{w}_3) = (0.095W, 0.247W, -0.924W)$$

$$\bar{T}_3 = \bar{R} - \bar{N}_3 = (-0.095W, -0.247W, -0.076W)$$

$$T_3 = 0.275W$$

$$F.S. = \frac{0.961W \tan 20^\circ}{0.275W} = 1.27$$

The preceding calculations have been carried out under the assumption that the critical rock wedges bounded by all the three joint planes. As has been pointed out earlier, in a majority of cases, there exists a rock wedge, bounded by only two joint planes, which is more critical than the one considered in the preceding analysis. As a matter of fact, in the present problem, the rock wedge bounded by planes 1 and 2 has a lower factor of safety with respect to sliding. The determination of the mode of failure and the factor of safety against sliding can be done as explained in section 3.4.1.3. The details of this analysis will not be given here except the fact that the sliding tends to occur down the line of intersection of planes 1 and 2 and that the factor of safety is 0.58 as compared to the previous value of 1.27.

### 3.7 Computer Techniques

The stability of rock slopes bounded by two or three joint sets can also be analyzed using digital computer techniques. This method avoids lengthy hand-calculations and is particularly useful when there is a need for solving a whole series of stability problems.

The basis of the procedure is the same as explained in the previous sub-sections. The essential steps in this procedure are as follows (see flow chart, Fig. 3.15):

1. Using the input data calculate all the required directional vector quantities.
2. Check to see if failure by lifting off the base planes of the rock wedge is possible.
3. If not, determine the probably mode of sliding failure.
4. Calculate the factor of safety for this mode of sliding failure.
5. Check for stability against the possible mode of rotation.
6. Print the results.

A documentation and listing of the computer programs using Fortran IV language is given in Appendix A.



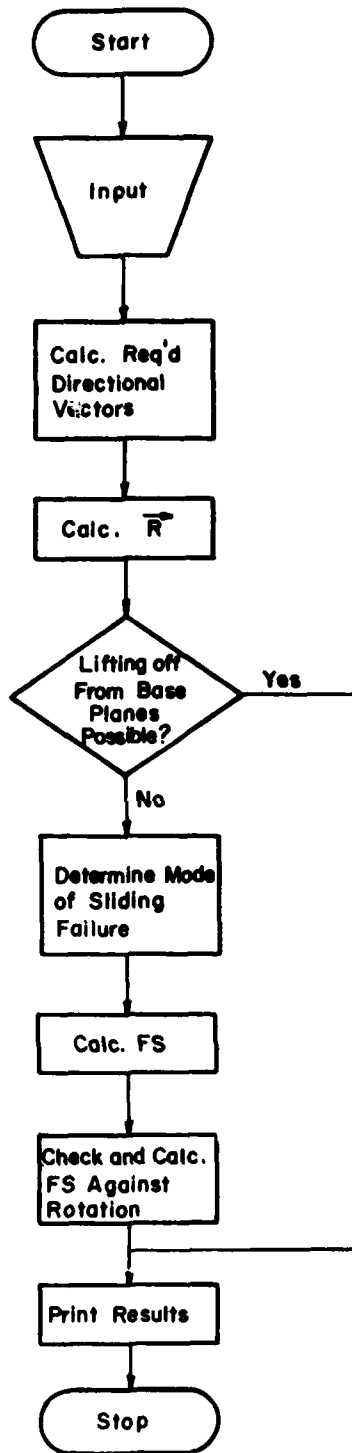


FIG. 3.15 FLOW CHART

## Chapter Four

### GRAPHICAL SLOPE STABILITY ANALYSIS BY USE OF STERONETS

#### 4.1 Properties of Spherical Projections

##### 4.1.1 General

The orientation (strike and dip) of planes or lines in space can be represented by the intersection of the plane or line with the surface of a reference sphere through whose center the plane or line passes. As can be seen in Figure 4.1, the intersection of a plane with the sphere is a great circle, while a line which parallels the plane will plot as two points, 180 degrees apart, on the great circle. A plane can also be represented by the intersection of its normal with the sphere (the pole of the plane), which will plot as a point located 90 degrees from the great circle, in both the upper and lower hemispheres of the sphere.

To communicate this information, a two-dimensional representation of the spherical projection is necessary. Several types of projection can be used to transfer great circles and points from the spherical surface to the equatorial plane of the sphere.

The equal angle projection (termed a Wulff net or stereonet) is the method used in this report because of the simplicity in plotting the projections. Each great circle on the sphere plots as an arc of a circle on the equatorial plane of the sphere.

Another type of projection, the equal area projection, is used for compiling statistical information on the frequency and orientation of lines or planes. It therefore should be used to plot and evaluate the

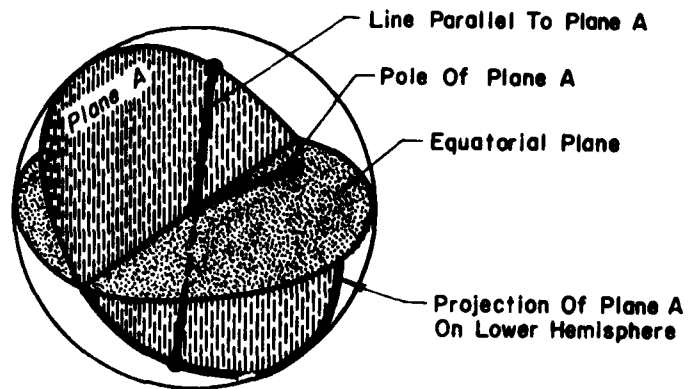


**FIG. 4.1 PROJECTION OF PLANE AND LINES ON A SPHERE**

raw data from field and borehole mapping of joints and other geologic discontinuities. The equal area projection of great circles from the sphere to the equatorial plane results in a distortion from the circular arc, and therefore is not quite as simple to use for stability analyses as the equal angle projection.

#### 4.1.2 Equal Angle Projections

Figures 4.2 and 4.3 show the lower hemisphere, equal angle method for projecting a point from the surface of the sphere to equatorial plane.

A line is drawn from point P on the sphere to the upper pole, U, of the equatorial plane (dashed line in Fig. 4.2 and 4.3). The intersection of this line with the equatorial plane (P') is the desired projection of point P. In Figure 4.2, the projection of plane A and point P from the lower hemisphere to the equatorial plane is shown; the projection of plane A plots as an arc of a circle (or line of meridian) on the equatorial plane.

The projection of a vertical plane will project as a straight line through the origin of the equatorial plane. A horizontal plane will project as a line of meridian having a radius equal to the radius of the sphere, with the same origin. All points projected from the lower hemisphere will plot within this circle on the equatorial plane. Points from the upper hemisphere projected on the equatorial plane will plot outside the radius of the sphere, as can be seen for the projection, Q', of point Q in Figure 4.3.

A diagram of the stereonet obtained from an equal angle, lower hemisphere projection is shown in Fig. 4.4. The lines of meridian

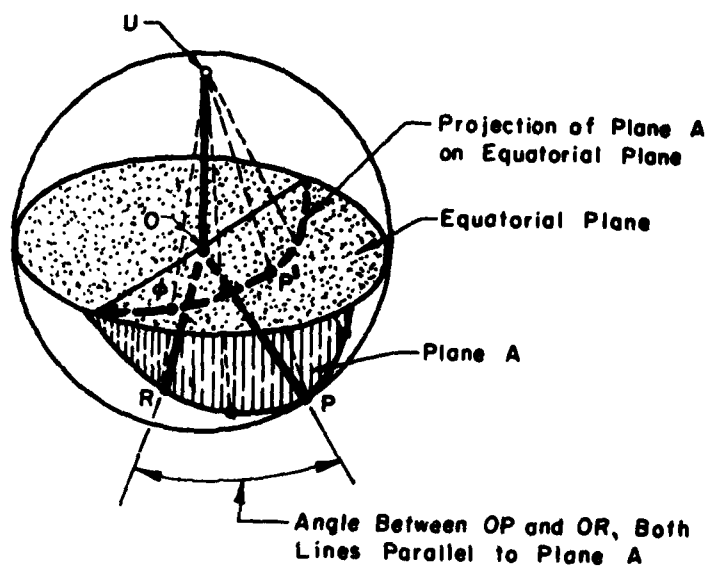


**FIG. 4.2 EQUAL ANGLE PROJECTION FROM LOWER HEMISPHERE TO EQUATORIAL PLANE OF THE SPHERE**

$Q'$  is a Projection of Point  $Q$  ( $Q$  is Above the Equatorial Plane)  $P'$  is a Projection of Point  $P$  ( $P$  is Below the Equatorial Plane)

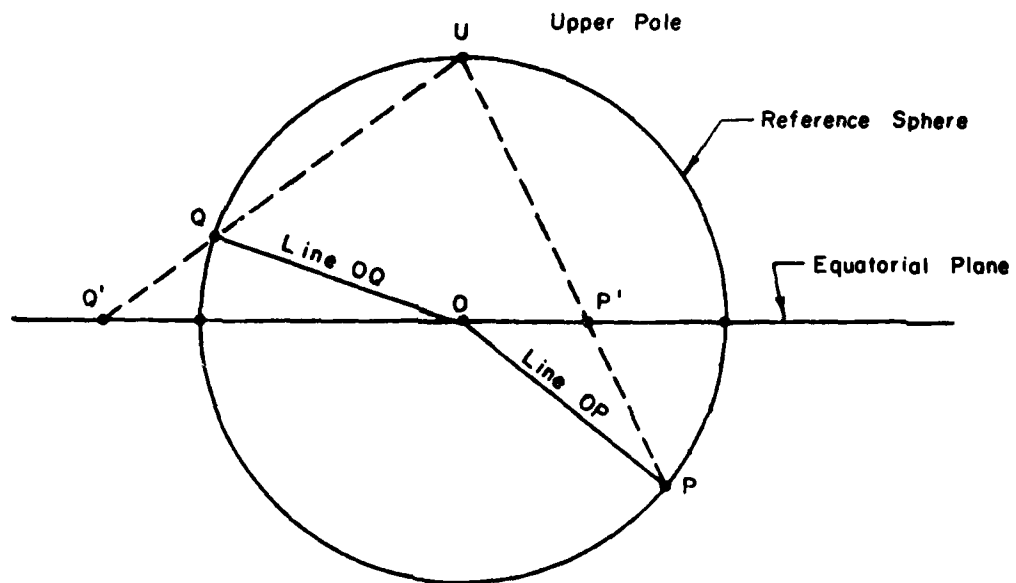


**FIG. 4.3 PROFILE OF SPHERE SHOWING METHOD OF EQUAL ANGLE, LOWER HEMISPHERE PROJECTION**

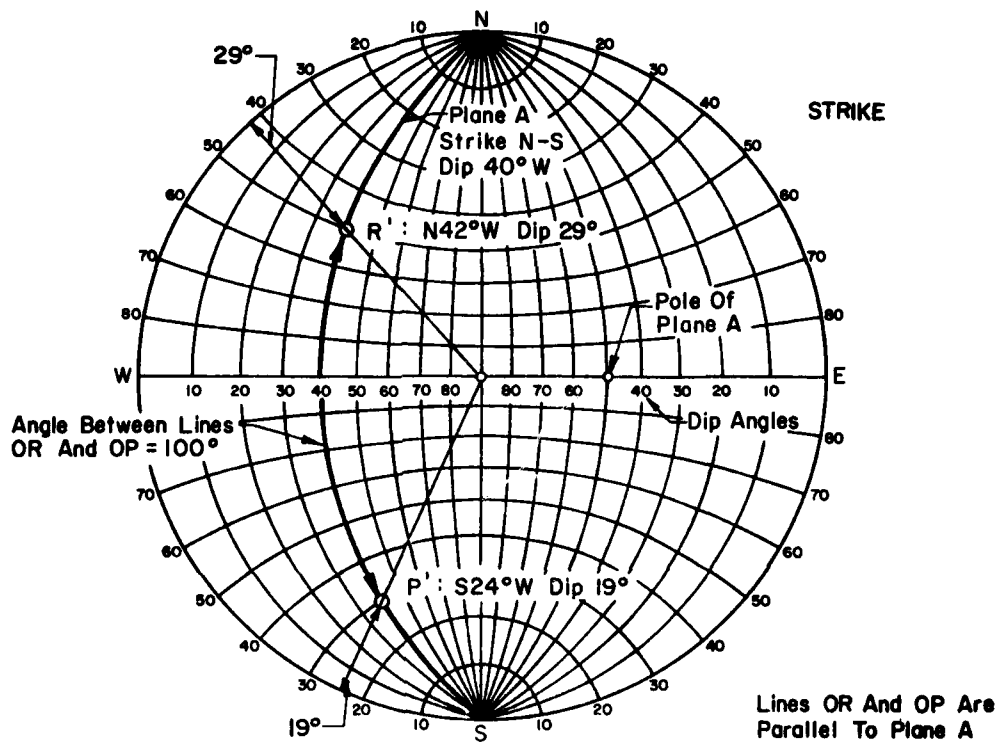


FIG. 4.4 STERONET (WULFF NET) (EQUAL ANGLE PROJECTION)

through the N and S poles of this diagram represent great circles resulting from the intersection of N-S striking planes with the reference sphere. Dip angles for these planes are shown on the E-W axis of the stereonet. The meridians for steeply dipping planes will approach straight lines on this plot, while the meridians for flat-lying planes will plot as arcs of circles having radii approaching the radius of the reference sphere. Each of the meridians is divided into 180 degrees by E-W lines of latitude, which plot as arcs of circles on the equal angle stereonet. To represent a plane which strikes other than N-S, the stereonet of Fig. 4.4 must be rotated so that its N-S axis is aligned in the direction of the strike of the given plane. The meridian can then be traced from the stereonet so that it is oriented in its proper strike direction. Note that the true dip of a plane or line should be determined by orienting the E-W axis of the stereonet so that it is in the direction of the dip of the line or plane.

Stereonets similar to that shown in Fig. 4.4 are available from graphic aid suppliers. It is suggested that such a stereonet be used for the example problems of this report by overlaying clear vellum on the stereonet and rotating the stereonet about its center, beneath the sheet of vellum, to plot planes and lines of various strikes and dips.

In Figure 4.4 the great circle projection of Plane A (dipping  $40^{\circ}$  west and striking N-S) plots as a line of meridian. The pole (or normal) of plane A is located  $90^{\circ}$  from the plane. Lines parallel to plane A plot as points on this line of meridian. The angle between two such lines, OP and OR is  $100^{\circ}$  and is found by counting the lines of latitude along the meridian, between points R' and P'.

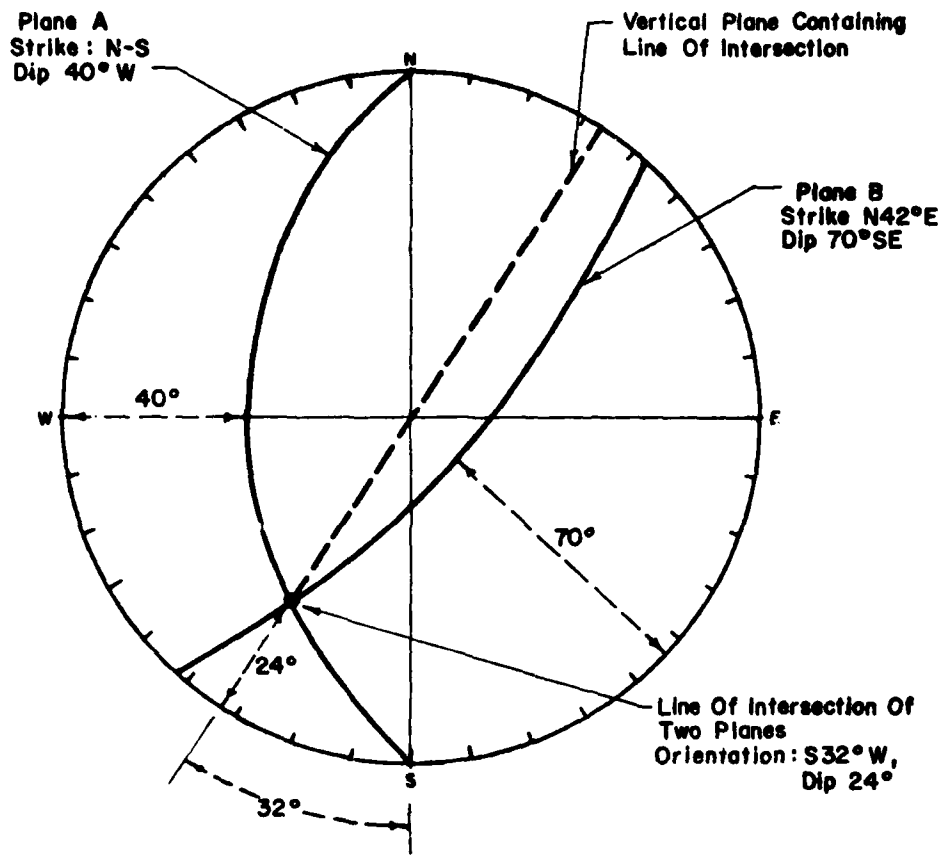


Figure 4.5 shows the projection of two planes on the stereonet, one striking N-S, the other N 42° E. The orientation of the line of intersection of the two planes is determined from the point of intersection of the two meridians. In this case the line of intersection dips at an angle 24° in a direction of S 32° W. All of this information can be determined by using the stereonet, rotating it as required to plot lines of meridian and read angles. The dip angle is read by rotating the stereonet until either the NS or EW axis coincides with the direction of dip. The dip angle is then read in degrees from the outer edge of the stereonet.

#### 4.2 Use of Stereonet to Evaluate Driving and Resisting Forces on a Potential Sliding Wedge of Rock

The use of the stereonet in stability analyses has been described by John (1968), Goodman (1964). The stereonet can be used to evaluate the stability of a three-dimensional wedge of rock resting on planes having frictional resistances. The method is very similar to the two-dimensional graphical force polygon used to sum forces. However, only the orientation (and not the magnitude) of forces is determined directly from the stereonet. If the resultant driving force acts at an angle further from the normal to the potential failure planes than the angle of the maximum resisting reaction on the planes, then sliding will occur. Note that the location of the forces and reactions is not known, and a summation of moments is not carried out.

The stability analysis is divided into two distinct parts. In the first part the orientation of the maximum resisting reaction on the potential failure planes is plotted on the stereonet. (For sliding on a



**FIG. 4.5 DETERMINATION OF LINE OF INTERSECTION OF TWO PLANES**

single plane, the maximum reaction would be oriented at  $\phi$  degrees to the normal of the plane.) Zones of stability and instability can thus be outlined on the stereonet, strictly by considering the orientation of the reactions on the potential sliding planes.

The second part involves determination of the orientation of the resultant driving force acting on the wedge. This force may include the weight of the wedge as well as acceleration forces, uplift water pressures on the planes of failure, and driving forces on the wedge from structures such as dam abutments. Graphical addition of vectors is used in conjunction with the stereonet to determine the orientation of the resultant vector force. If the orientation of the resultant driving force falls within the zone of stability on the stereogram, then the wedge is stable; if the orientation of the resultant driving force lies outside the stable zone, then the wedge is unstable.

Not only is the stereonet method of evaluating the stability of a wedge simple and rapid, it also possesses the advantage that a variety of forces required to cause failure or, conversely, to ensure stability can be clearly visualized, without resorting to extensive computations.

#### 4.3 Sliding on a Single Frictional Plane

The simple case of sliding on a single plane is described, to illustrate the use of the stereonet in stability analysis. Of course, a true two-dimensional problem (where the resultant driving vector force,  $\bar{R}$ , acts in the direction of the dip) is more simply solved using a conventional two-dimensional force polygon. However, for cases where the driving vector is not in the direction of the dip (such as might occur when an abutment load acts on a wedge), the stereographic method can

be used to solve problems which cannot be readily solved using a two-dimensional force polygon.

#### 4.3.1 Orientation of reaction force on the plane of failure

The reaction force at failure,  $\bar{R}_L$  (summation of the normal force,  $\bar{N}$ , and maximum shear force,  $\bar{S}$ ) is oriented at the angle of friction  $\phi$ , from the normal to the plane. Should the tendency for sliding be down-dip, then  $\bar{S}$  acts upslope and  $\bar{R}_L$  is as shown in Fig. 4.6a. A friction cone can be drawn to show the possible orientations of  $\bar{R}_L$  for sliding in other directions. The sides of the cone are oriented at  $\phi$  degrees to the normal, as shown in Fig. 4.6a and b. As long as the resultant driving vector,  $\bar{R}$ , acts at an angle less than  $\phi$  degrees to the normal, then sliding will not occur in any direction. When  $\bar{R} = \bar{R}_L$ , sliding is initiated.

A friction cone will plot as a circle on an equal angle stereonet, as shown in Fig. 4.6c. The position of the normal force is first located on the stereonet. (The position of the normal force is located at the pole of the plane.) The friction circle can then be drawn by marking off 40 degree angles from  $\bar{N}$ , on great circles passing through  $\bar{N}$ . (Note that  $\bar{N}$  is not in the center of the circle formed by the friction cone.)

#### 4.3.2 Stability of wedge of weight $\bar{W}$ with uplift force, $\bar{U}$ , acting on the failure plane

It is immediately apparent that a wedge of weight  $\bar{W}$  will not slide on the plane of failure because  $\phi$  is 40 degrees and exceeds the slope angle of 30 degrees. This is also apparent from Fig. 4.6c, where the weight vector,  $\bar{W}$ , falls within the friction cone.

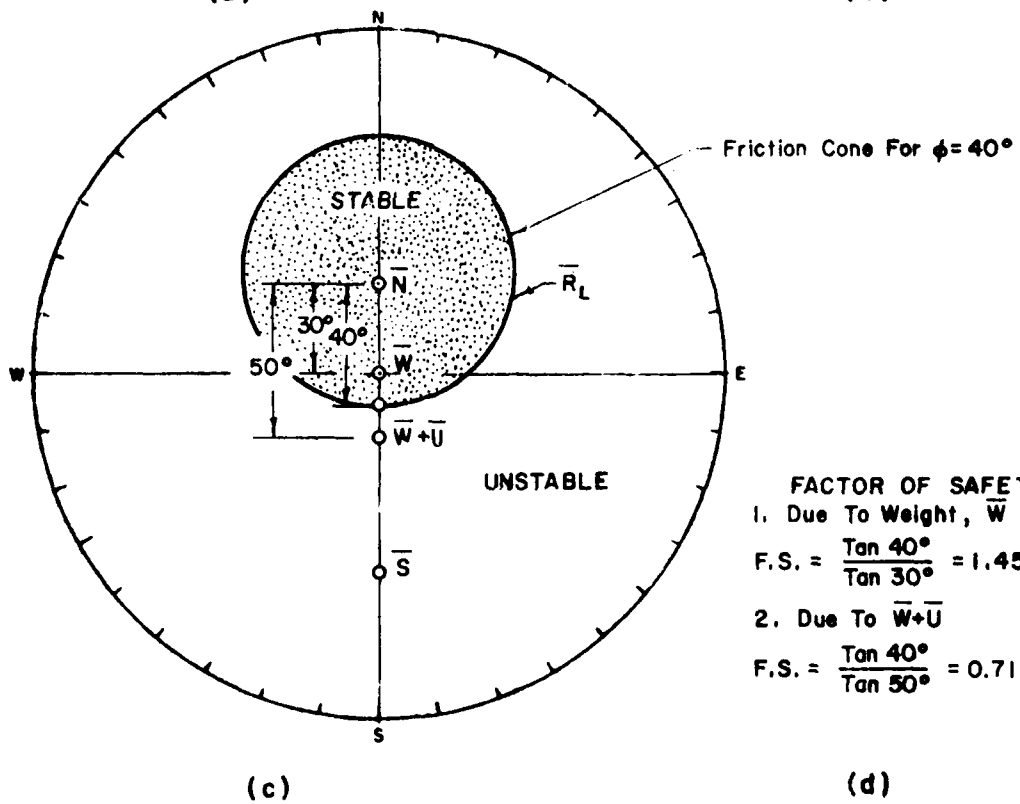
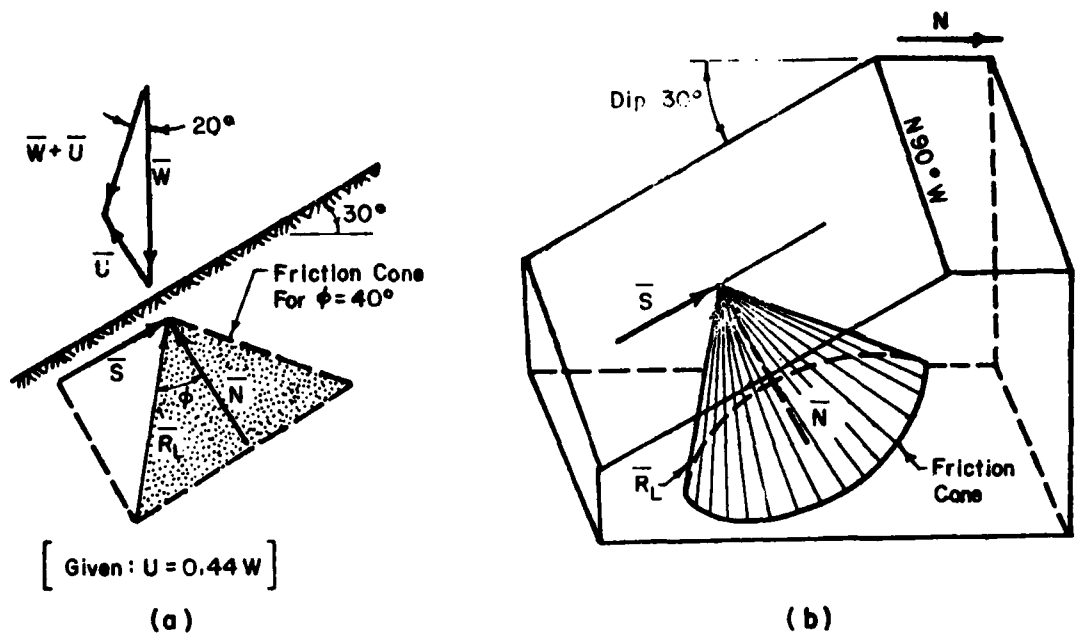


FIG. 4.6 SLIDING ON A SINGLE PLANE

If a porewater pressure were acting on the plane of failure, the stability of the wedge would be reduced. The porewater vector force,  $\bar{U}$ , acts normal to the plane of failure, as shown in Fig. 4.6a. The resultant driving vector,  $\bar{R} = \bar{W} + \bar{U}$ , can be determined by drawing the two vectors to scale (see Fig. 4.6a) and determining the angle of the resultant. In this case, the magnitude of  $U$  is given as  $0.44 W$  and therefore the angle of  $\bar{R}$  from the vertical is found to be 20 degrees.  $\bar{R}$  is thus located  $10^\circ$  outside the friction circle, in the unstable zone.

The factor of safety for the two cases, with and without the uplift force acting, is shown in Fig. 4.6d. The tangent of the angle between the normal and the resultant driving force determines the denominator in each case.

#### 4.3.3 Graphical procedure for determining the direction of resultant vector force

The summation of a series of vectors cannot be performed using the stereographic projection alone, because there is no method for showing magnitudes of forces on the stereographic projection. However, the orientation of the resultant vector can be determined using the stereographic projection in combination with the graphical addition of vectors, two at a time. Three vectors,  $\bar{W}$  and  $\bar{U}$  of the preceding example and an additional vector  $\bar{A}$ , are illustrated in Fig. 4.7. The graphical addition of these vectors is performed as shown in Fig. 4.8. As described in the preceding example, vectors  $\bar{W}$  and  $\bar{U}$  are added graphically thus determining the orientation of  $\bar{W} + \bar{U}$ , which is found to be 20 degrees from the vertical (Fig. 4.8a). Vectors  $\bar{W} + \bar{U}$  and  $\bar{A}$  are then added, determining the orientation of  $\bar{W} + \bar{A}$ , 30 degrees from the vertical (Fig. 4.8b).

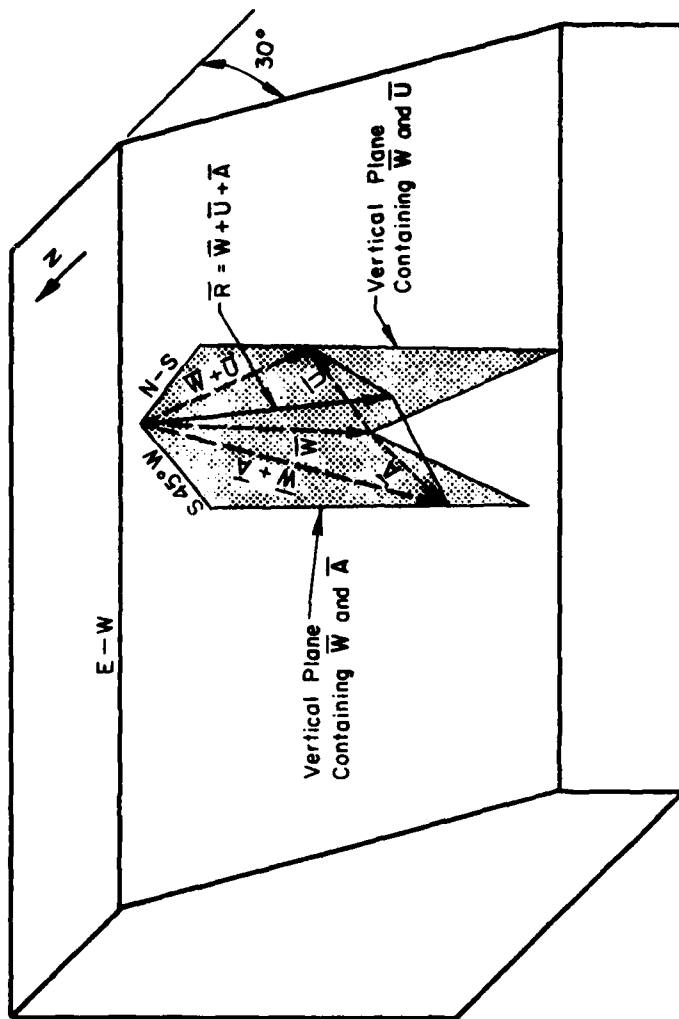
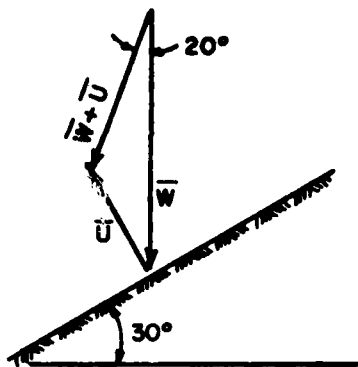
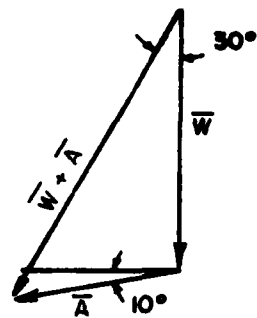


FIG. 4.7 GRAPHICAL SUMMATION OF 3 VECTORS

- GIVEN: 1. Weight of Wedge =  $\bar{W}$   
 2. Porewater Force,  $\bar{U}$ , Equal to  $0.44W$ , on  $30^\circ$  Plane  
 3. Force  $\bar{A}$ , Equal to  $0.6W$ , Acting  $S 45^\circ W$ , Dip  $10^\circ$



(a) Vertical Plane Oriented N-S Containing Vectors  $\bar{W}$  and  $\bar{U}$



(b) Vertical Plane Oriented  $S 45^\circ W$  Containing Vectors  $\bar{W}$  and  $\bar{A}$

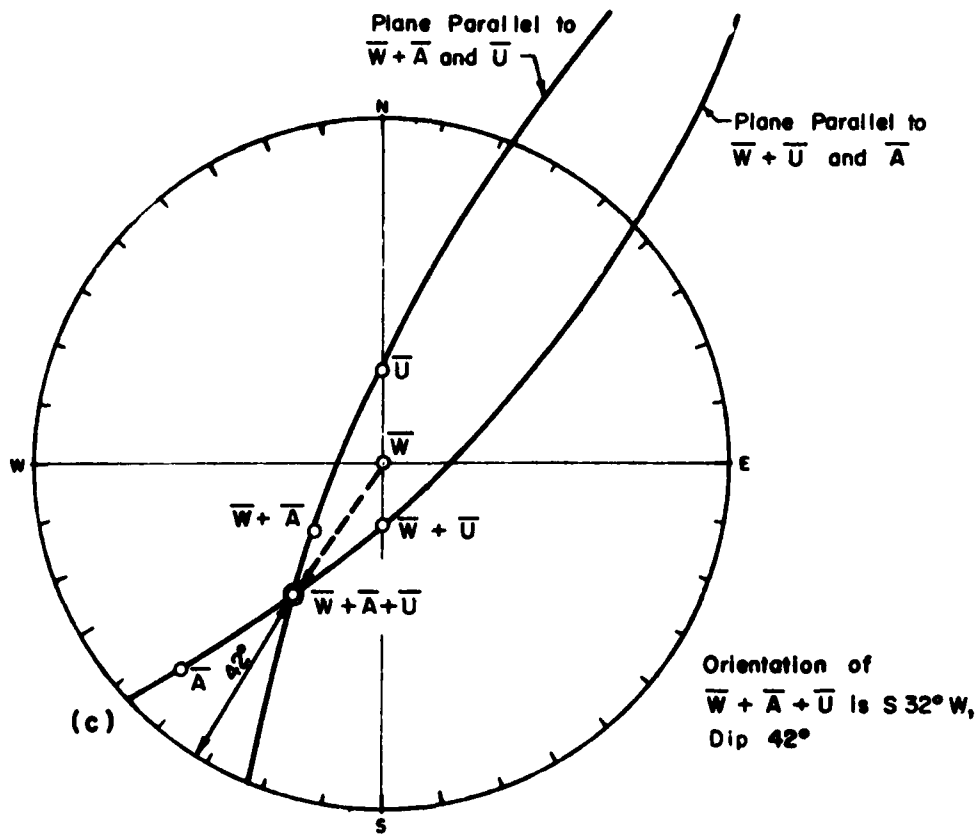


FIG. 4.8 GRAPHICAL DETERMINATION OF ORIENTATION OF RESULTANT VECTOR,  $\bar{W} + \bar{A} + \bar{U}$



The orientations of vectors  $\bar{W}$ ,  $\bar{U}$ ,  $\bar{A}$ ,  $\bar{W} + \bar{U}$ , and  $\bar{W} + \bar{A}$  are then plotted on the stereogram (Fig. 4.8c, solid arcs).

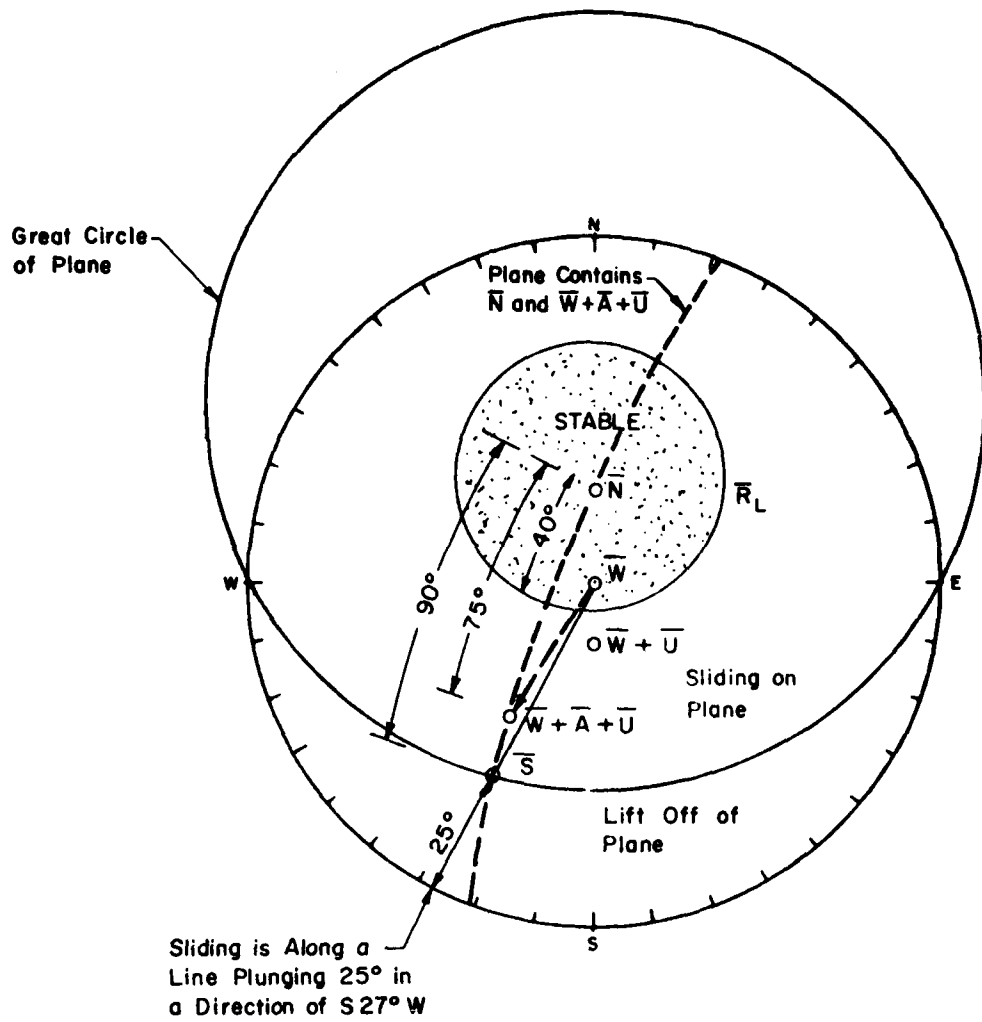
Once these vectors have been plotted, the orientation of the resultant vector,  $\bar{R} = \bar{W} + \bar{A} + \bar{U}$ , can be found using only the stereogram. This is accomplished by finding the line of intersection of two planes. One plane contains  $\bar{W} + \bar{A}$  and  $\bar{U}$ , the other contains  $\bar{W} + \bar{U}$  and  $\bar{A}$  (Fig. 4.7). The intersection of the two planes is the resultant vector,  $\bar{R} = \bar{W} + \bar{A} + \bar{U}$ . On the stereogram in Figure 4.8b, a great circle is drawn through  $\bar{W} + \bar{A}$  and  $\bar{U}$ , another great circle is drawn through  $\bar{W} + \bar{U}$  and  $\bar{A}$ . The two great circles intersect at  $\bar{R} = \bar{W} + \bar{U} + \bar{A}$ , which is thus determined as dipping 42 degrees from the horizontal in a direction of S 32° W.

#### 4.3.4 Determination of direction of movement and factor of safety for case of resultant driving vector, $\bar{W} + \bar{U} + \bar{A}$ , acting on the wedge

In Fig. 4.9 the resultant driving vector,  $\bar{R} = \bar{W} + \bar{U} + \bar{A}$  has been combined with the friction cone diagram.  $\bar{R} = \bar{W} + \bar{A} + \bar{U}$  lies outside of the friction cone, therefore sliding of the wedge will occur. The direction of sliding on the plane will be in the direction of the shear force, S. Sliding is along a line plunging 25° in a S 27° W direction (down an apparent dip slope). Note that this direction is not the same as the S 32° W direction of the resultant driving vector,  $\bar{R}$ .

The factor of safety is determined from the angular distances along this great circle. From  $\bar{N}$  to  $\bar{R}_L$ , the angle is 40 degrees, while from  $\bar{N}$  to  $\bar{R}$  the angle is 75 degrees. The factor of safety is therefore:

$$\frac{\tan 40^\circ}{\tan 75^\circ} = 0.22$$



$$F.S. = \frac{\tan 40^\circ}{\tan 75^\circ} = 0.22$$

FIG. 4.9 THREE VECTORS ON SINGLE PLANE

#### 4.3.5 Minimum force $\overline{NW}$ required to cause failure

The orientation of the minimum force,  $\overline{NW}$ , required to cause failure on an otherwise stable slope can be rapidly determined from the stereonet. To determine the magnitude of the minimum force, one auxiliary graphical construction is required (Fig. 4.10).

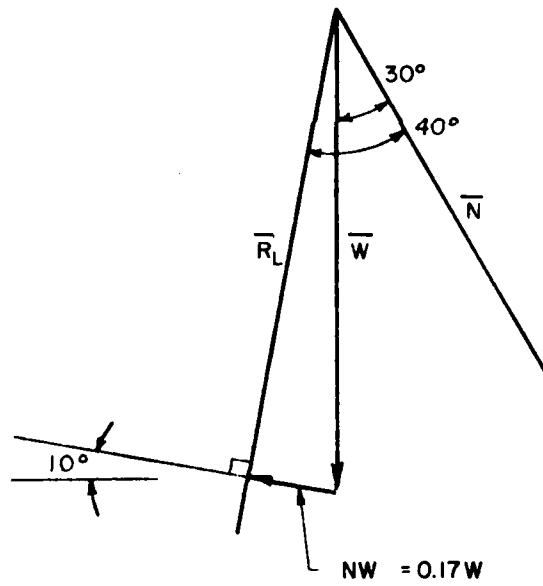
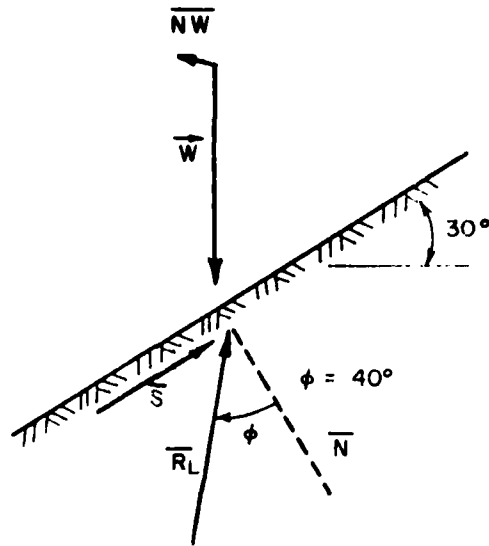
For the single  $30^\circ$  plane shown in Fig. 4.6, the wedge is stable under its own weight,  $\overline{W}$ . To reduce the factor of safety to unity, the angle between the weight,  $\overline{W}$ , and the limiting reaction,  $\overline{R}_L$  must be closed. The minimum angle is 10 degrees and will be obtained when the driving forces cause sliding directly down-dip (to the south). Any other direction of sliding will result in a larger angle between  $\overline{R}_L$  and  $\overline{W}$  and therefore a larger value for  $\overline{NW}$ .

The minimum force,  $\overline{NW}$  will therefore be directed to the south and will be directed upward 10 degrees so that it is normal to  $\overline{R}_L$  (Fig. 4.10). The minimum force will be almost horizontal for the case of frictional sliding on a wedge loaded only by its own weight, where the factor of safety is near unity.

#### 4.4 Sliding on Two Frictional Planes

##### 4.4.1 General

The possible modes of failure of a wedge on two planes can be rapidly determined from the stereonet. The orientation of the driving forces determines whether sliding along the line of intersection of the planes or sliding on either one of the planes will occur. An example problem for sliding on two planes has been used to clarify the following discussion. The problem is illustrated in Figs. 4.11 through 4.15.



Force Polygon

FIG. 4.10 MINIMUM FORCE REQUIRED TO CAUSE FAILURE

#### 4.4.2 Orientation of line of intersection of the two planes

The orientation of the line of intersection of two potential failure planes is determined using the stereonet as illustrated in Fig. 4.11. The great circles for the two planes are drawn on the stereonet and their intersection is determined as described in section 4.1. For the example problem illustrated in Fig. 4.11, the line of intersection is oriented S 27° W and plunges 40 degrees from the horizontal.

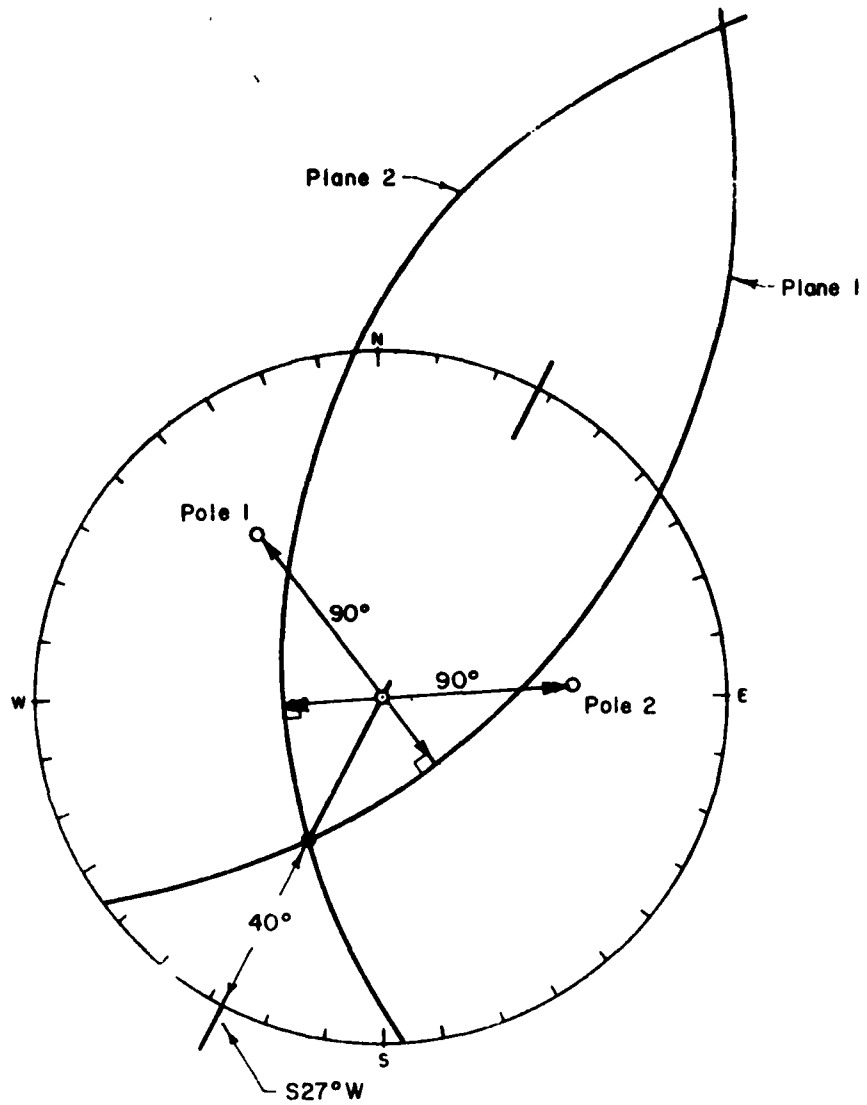
Figure 4.12 is a block diagram of the two planes, showing their line of intersection and the friction cones acting on each plane. For convenience, the friction cones are shown above the sliding plane.

#### 4.4.3 Reaction forces on the failure planes

Stable and unstable zones are separated on the stereonet (Fig. 4.13) by the limiting reaction forces,  $\bar{R}_{L1}$  and  $\bar{R}_{L2}$ . The unstable zones include zones for sliding down the intersection, sliding up the intersection, sliding on single planes, and lifting of the wedge off the planes. For the case of sliding on plane 1 alone, the orientation of  $\bar{R}_{L1}$ , as defined by the friction cone on plane 1, separates the stable and unstable zones. For sliding along the intersection of planes 1 and 2, the orientation of  $\bar{R}_{L1} + \bar{R}_{L2}$  separates the stable and unstable zones. The boundary between sliding on the intersection and sliding on plane 1 is the great circle which passes through  $\bar{N}_1$  and  $\bar{S}_1$ , the normal and shear forces, respectively, on plane 1. This great circle represents a plane normal to plane 1 and parallel to the line of intersection.

#### 4.4.4 Method of locating boundary between stable and unstable zones for the case of sliding along the line of intersection

The location of the resultant,  $\bar{R}_{L1} + \bar{R}_{L2}$ , must be determined in



Given :

Plane 1 : Strike  $N54^{\circ}E$ , Dip  $62^{\circ}SE$ ,  $\phi = 20^{\circ}$   
 Plane 2 : Strike  $N04^{\circ}W$ , Dip  $59^{\circ}SW$ ,  $\phi = 40^{\circ}$

**FIG. 4.11 SLIDING ON TWO PLANES: ORIENTATION OF LINE OF INTERSECTION**

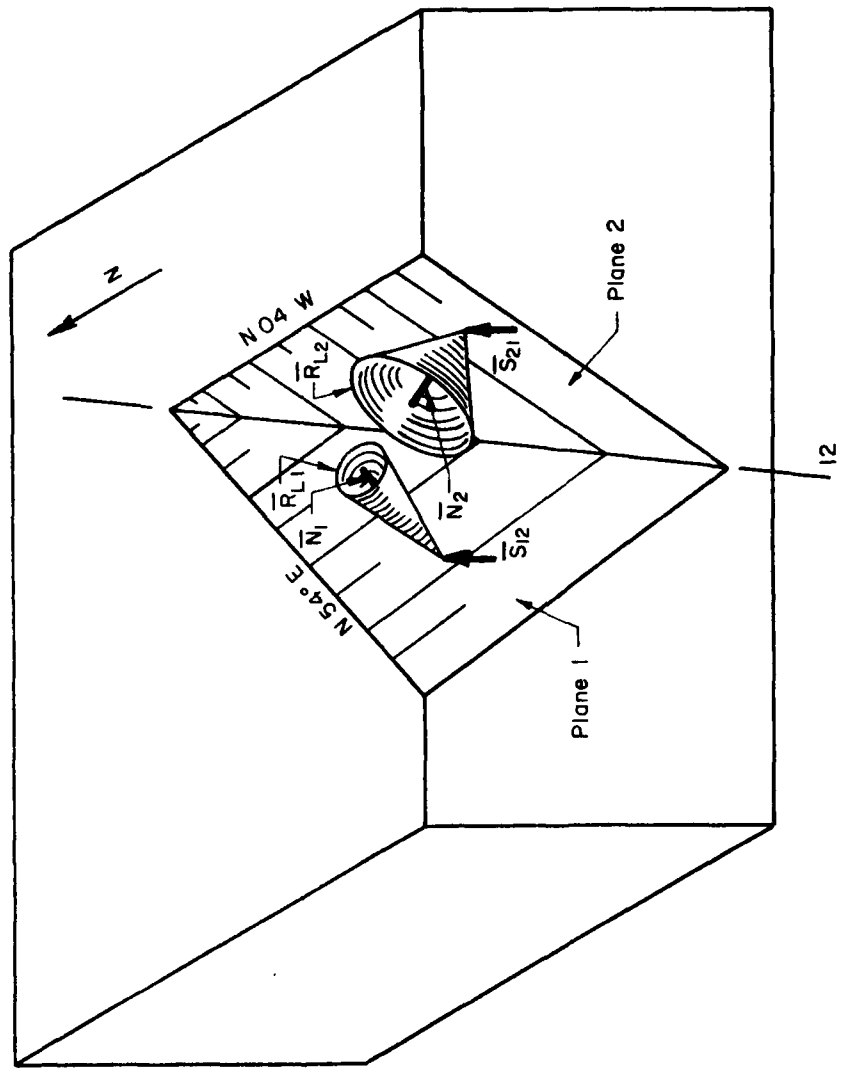


FIG. 4.12 SLIDING ON TWO PLANES : BLOCK DIAGRAM

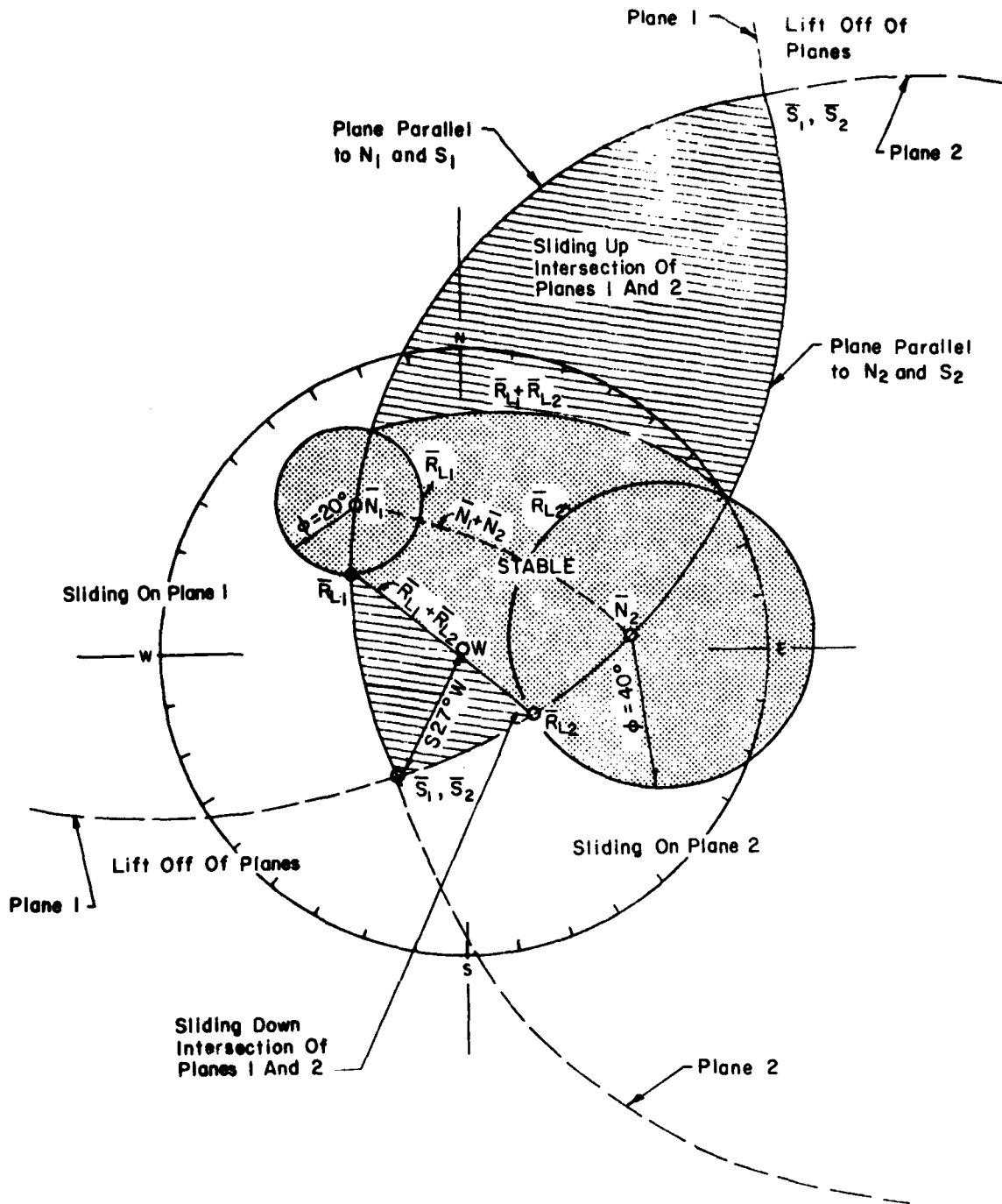


FIG. 4.13 SLIDING ON TWO PLANES : STERONET



order to outline the stable and unstable zones for the case of sliding along the line of intersection. The shear forces on planes 1 and 2 will act in the direction of sliding, which in this case is parallel to the line of intersection. Therefore, the shear forces,  $\bar{S}_1$  and  $\bar{S}_2$ , will both plot on the stereogram at the same point as does the line of intersection (point  $\bar{S}_1, \bar{S}_2$  in Fig. 4.13).

The direction of the reaction force on each plane is known, since the direction of its components, the normal and shear forces on that plane, are fixed. The reaction force,  $\bar{R}_{L1}$ , must act within the plane in which  $\bar{N}_1$  and  $\bar{S}_1$  act. Therefore, the direction of the reaction force,  $\bar{R}_{L1}$ , can be located by drawing a great circle through  $\bar{N}_1$  and  $\bar{S}_1$ .  $\bar{R}_{L1}$  is located where this circle intersects the friction cone of plane 1. Similarly,  $\bar{R}_{L2}$  is located where the great circle drawn through  $\bar{N}_2$  and  $\bar{S}_2$  intersects the friction cone of plane 2. No matter what driving forces act on the wedge, as long as the limiting case of sliding along the intersection is considered, then the orientation of both  $\bar{R}_{L1}$  and  $\bar{R}_{L2}$  are fixed.

If  $\bar{R}_{L1}$  and  $\bar{R}_{L2}$  are summed, their resultant,  $\bar{R}_{L1} + \bar{R}_{L2}$ , must act in a plane parallel to  $\bar{R}_{L1}$  and  $\bar{R}_{L2}$ . This plane can be located on the stereonet of Fig. 4.13 by drawing a great circle through  $\bar{R}_{L1}$  and  $\bar{R}_{L2}$ . For sliding along the intersection of plane 1 and 2, the reaction  $\bar{R}_{L1} + \bar{R}_{L2}$  will be located somewhere on this great circle, but its position along the great circle will depend on the orientation of the driving forces acting on the wedge, since the orientation of the driving vector affects the relative magnitudes of  $\bar{R}_{L1}$  and  $\bar{R}_{L2}$ . Should the orientation of the resultant vector forces lie outside the stable zone outlined by  $\bar{R}_{L1} + \bar{R}_{L2}$ , then sliding will occur on the intersection of the two planes.

In Fig. 4.13, the weight vector,  $\bar{W}$ , is located just within the stable zone. Only a very small force directed toward the south would be required to move the driving vector out of the stable zone and cause sliding down the line of intersection of planes 1 and 2.

#### 4.4.5 Minimum force ( $\bar{NW}$ ) required to cause sliding of the wedge

In order to cause sliding of the wedge, the resultant driving vector must lie outside the stable zone. The minimum force,  $\bar{NW}$  required to cause sliding can be determined by means which is directly analogous to the method for determining the minimum force for sliding on a single plane (Refer to Section 4.3.4). To close the force polygon (and obtain a factor of safety of one) a force must be added which connects the tip of the existing vector (Weight,  $\bar{W}$ , in this case) to the plane of the reaction,  $\bar{R}_{L_1} + \bar{R}_{L_2}$ . The minimum force will be the one acting normal to the plane of  $\bar{R}_{L_1} + \bar{R}_{L_2}$  as shown in Fig. 4.14.

The orientation of the minimum force can be determined from the stereonet. Its magnitude can be determined by graphical construction of the force polygon (such as Fig. 4.14). In Fig. 4.14, the minimum angle between  $\bar{W}$  and  $\bar{R}_{L_1} + \bar{R}_{L_2}$ , which must be closed for a factor of safety of one, is 4 degrees. The minimum force is also directed upward (in this case at an angle of  $4^{\circ}$ ) in order to intersect the plane of  $\bar{R}_{L_1} + \bar{R}_{L_2}$  at right angles. Note that the strike of the minimum force (in this case S40W) is not the same as the strike of the line of intersection (in this case S27W). In general, the minimum force,  $\bar{NW}$ , will not be oriented directly along the strike of the line of intersection unless the wedge is acted on only by its own weight and the friction angles on the two planes are the same.

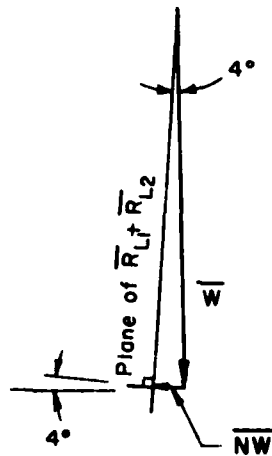
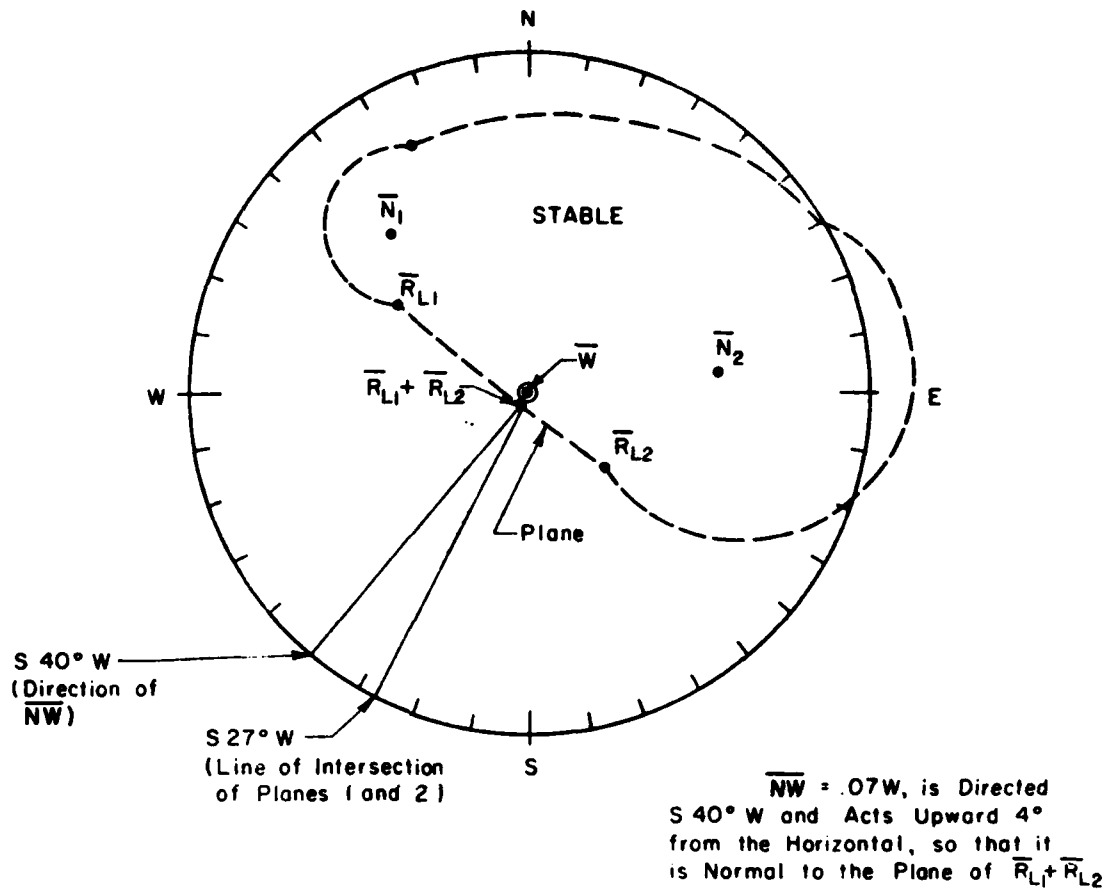


FIG. 4.14 SLIDING ON TWO PLANES: MINIMUM FORCE REQUIRED TO CAUSE SLIDING

It should be noted that the difference in magnitude between the minimum force,  $\overline{NW}$ , and the force  $\overline{NW}$  directed horizontally and parallel to the strike of the line of intersection will be very small in most cases, particularly for cases when the primary force acting on the wedge is its own weight, and the factor of safety is only slightly greater than one. In these cases, a reasonable (but slightly unconservative) approximation is that  $\overline{NW}$  acts horizontally, parallel to the strike of the line of intersection.

#### 4.4.6 Factor of safety and minimum forces required to stabilize the wedge

Two separate conditions exist for determination of the factor of safety of the wedge and the forces required to stabilize the wedge. Consider the two conditions illustrated in Fig. 4.15: case 1, where the wedge is acted on by a driving force,  $\overline{D}$ , causing sliding on a single plane (plane 1), and case 2, where the wedge is acted on by a driving force,  $\overline{B}$ , causing sliding along the line of intersection of planes 1 and 2.

Case 1: The wedge is acted upon by the driving force,  $\overline{D}$ , and will slide on plane 1 alone. There will be no normal force on plane 2. In this case, the orientations of both the normal force,  $\overline{N}_1$ , on plane 1, and the driving force,  $\overline{D}$ , are known, while the orientation of the shear force,  $\overline{S}_1$ , and the reaction,  $\overline{R}_{L1}$ , on plane 1 remain to be determined.  $\overline{S}_1$  and  $\overline{R}_{L1}$  are known to act within the plane of  $\overline{N}_1$  and  $\overline{D}$ . Thus, their position is obtained by drawing a great circle (solid line in Fig. 4.15a) through  $\overline{N}_1$  and  $\overline{D}$ , then locating  $\overline{S}_1$  at 90 degrees from  $\overline{N}_1$  and locating  $\overline{R}_{L1}$  at  $\theta$  degrees from  $\overline{N}_1$ , along the great circle. In the example shown, the angle between  $\overline{N}_1$  and  $\overline{R}_{L1}$  is  $\theta = 20^\circ$ , and the angle between

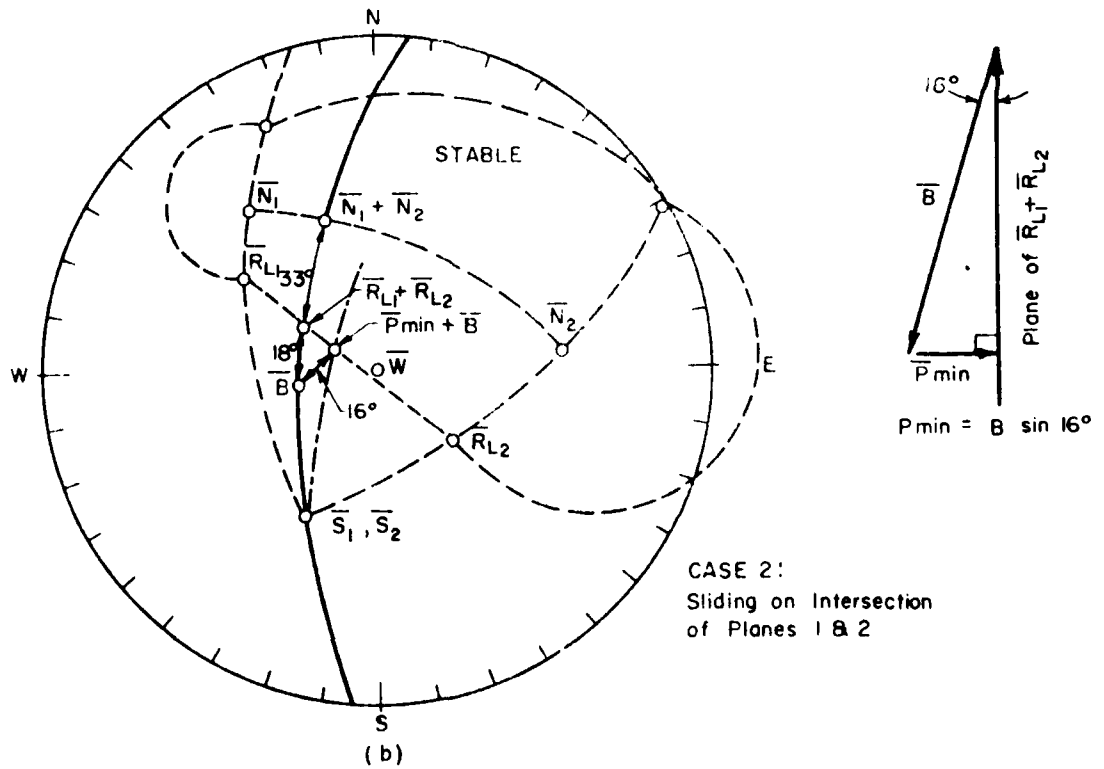
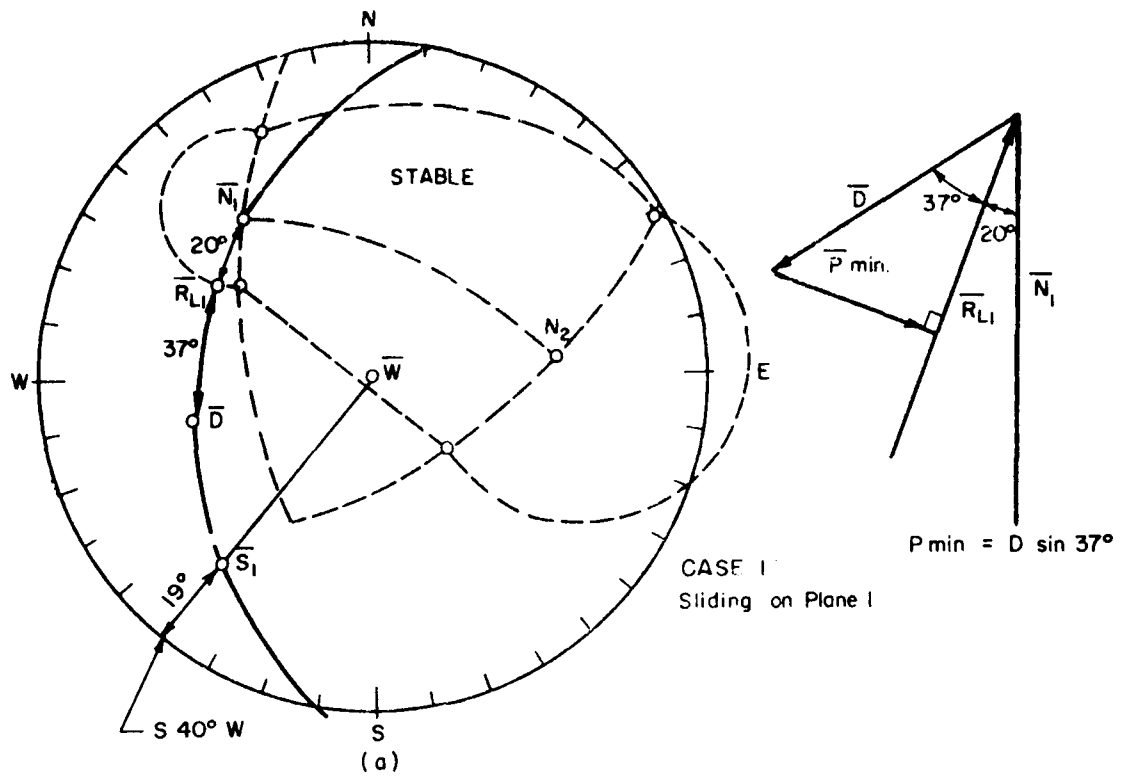


FIG. 4.15 MINIMUM FORCES REQUIRED TO STABILIZE THE WEDGE

$\bar{R}_{L_1}$  and  $\bar{D}$  is  $37^\circ$ . Therefore, the factor of safety is:

$$F.S. = \frac{\text{Maximum shear force available}}{\text{Actual shear force mobilized}} = \frac{\tan 20^\circ}{\tan (20^\circ + 37^\circ)} = 0.24$$

(Refer to Fig. 4.15a.) Sliding of the wedge will be in the direction of the shear force,  $S$ , in this case plunging  $19^\circ$  in a direction  $S 40^\circ W$ , on plane 1.

The magnitude of the minimum force,  $\bar{P}$ , required to close the  $37^\circ$  angle between  $\bar{R}_{L_1}$  and  $\bar{D}$  (and thereby increase the factor of safety to one) can be determined from the graphical construction in Fig. 4.15a. If the magnitude of  $\bar{D}$  is known, then the minimum force is:

$$P_{\min} = D \sin 37^\circ$$

Case 2: The wedge is acted upon by the driving vector,  $\bar{B}$ , and will slide on the intersection of planes 1 and 2. The direction of the shear forces,  $\bar{S}_1$  and  $\bar{S}_2$ , are fixed parallel to the line of intersection of planes 1 and 2, while the positions of  $\bar{N}_1 + \bar{N}_2$  and  $\bar{R}_{L_1} + \bar{R}_{L_2}$  remain to be determined. They can be found by drawing a great circle (solid line in Fig. 4.15b) through  $\bar{S}_1$ ,  $\bar{S}_2$  and  $\bar{B}$ .  $\bar{R}_{L_1} + \bar{R}_{L_2}$  is located at the intersection of this great circle and the great circle through  $\bar{R}_{L_1}$  and  $\bar{R}_{L_2}$ .  $\bar{N}_1 + \bar{N}_2$  is located at the intersection of the great circle through  $\bar{S}_1 + \bar{S}_2$  and  $\bar{B}$ , and the great circle through  $\bar{N}_1$  and  $\bar{N}_2$ .

The factor of safety in this case is determined by the  $51^\circ$  angle between  $\bar{N}_1 + \bar{N}_2$  and  $\bar{B}$  and the  $33^\circ$  angle between  $\bar{N}_1 + \bar{N}_2$  and  $\bar{R}_{L_1} + \bar{R}_{L_2}$ . The factor of safety is therefore:

$$F.S. = \frac{\tan (33^\circ)}{\tan (33^\circ + 18^\circ)} = \frac{\tan 33^\circ}{\tan 51^\circ} = .53$$

The direction of sliding is along the line of intersection,  $S 27^\circ W$ ,

downdip at  $40^\circ$ .

The concept of a factor of safety is somewhat misleading in this case, because the force required to stabilize the wedge does not have to close the  $18^\circ$  angle between  $\bar{R}_{L_1} + \bar{R}_{L_2}$  and  $\bar{B}$ . Instead, the minimum force,  $P_{\min}$  is  $B \sin 16^\circ$ . Note that the new resultant driving vector,  $\bar{P}_{\min} + \bar{B}$ , acts in a plane which is different from the plane in which  $\bar{B}$  originally acted.

#### 4.5 Sliding of a Wedge Bounded by Three Planes

The case for sliding of a wedge bounded by three or more planes is only slightly more complicated than the case for a wedge bounded by two planes. With three planes another friction circle is added to the stereonet. Depending on the orientation of the driving forces, sliding will occur on any one of the three planes, on any one of the three lines of intersection, or the wedge will lift off the three planes. Methods for determining the minimum forces to cause sliding, for determining factors of safety, etc., are identical to those described for the two plane case (section 4.4). Prior to performing the stability analysis, a basic decision must be made as to which planes are potential sliding planes and which wedges are critical.

Figures 4.16 and 4.17 illustrate the three plane case. The orientations and friction angles for the three planes are given in the block diagram of Fig. 4.16. The corresponding stereonet is illustrated in Fig. 4.17. For this case it is readily apparent that, regardless of the presence of the third plane, the wedge is still closest to a failure by sliding (under its own weight) along the intersection of planes 1 and 2. In order for failure to occur by sliding up plane 3, or by

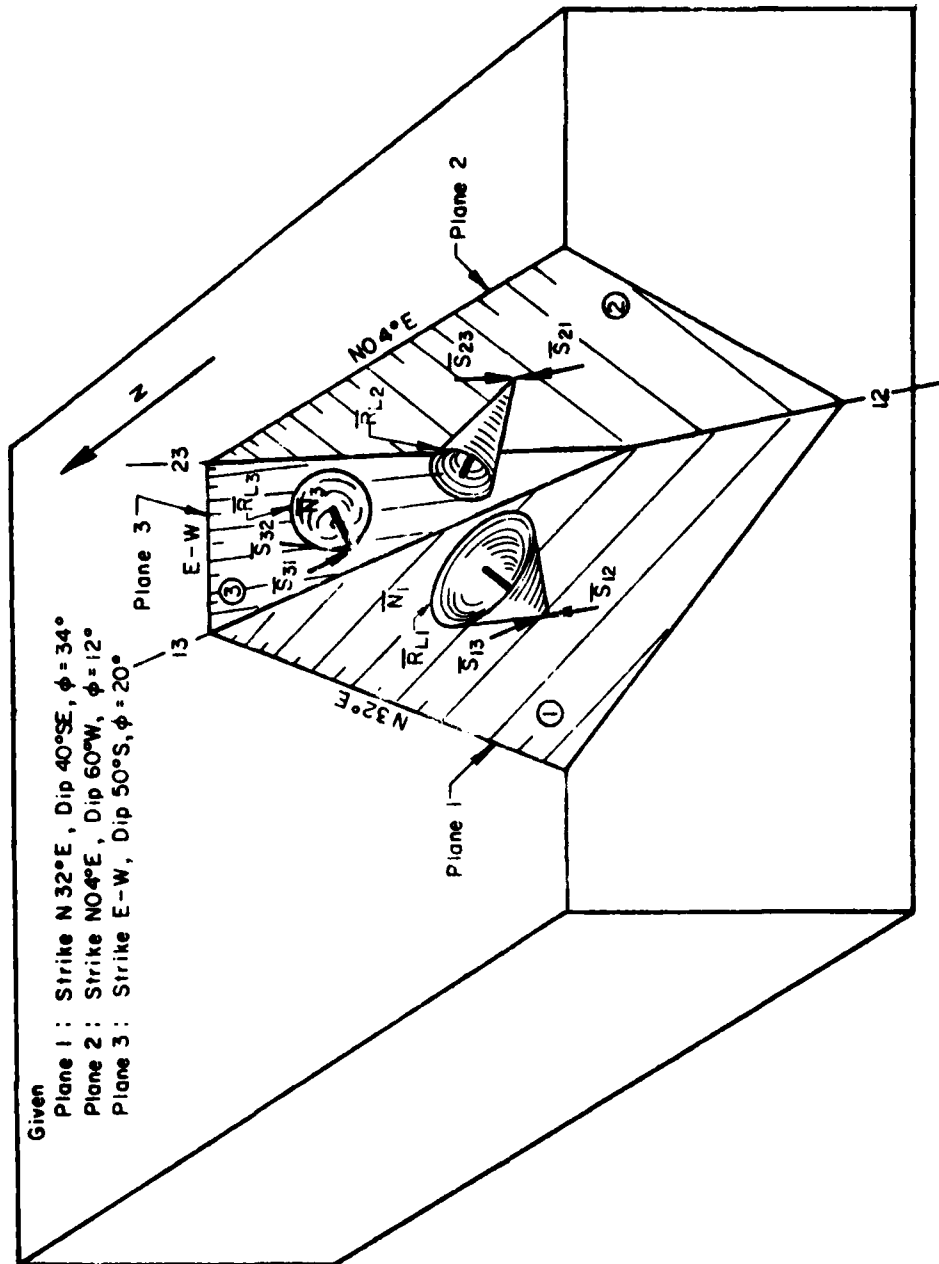


FIG 4.16 WEDGE BOUNDED BY THREE PLANES : BLOCK DIAGRAM



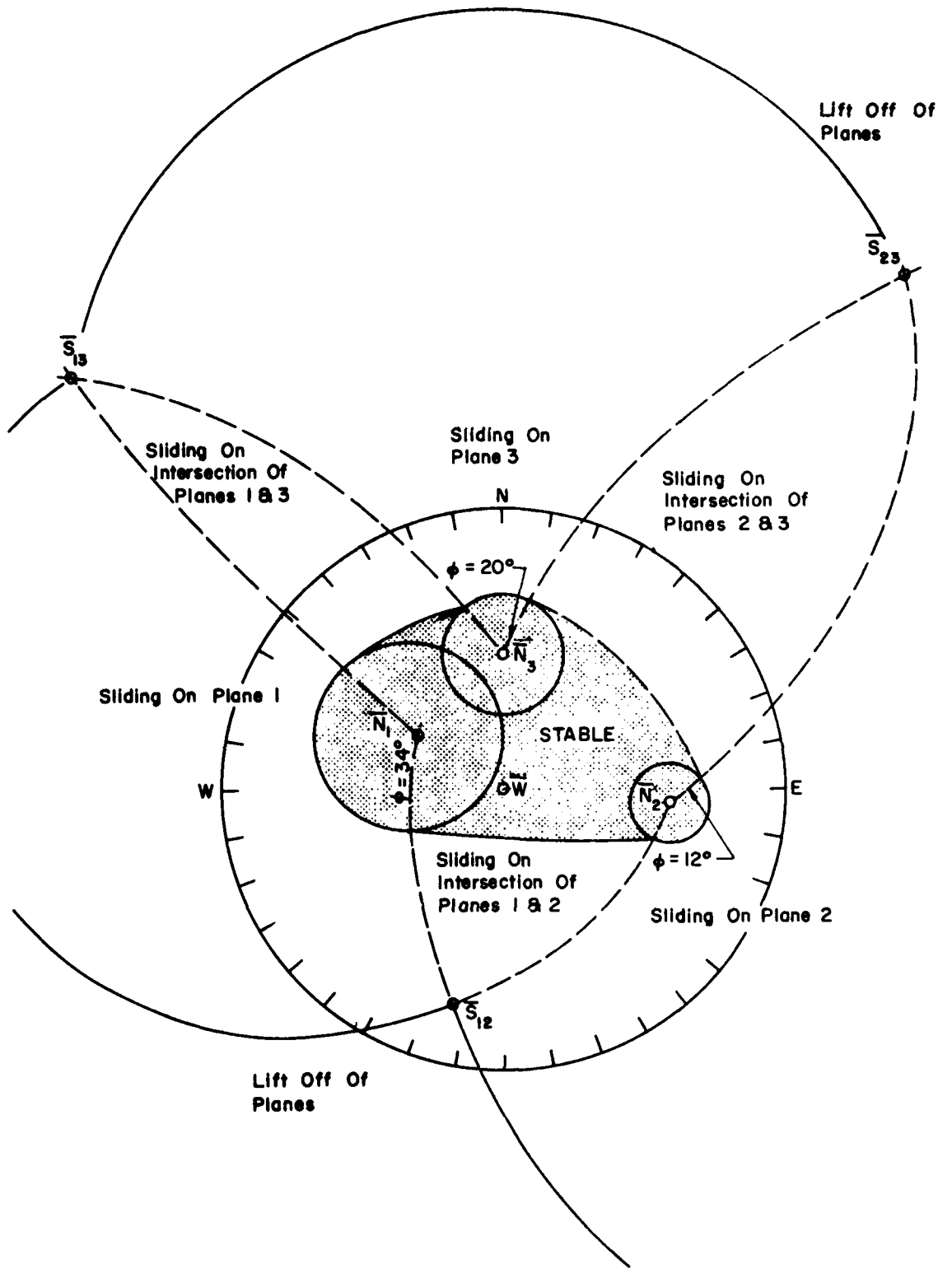


FIG. 4.17 WEDGE BOUNDED BY THREE PLANES; STERONET

sliding along the intersection of plane 3 and 1, or by sliding along the intersection of plane 3 and 2, an appreciable driving force acting upward (toward the North) would be required.

#### 4.6 Wedge Bounded by Three Planes but Daylighted by Cut Face

Although the wedge bounded by planes 1, 2, and 3 is stable for the condition illustrated in Fig. 4.17, it will not be stable if plane 3 is daylighted at the base and sides of the cut, as shown in Fig. 4.18. Cases similar to this will commonly occur in rock masses where joint sets form multiple wedges, rather than a single wedge.

If planes 1 and 2 are present, as shown in Fig. 4.18a, then wedge A would still be stable under its own weight, as was previously shown in Fig. 4.17. However, if plane 3 is daylighted at the edge of the cut, then plane 2 no longer restrains wedges A and B, thus sliding will occur along the intersection of planes 1 and 3, as indicated in the stereonet of Fig. 4.18b.

Another possible mode of failure would be for wedges A and B (acting as a single wedge) to rotate away from the line of intersection of planes 1 and 3 and slide on plane 3 alone. This is likely to occur if the mass of the wedges is concentrated over plane 3, away from the line of intersection of planes 1 and 3. (Rotational wedge failures are analyzed in section 4.7.)

Another possibility is that wedges A and B would break up and slide as individual blocks, wedge A possibly sliding on the intersection and wedge B sliding on plane 3 alone.

When the planes represent joint sets rather than single discontinuities, then modes of failure similar to those described above become

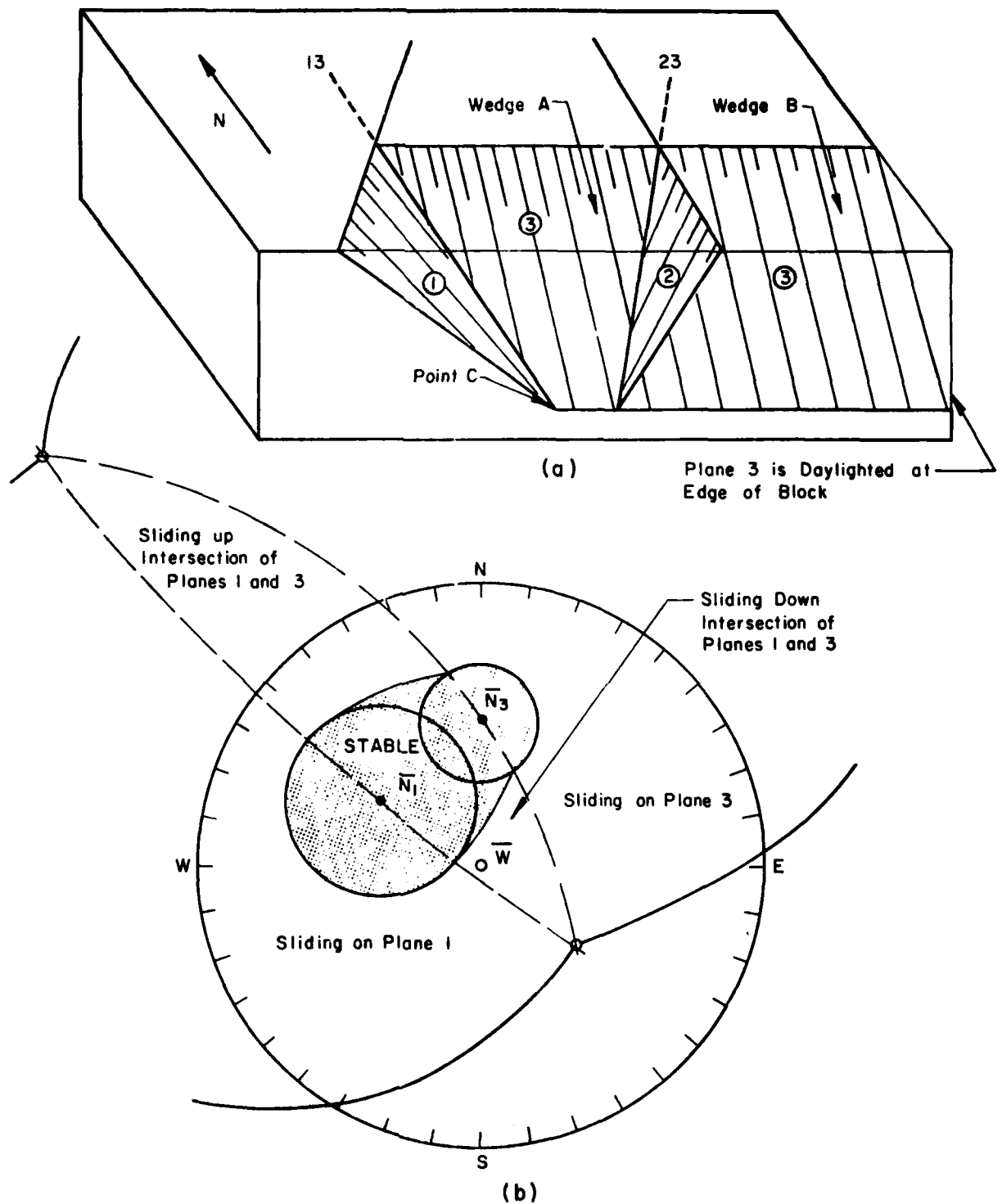


FIG 4.18 WEDGE BOUNDED BY THREE PLANES: PLANE 3 DAYLIGHTED AT EDGE OF BLOCK

quite possible. Some of the joints within a set may daylight on the sides or edges of slopes and allow failure of wedges on single planes rather than multiple planes. Joints of other sets may also free the edges of wedges, facilitating sliding on a single plane. In general, a lower factor of safety will be obtained if the mass has a tendency to move as several rigid bodies broken up by the joint sets, rather than moving as a single rigid body. It is very important that these possibilities be considered during the exploratory phase of the slope stability study, prior to selecting the critical wedges on which the stability analyses will be performed.

#### 4.7 Rotation of Wedge on Plane 3

The factor of safety against rotation of a wedge can be estimated using the stereonet if the point of application of the driving forces on the failure plane is known. Consider the example of Fig. 4.19. The wedge illustrated here is the same as the wedge of Fig. 4.18 except for an increase in the angle of friction on plane 1 from  $34^\circ$  to  $40^\circ$ , so that the wedge is now stable against sliding under its own weight down the intersection of planes 1 and 3. It is assumed for a rotational failure that the wedge rotates about point C, at the base of the slope. It is also assumed that the limiting shear and normal stresses on plane 3 can be summed as forces  $\bar{N}_3$  and  $\bar{S}_3$ , acting at point D (at the point of intersection of the resultant driving vector,  $\bar{W}$ , with plane 3). This implies that there is no variation in the angle of friction on plane 3. Based on these assumptions the direction of the shear force,  $\bar{S}_3$ , will be perpendicular to line  $\overline{CD}$ , as shown in Fig. 4.19.



The given conditions for the wedge of Fig. 4.19a are:

Plane 1: Strike N32°E, dip 40°SE,  $\phi = 40^\circ$

Plane 3: Strike E-W, dip 50°S,  $\phi = 20^\circ$

In addition, it is assumed that the center of gravity of the wedge is known, so that the orientation of line  $\overline{CD}$  is known. Line  $\overline{CD}$  is the moment arm from the center of rotation, C, to the point of intersection of the weight vector,  $\bar{W}$ , with plane 3 (point D). Its orientation is assumed to be S45°W on plane 3.

It is immediately apparent from the given conditions on planes 1 and 3 that the wedge, under its own weight,  $\bar{W}$ , is stable against sliding on plane 1 alone, since the dip of plane 1 equals the angle of friction on plane 1 (40°). The wedge is therefore also stable against sliding on the intersections of planes 1 and 3.

The wedge is not stable against sliding on plane 3 alone, since the dip of that plane exceeds its angle of friction. If the wedge were to extend an infinite distance to the right of the diagram, then the wedge would behave as if it were sliding on plane 3 alone, since all of the weight of the wedge would be over plane 3 and an infinitesimal portion of the weight would act on plane 1. In this case the moment arm for rotation of the wedge would extend parallel to the strike of plane 3 (line  $CD'$ ). Thus the shear force,  $\bar{S}_3$ , would act directly up the dip-slope of plane 3, the identical condition for sliding on a single plane. The factor of safety against rotational sliding would be:

$$\text{F.S.} = \frac{\text{RESISTING MOMENT}}{\text{DRIVING MOMENT}} = \frac{\overline{CD'} (W \tan 20^\circ)}{\overline{CD'} (W \tan 50^\circ)} = \frac{\tan 20^\circ}{\tan 50^\circ} = 0.3$$

the identical factor of safety for sliding directly down plane 3.

Another extreme would be the case where the weight of the wedge was concentrated near the intersection of planes 1 and 3 so that the moment arm extended directly up-slope on plane 3 (line  $CD''$ ). The limiting shear force,  $\bar{S}_3$ , in this instance would be directed along the strike of plane 3. The driving force,  $\bar{W}$ , has no component in this direction, so that rotation would not occur, regardless of the frictional resistance on plane 3. The factor of safety against rotation is therefore:

$$F.S. = \frac{\overline{CD''}(\tan 20^\circ)}{\overline{CD''}(\tan 0^\circ)} = \infty$$

An intermediate case, where line  $CD$  is directed  $S45^\circ W$  on plane 3, is shown in the stereonet of Fig. 4.19. The rotational stability of the wedge is determined as follows: The great circle representing plane 3 is drawn on the stereonet, as well as the normal force and friction circle for plane 3. Line  $\overline{CD}$  is located in its given direction on the stereonet at the intersection of plane 3 and a vertical plane oriented  $S45^\circ W$ .  $\bar{S}_3$  is then located on plane 3, at a  $90^\circ$  angle from line  $\overline{CD}$ . A great circle is then drawn through  $\bar{S}_3$  and  $\bar{N}_3$ , representing the plane containing  $\bar{S}_3$  and  $\bar{N}_3$ . This great circle will also be located  $90^\circ$  from  $\overline{CD}$ , along a great circle (in this case a straight line) passing through  $\overline{CD}$  and  $\bar{W}$ . The component of  $\bar{W}$  which is normal to  $\overline{CD}$  is located at this point. The factor of safety against rotation is:

$$F.S. = \frac{\tan \phi}{\tan (\text{angle between } \bar{N}_3 \text{ and the component of } \bar{W} \perp \text{ to } \overline{CD})}$$

$$= \frac{\tan 20^\circ}{\tan (20^\circ + 12^\circ)} = \frac{\tan 20^\circ}{\tan 32^\circ} = .58$$

Although the wedge is stable against sliding along the intersection of planes 1 and 3, it is unstable for the case of rotation on plane 3.

However, the factor of safety against rotation (F.S. = 0.58) is still appreciably higher than the factor of safety against sliding on plane 3 alone (F.S. = 0.30).

In order for the factor of safety against rotation on plane 3 to be equal to one, the center of gravity must be located so that line  $\overline{CD''}$  is oriented  $S27^{\circ}W$  on plane 3, as indicated by the dashed line tangent to the friction circle in the stereonet of Fig. 4.19.



CHAPTER FIVE  
DYNAMIC STABILITY OF ROCK SLOPES

5.1 Introduction

The stability of rock slopes subjected to dynamic loads has usually been treated as a pseudo-static problem by engineers assessing the "dynamic factor of safety." In this approach, the dynamic forces on a potential sliding mass of weight  $W$  are assumed to be equivalent to a horizontal force of  $\overline{KW}$  acting through the center of gravity toward the free surface of the slope. The constant  $K$  is called the seismic coefficient, the value of which is commonly taken between 0.05 and 0.20 for earthquake design in seismically active areas. If this method is used, the factor of safety is computed by the methods outlined in Chapters 3 and 4 for static problems. The only adjustment which has to be made is that the resultant force  $R$  acting on a three dimensional tetrahedron includes not only the weight and pore pressures, but also the force  $\overline{KW}$  directed in a horizontal direction. Wittke (1965) has presented this type of analysis to assess the dynamic stability of slopes and has suggested that the horizontal force  $\overline{KW}$  be directed along the line of intersection of the two planes on which sliding takes place for the most critical effect. The meaning of the factor of safety calculated for dynamic loading is somewhat nebulous however because the dynamic forces are not constant static forces acting in one direction. The actual factor of safety of a slope subjected to dynamic loading varies with time, and movements of the slope only occur when the factor of safety is momentarily below 1.0. Thus the average factor of safety computed

from a pseudo-static analysis using the seismic coefficient  $K$  is not meaningful because the analysis does not indicate the magnitude of the strains or displacements which may develop in the slope. An estimate of the displacement or strain in the slope after shaking enables the engineer to make a judgment on whether the displacements are harmful in terms of either structural damage or are large enough to cause a considerable decrease in shear strength of the slope materials.

In this chapter the basic analysis given by Newmark (1965) for the dynamic analysis of earth slopes is modified to assess the displacement rock slopes might experience under dynamic loadings. A criterion is also given for determining if the computed displacement may be harmful to the stability of the slope.

## 5.2 Dynamic Analysis of Rock Slopes

The first step in the dynamic analysis of a rock slope is to evaluate the dynamic resistance of the slope. The dynamic resistance is defined as the minimum force applied through the center of gravity of the potential sliding mass which will just begin to move the mass above the assumed failure surface. The dynamic resistance is usually denoted by  $\bar{N}W$  (Fig. 3.4a) where  $N$  is a coefficient and  $W$  is the weight of the potential sliding mass. Physically the dynamic resistance is the minimum shearing resistance which can be mobilized, in addition to that required for static stability, to resist the effects of a dynamic load.

For the three dimensional analysis of rock slopes, as shown in Figs. 3.4 and 3.5, the problem is to find the direction which will minimize  $N$  and solve for the magnitude of  $\bar{N}W$ . Graphical and analytical procedures have been developed for finding the minimum dynamic resistance in

sections 3.2.2 and 3.4.2 respectively.

The quantity  $N_g$  is the steady acceleration in the direction of  $\overline{NW}$  which will just overcome the resistance of the sliding mass. If the maximum acceleration  $A_g$  in the area of the slope is less than  $N_g$  then the slope is definitely safe. However, if  $A_g$  exceeds  $N_g$ , the slope does not necessarily fail because the ground acceleration may only exceed  $N_g$  for a very short period of time. During this time, a relative displacement occurs between the portions above and below the failure surface. Figure 5.1 shows a plot of the ground motions observed during the 1940 El Centro earthquake. Note that the maximum acceleration,  $A_g (= \gamma_0)$ , of 0.32 g occurred only for a short period of time and also note that if a slope in the area of this record had a dynamic resistance,  $\overline{NW}$ , of 0.2 W that the dynamic resistance would only be exceeded for very short periods of time during 6 pulses. Although some relative displacement would occur during these short times the slope would not necessarily fail. Newmark's method of analysis provides a means of calculating the displacements which occur for the case when  $A > N$ .

The following example illustrates Newmark's analysis for the case of a single acceleration pulse acting on the base beneath a sliding mass with a rigid plastic resistance between the base and mass with a resistance of  $\overline{NW}$ .

Consider the rigid body shown in Fig. 5.2 having a weight  $W$ , mass  $M$ , and having a motion  $x$ . The motion of the ground on which the mass rests is designated by  $y(t)$ , where  $y$  is a function of time  $t$ . The relative motion of the mass, compared with that of the ground, is given by  $u$ , where

$$u = x - y \quad (5.1)$$

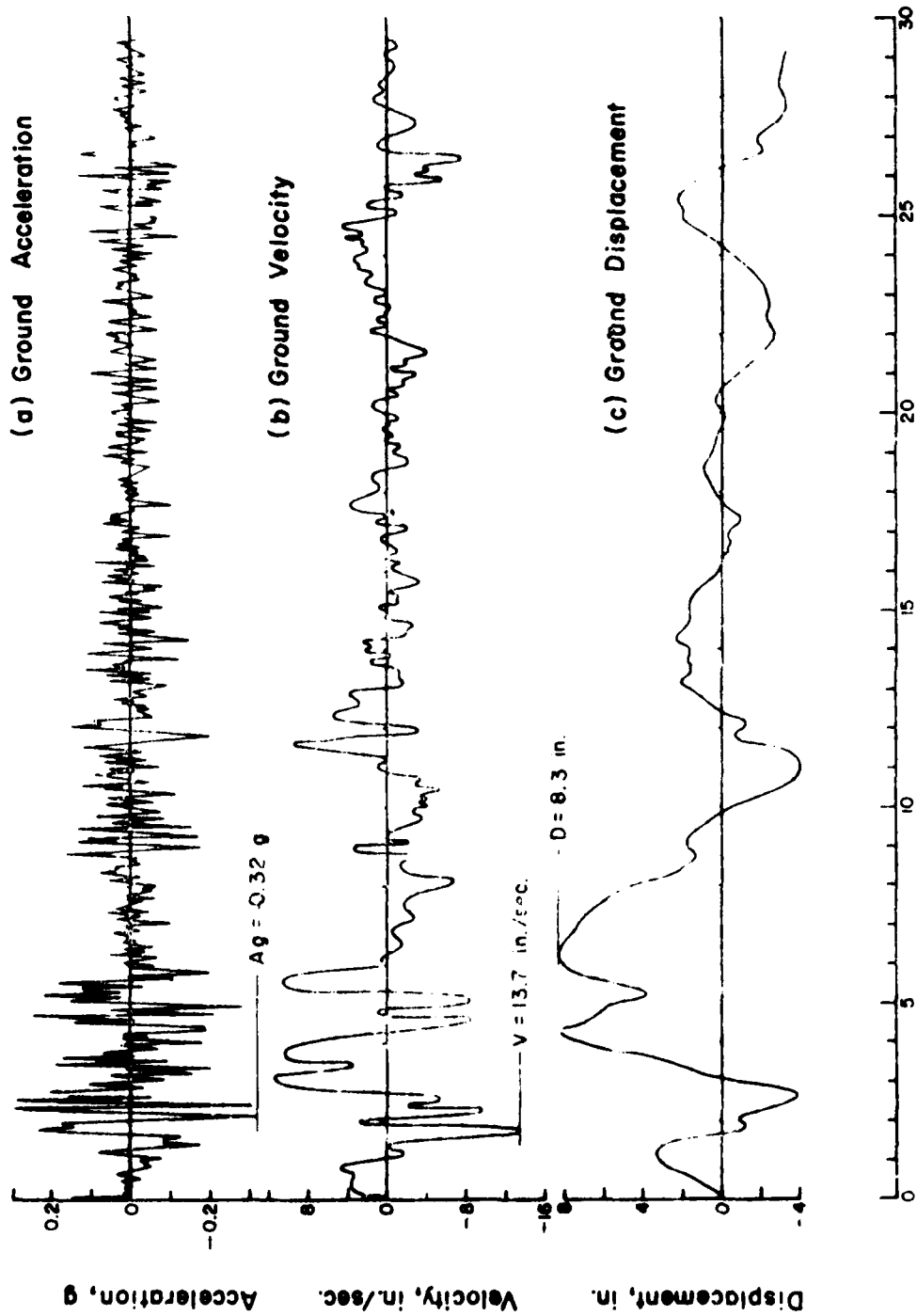


FIG. 5.1 EL CENTRO, CALIFORNIA, EARTHQUAKE OF MAY 18, 1940,  
N-S COMPONENT

The resistance to motion is accounted for by a shearing resistance, which can be expressed as being proportional to the weight  $W$ , and having a magnitude of  $\overline{NW}$ . This shearing resistance corresponds to an acceleration of the ground of magnitude  $Ng$  that would cause the mass to move relative to the ground.

The accelerating forces acting on the mass  $M$  are shown in Fig. 5.3. The acceleration considered is a single pulse of magnitude  $Ng$ , lasting for a time interval  $t_0$ . The resisting acceleration,  $Ag$ , is shown by the dashed line in Fig. 5.3. The accelerating force lasts only for the short time interval indicated, but the decelerating force lasts until the direction of motion changes.

In Fig. 5.4 the velocities are shown as a function of time for both the accelerating force and the resisting force. The maximum velocity for the accelerating force has a magnitude  $V$  given by the expression

$$V = Agt_0 \quad (5.2)$$

After the time  $t_0$  is reached, the velocity due to the accelerating force remains constant. The velocity due to the resisting acceleration has the magnitude  $Ng$ . At a time  $t_m$ , the two velocities are equal and the relative velocity becomes zero, or the body comes to rest relative to the motion of the ground. The formulation for  $t_m$  is obtained by equating the velocity  $V$  to the quantity  $Ng$ , which results in the expression

$$t_m = \frac{V}{Ng} \quad (5.3)$$

The maximum displacement of the mass relative to the ground,  $u_m$ , is obtained by computing the shaded triangular area in Fig. 5.4. The

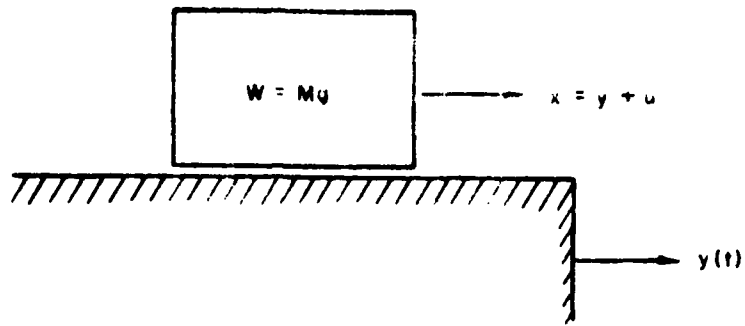


FIG. 5.2 RIGID BLOCK ON A MOVING SUPPORT.

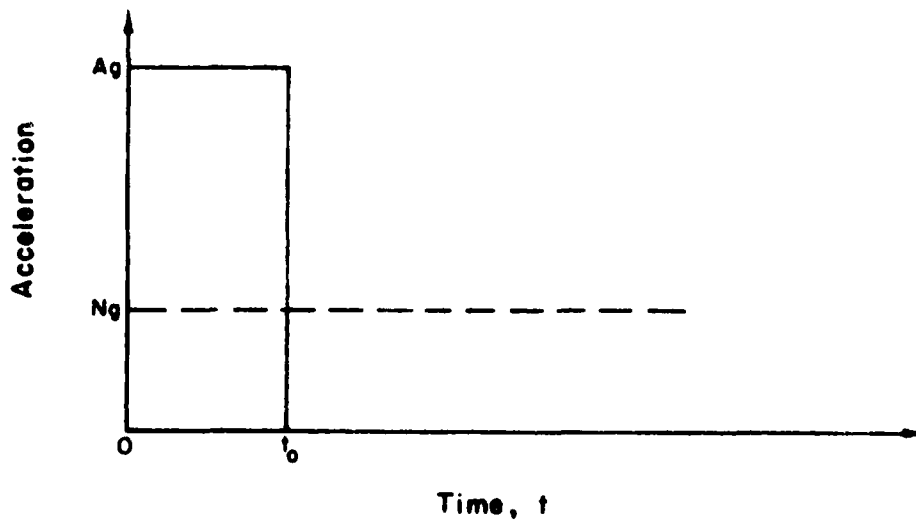


FIG. 5.3 RECTANGULAR BLOCK ACCELERATION PULSE

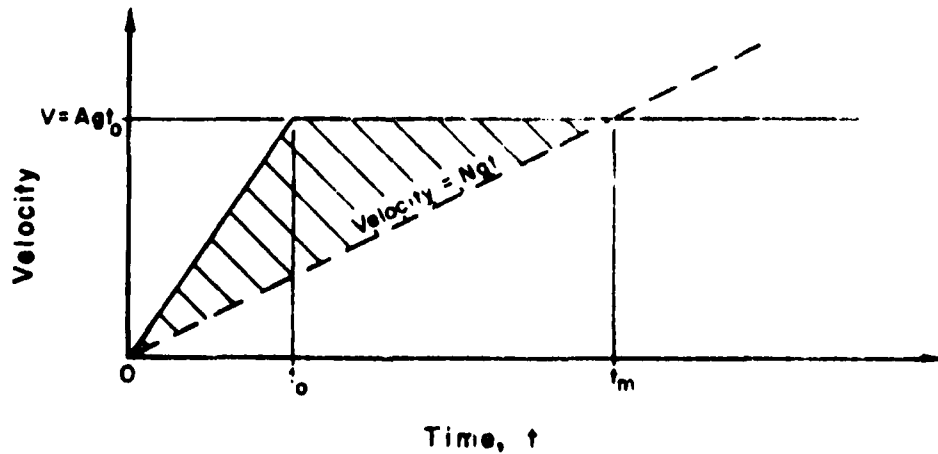


FIG. 5.4 VELOCITY RESPONSE TO RECTANGULAR BLOCK ACCELERATION

calculation is made as follows:

$$u_m = \frac{1}{2} V t_m - \frac{1}{2} V t_o$$

or

$$u_m = \frac{1}{2} \frac{V^2}{Ng} - \frac{1}{2} \frac{V^2}{Ag}$$

hence

$$u_m = \frac{V^2}{2gN} \left(1 - \frac{N}{A}\right) \quad (5.4)$$

The acceleration pulse shown in Fig. 5.3 corresponds to an infinite ground displacement. During a real earthquake a mass would undergo a number of pulses occurring in random order, some positive and some negative as shown in Fig. 5.1. If we now consider a second pulse of a negative magnitude that is sufficient to bring the velocity to zero even without the resisting force, then it can be shown that the net displacement occurring with the resistance generally cannot exceed that which would occur without the resistance.

The result of using Eq. (5.4) is to generally overestimate the relative displacement for an earthquake because the equation does not take into account the fact that the pulses occur in opposite directions. However, Eq. (5.4) should give a reasonable order of magnitude for the relative displacement and it does indicate that the displacement is proportional to the square of the maximum ground velocity.

The result derived above is also applicable to the case for a group of pulses in which the resistance in either direction of possible motion is the same. For a situation in which the body has a resistance to motion greater in one direction than in another, one must take into account the cumulative effect of the displacements. A simple example where this effect must be considered is found by rotating Fig. 5.2 clockwise so that the body has a tendency to slide downhill. In this

situation, ground motions in an upslope direction leave the mass without any additional relative motion except where the magnitudes of the motions are extremely large. One may consider this model applicable to a slope.

Similar calculations using wave forms of 4 different earthquake records were made for a resistance of  $\overline{NW}$  for downhill movement and an infinite resistance for uphill movement on a digital computer at the University of Illinois. These results are shown in Fig. 5.5. A conservative upper bound to the displacement is given by

$$\delta = \frac{V^2}{2gN} \cdot \frac{A}{N} \text{ for } 0.2 < \frac{N}{A} < 0.4 \quad (5.5)$$

For  $\frac{N}{A} > .4$  a reasonable upper bound is given by

$$\delta = \frac{V^2}{2gN} \left(1 - \frac{N}{A}\right) \frac{A}{N} \quad (5.6)$$

And for  $\frac{N}{A} < 0.2$  a reasonable upper bound for the displacement is given by

$$\delta = \frac{6V^2}{2gN} \quad (5.7)$$

The simplified calculation presented for one acceleration pulse and the calculation of displacements for actual earthquake records show that the slope movements relative to the base are proportional to the square of the maximum particle velocity,  $V^2$ , at a given ratio of  $N/A$ . Since the calculations of Newmark, presented in Fig. 5.5, are for four different earthquake records, it is conservative to use the relations given in Eqs. 5.5, 5.6, and 5.7 for ground motions from nuclear explosions because the duration of shaking is significantly shorter.

### 5.3 Permissible Movement of Rock Slopes

Ultimately, the engineer must decide if the dynamic displacement calculated from Eqs. 5.3 - 5.5 is acceptable. Many slopes in soil and



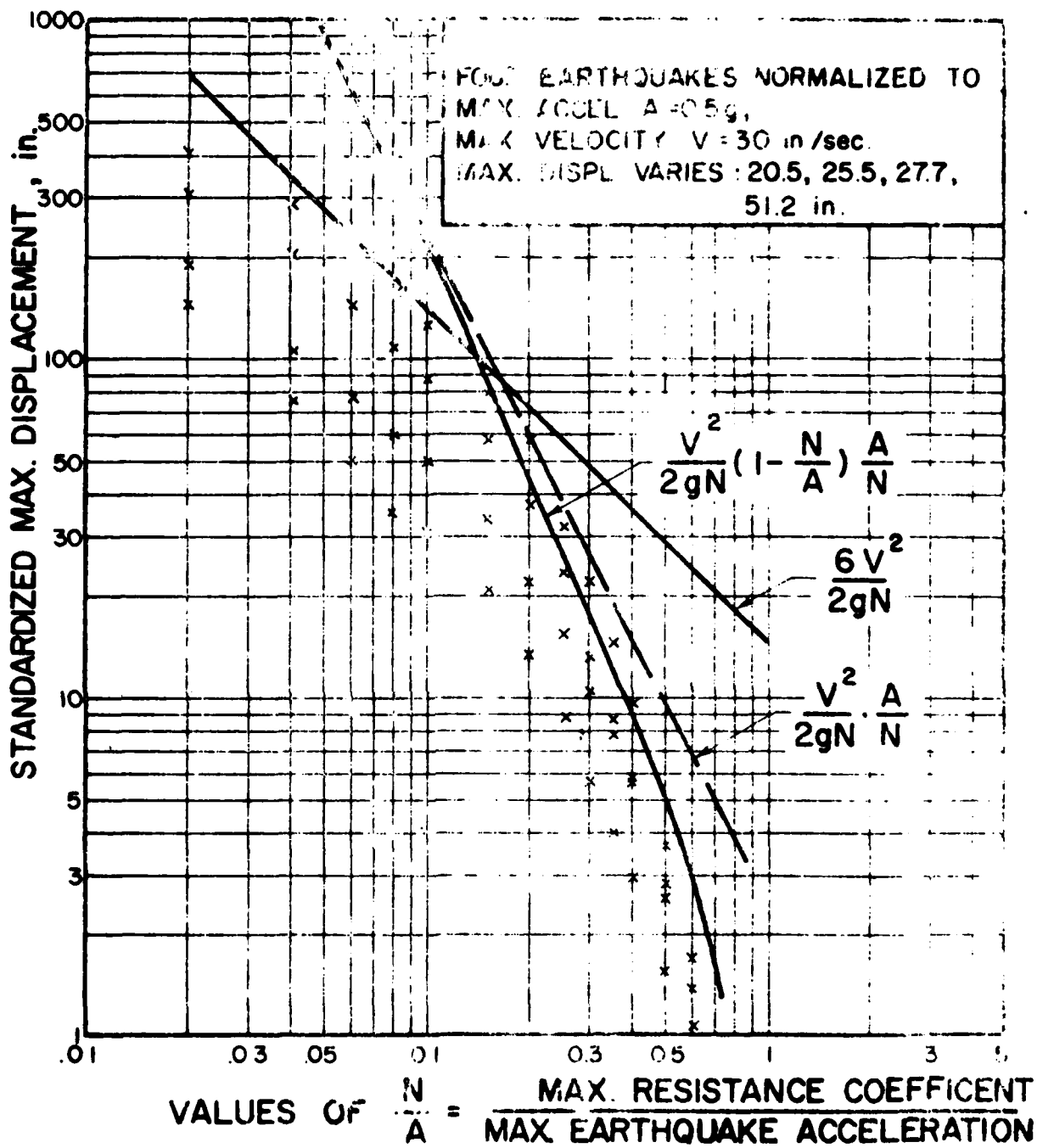


FIG. 5.5 STANDARDIZED DISPLACEMENT FOR  
 NORMALIZED EARTHQUAKES.  
 (UNSYMMETRICAL RESISTANCE)

soft shales have undergone considerable movement (as much as 6-10 ft) under earthquake loading without catastrophic consequences. On the other hand, there have been catastrophic failures of some rock slopes during dynamic loading, such as the Madison Valley, Montana slide and catastrophic slope failures have also been observed in sensitive marine clays in Anchorage, Alaska under earthquake loading. Jointed rock slopes and slopes composed of sensitive marine clays are similar in that they are composed of materials which are strain softening for displacements beyond those required to develop the maximum shearing resistance. A qualitative diagram of shearing strength mobilized versus displacement parallel to the discontinuity is shown in Fig. 5.6b for rough rock surfaces. The peak shearing strength given by point C on this diagram is given by

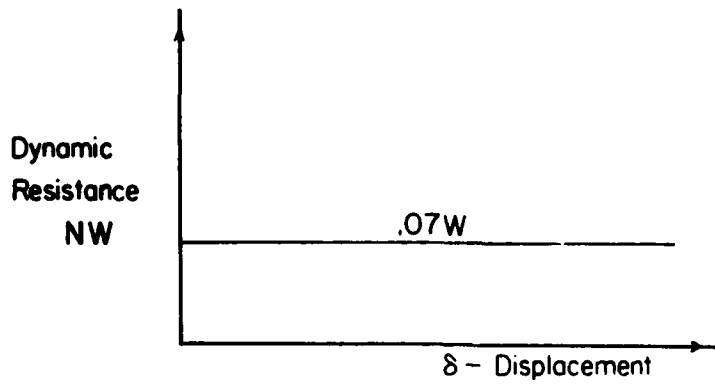
$$\tau = \sigma_n \tan (\phi_r + i) \quad (5.8)$$

where  $i$  is the geometrical component of resistance given by the roughness along the discontinuities and  $\phi_r$  is the residual angle of shearing resistance.

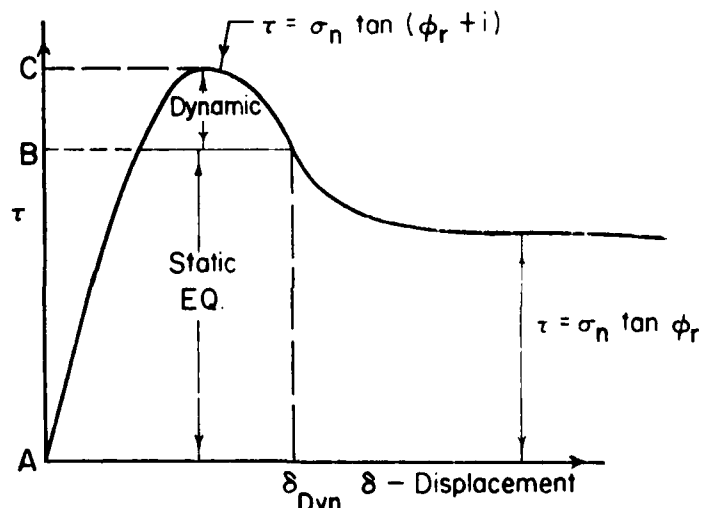
With further displacement the asperities are sheared off to a certain extent along the discontinuity and eventually at larger displacements the shear strength will be reduced to a value given by

$$\tau = \sigma_n \tan \phi_r \quad (5.9)$$

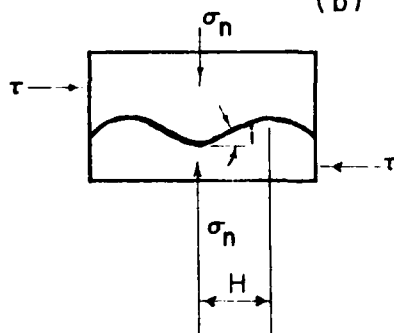
where  $\phi_r$  is the residual angle of shearing resistance along the discontinuity. Thus in any given case, the potential fall off in strength between the peak strength and the residual strength is  $\sigma_n \tan i$ , where  $i$  is the angle which the roughness makes with the average direction of movement along the discontinuity, as shown in Fig. 5.6c. The value of



(a)



(b)



$\delta_{Dyn} \ll H, OK$

$\delta_{Dyn} \cong H, \text{ Static Stability Impaired}$

(c)

FIG. 5.6 RELATIONSHIP BETWEEN PEAK SHEAR STRENGTH AND THE COMPONENT OF STRENGTH DUE TO SURFACE ROUGHNESS

$\phi_r$  is a function of the type of rock of which the slope is composed and can be relatively easily determined from smooth samples in the laboratory. The selection of the  $i$  value, however, is somewhat difficult in that there are usually several groups of undulations on a discontinuity which have different  $i$  values. For instance, there may be broad undulations (first order irregularities) with wave lengths on the order of 8-10 ft which may have an  $i$  associated with them which may only be on the order of  $5-15^\circ$  (Fig. 5.7). Whereas there are shorter undulations (second order irregularities), which may have higher  $i$  values ( $10-46^\circ$ ) as shown in Fig. 5.7. If the dynamic resistance  $\overline{NW}$  is calculated on the basis of a peak shearing strength such as point C on diagram 5.6b, then it is of utmost importance to know approximately the wave length of the asperity associated with the value of the angle  $i$  chosen in the analysis. For instance, if the value of  $i$  is associated with a quarter wave length denoted by  $H$  in Fig. 5.6c, then it is obvious that the dynamic displacement as computed by Newmark's method must be less than  $H$  or the shear strength value upon which the calculation of  $\overline{NW}$  was computed is no longer valid. The displacement in this case would have been enough to roll up and over the asperity shown in Fig. 5.6c and the shear strength would have been reduced to some value lower than the peak shear strength. The full value of  $i$  would not be effective because of the lower slope of the surface roughness near the top and possibly because part of the roughness could have been sheared off by the dynamic movement. On the other hand, a value of  $i$  used in estimating the peak shear strength used in the calculation of  $\overline{NW}$  could be a relatively low value of about  $5-10^\circ$ ; and this value of  $i$  could be consistent with a length  $H$  (Fig. 5.6c)

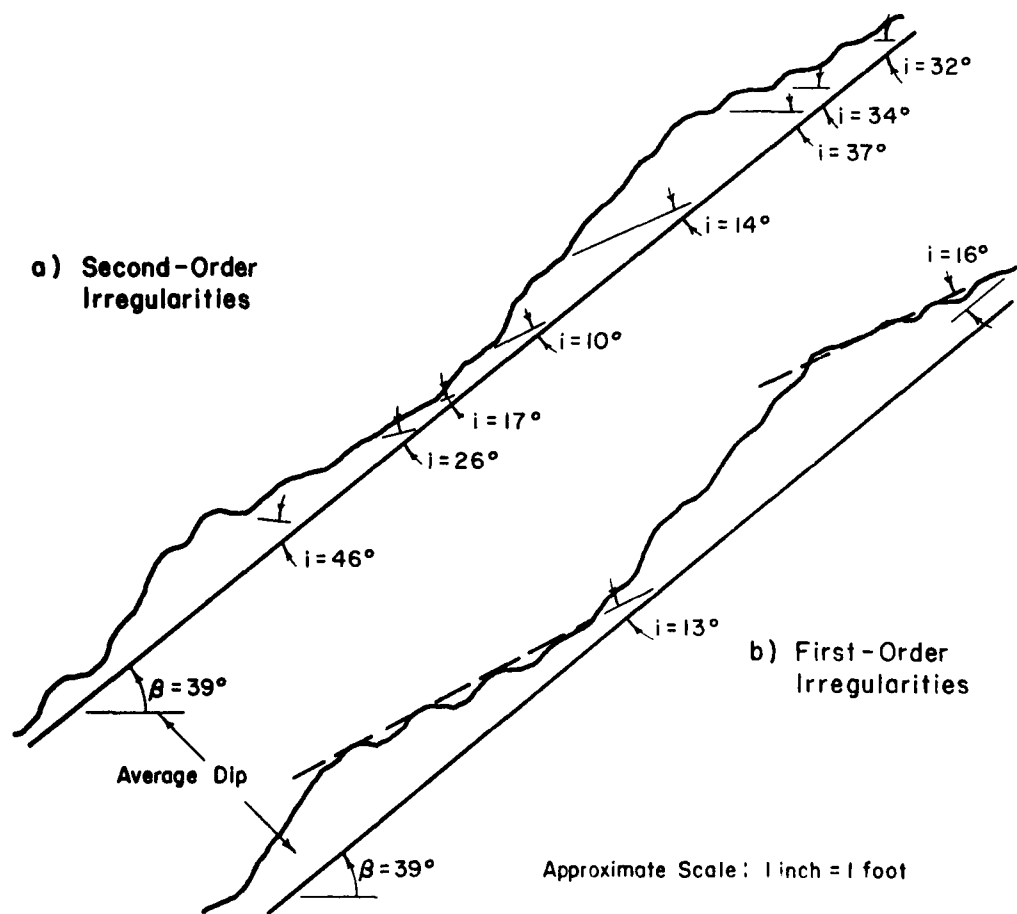


FIG. 5.7 AN EXAMPLE OF A DISCONTINUITY ILLUSTRATING FIRST AND SECOND-ORDER IRREGULARITIES

on the order of 5 or 6 ft. In this case if the calculated dynamic displacement caused by a given earthquake turns out to be something like 6 inches, then we would definitely say that the slope is probably stable or no problems would result from dynamic loading. This is true because the 6 inch displacement will not significantly reduce the strength assumed in calculations of  $\overline{NW}$ . The relative displacement would have to be on the order of 3 or 4 ft to significantly lower the peak shearing resistance in this case. Thus, in general, the criterion which should be used to decide if a certain displacement is detrimental or not is the wave length of the asperities giving the geometrical component of resistance because this is the resistance which can be destroyed by the dynamic displacement. If preliminary calculations indicate that the dynamic displacements will not be large in comparison with the displacements necessary to significantly lower the shear strength, then the dynamic displacement calculated will probably be acceptable and the slope can be judged safe. However, if the dynamic displacement computed is on the same order of magnitude as the wave length of the discontinuities or the order of displacement necessary to significantly reduce the shear strength along a discontinuity, then the slope may not be safe.

CHAPTER SIX  
SUMMARY AND CONCLUSIONS

6.1 Static Stability of Rock Slopes

In this report the methods of analysis for assessing the static stability of rock slopes in three dimensions have been described and a method for calculating the dynamic resistance and displacement of rock slopes subjected to earthquake loading has been given.

The general procedures for determining the static factor of safety of rock slopes analytically by vector analysis and graphically with stereonets are given in Chapter 3 and Chapter 4 respectively. Although the mechanics of the calculation are different in each of these approaches, the same basic steps are followed in each method for determining the static factor of safety. The steps in the analysis are as follows:

- (1) the intersection of the various joint sets with each other and with the slope face must be inspected to determine the tetrahedra which may be potential failure wedges. These wedges must then be analyzed in detail.
- (2) the forces tending to disturb the equilibrium of the wedge should be added vectorially to give a resultant driving force. These disturbing forces are the weight of the wedge,  $\bar{W}$ , the external load applied to the wedge by a structure,  $\bar{Q}$ , and the porewater forces acting on various faces of the tetrahedron given as  $\bar{U}_1$ ,  $\bar{U}_2$ , and  $\bar{U}_3$ . This step is illustrated by equations 3.10 and 3.68 for the vector analysis and is shown in Figs. 4.7 and 4.8 for the graphical method using stereonets.

(3) the mode of failure must then be determined. For example a wedge supported on two base planes can either slide along the line of intersection of the two planes, slide on either plane or rotate on either plane. The kinematics of failure will depend upon the orientation of the disturbing force in relation to the orientation of the supporting planes. These kinematic tests for sliding are illustrated by equations 3.16, 3.17, 3.20, 3.21, 3.22 and 3.23 for a tetrahedron supported on two base planes. The kinematic tests for rotation are given in Table 3.1. The orientation of the resultant disturbing force which will cause various modes of failure for a wedge supported on two base planes as shown in Fig. 4.13 by the graphical method using stereonets. Equations 3.81-3.93 are kinematic tests to determine the sliding mode for a tetrahedron bounded by 3 base planes by means of vector analysis. Fig. 4.17 illustrates the method of determining the mode of sliding of a tetrahedron bounded by 3 base planes by utilization of stereonets.

(4) after the mode of failure is determined the maximum shearing resistance which can be mobilized in the direction of movement is compared to the shearing forces necessary for equilibrium to obtain a factor of safety. This step has been illustrated by the many example problems worked in Chapters 3 and 4.

The detailed analyses given in Chapters 3 and 4 can be used to solve most of the problems which arise in the calculation of rock slope stability. A majority of the real problems which arise however are



wedges acted on by their own weight, partially submerged beneath a phreatic surface, and resting on two base planes. The influence of external loads is small relative to the weight of the wedge. For this case, which has been the most common field case encountered by the authors, there are several approximate generalizations which can be made such that all the details of analyses presented in Chapters 3 and 4 are not necessary to obtain a fairly accurate answer to the problem. First of all for a wedge resting on two base planes, acted on by only its own weight, sliding will occur along the line of intersection of the two planes if a line drawn down the dip in both planes tends to intersect the line of intersection. If in either one of the planes a line drawn down the dip is directed away from the line of intersection then sliding will occur on that plane only and the wedge will move away from the line of intersection. If a wedge is acted on by its own weight, it will slide down the maximum dip if sliding occurs on one plane and the factor of safety can be easily computed. If it is determined above that sliding will take place along the line of intersection, the slope of the line of intersection,  $\alpha$ , as shown in Fig. 6.1, should be determined immediately by means of graphics. The angle of friction  $\phi$  required for stability will always be equal to or less than  $\alpha$  if there are no pore pressures on the joint surfaces. The next step is to determine the angle,  $\beta$ , included between planes 1 and 2 in a plane perpendicular to the line of intersection OA as shown in Fig. 6.1. The smaller angle  $\beta$ , the lower the value of  $\phi$  required for stability. As  $\beta$  approaches zero, the value of  $\phi$  required for stability approaches zero; and, as  $\beta$  approaches  $180^\circ$  the value of  $\phi$  required for stability

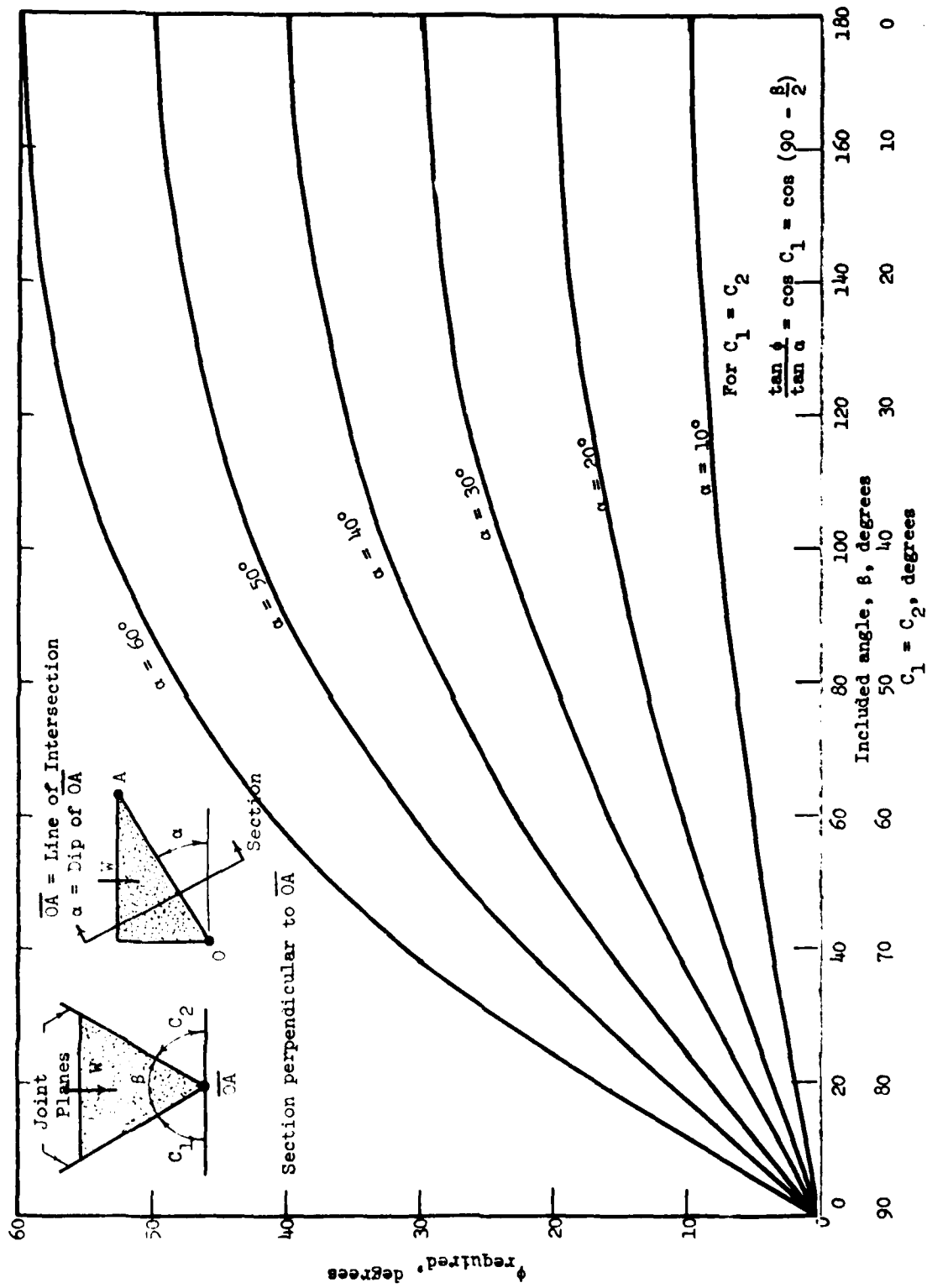


FIG. 6.1.1. FRICTION ANGLE REQUIRED FOR STABILITY OF WEDGE OF WEIGHT,  $W$ , FOR  $C_1 = C_2$

approaches  $\alpha$ . The next step is to determine the skewness  $\gamma$  of the wedge as shown in Fig. 6.2. For the non-skewed or symmetrical case ( $C_1 = C_2$  and  $\gamma = 0$ , as shown in Fig. 6.1) the  $\phi$  required for a factor of 1.0 for various values of  $\beta$  and  $\alpha$  are shown in Fig. 6.1. If the angle of shearing resistance  $\phi$  is the same on both planes 1 and 2, the value of  $\phi$  required for stability is less for the symmetrical case ( $C_1 = C_2$ , Fig. 2) than for the skewed case ( $C_1 \neq C_2$ ) for the same values of  $\alpha$  and  $\beta$ . Figure 6.2 illustrates the effect of skewing the planes on the value of  $\phi$  required for a factor of safety of 1.0. From Fig. 6.2 the value of  $\phi$  required for a factor of safety of 1.0 can be determined from the value of  $\tan \phi / \tan \alpha$  for various values of  $\beta$  and  $\gamma$  where  $\gamma$  is a measure of the skewness of the wedge as shown in Fig. 6.2. The curve labeled  $C_1 = C_2$  ( $\gamma = 0$ ) in Fig. 6.2 summarizes the curves presented in Fig. 6.1 for the symmetrical case. The additional curves presented in Fig. 6.2 illustrate the effect of skewing. These curves illustrate the sensitivity of the value of  $\phi$  required to skewing. For values of  $\gamma$  less than  $20^\circ$  the  $\tan \phi_{\text{required}} / \tan \alpha$  values are increased by only 6 percent above the values for  $\gamma = 0$ . However if the wedge is skewed  $60^\circ$  ( $\gamma = 60^\circ$ ) then values of  $\tan \phi_{\text{required}} / \tan \alpha$  are approximately twice the values for  $\gamma = 0$ . For  $\gamma = 40^\circ$   $\tan \phi_{\text{required}} / \tan \alpha$  values are increased by approximately 30 percent from the case where  $\gamma = 0$ .

The five example problems shown below in Table 6.1 illustrate all the conditions which are considered in Fig. 6.2.

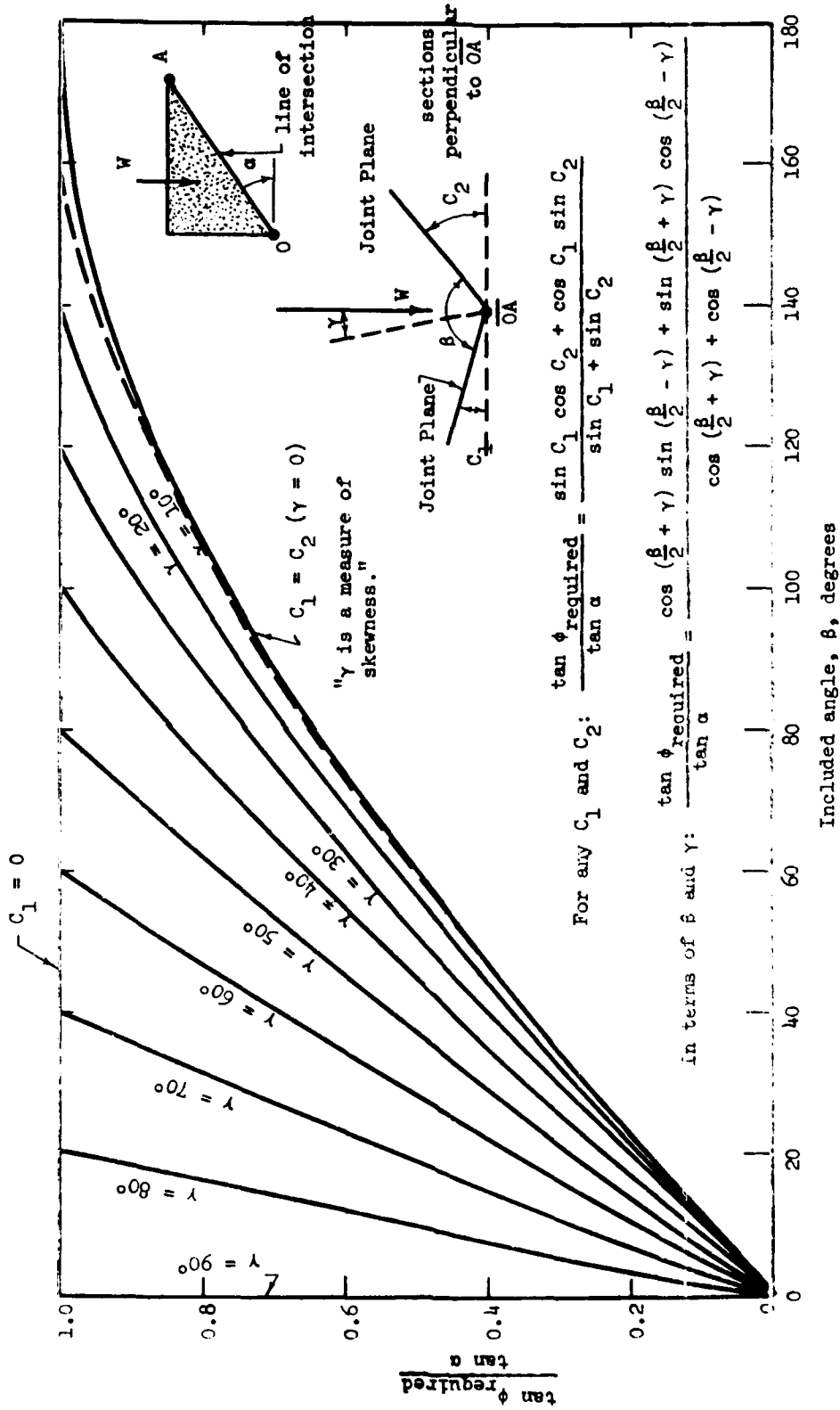


FIG. 6.2. TAN  $\phi$  REQUIRED FOR STABILITY OF A WEDGE OF WEIGHT, W FOR VARIOUS VALUES OF  $\beta$ ,  $\gamma$ , AND  $\alpha$

TABLE 6.1

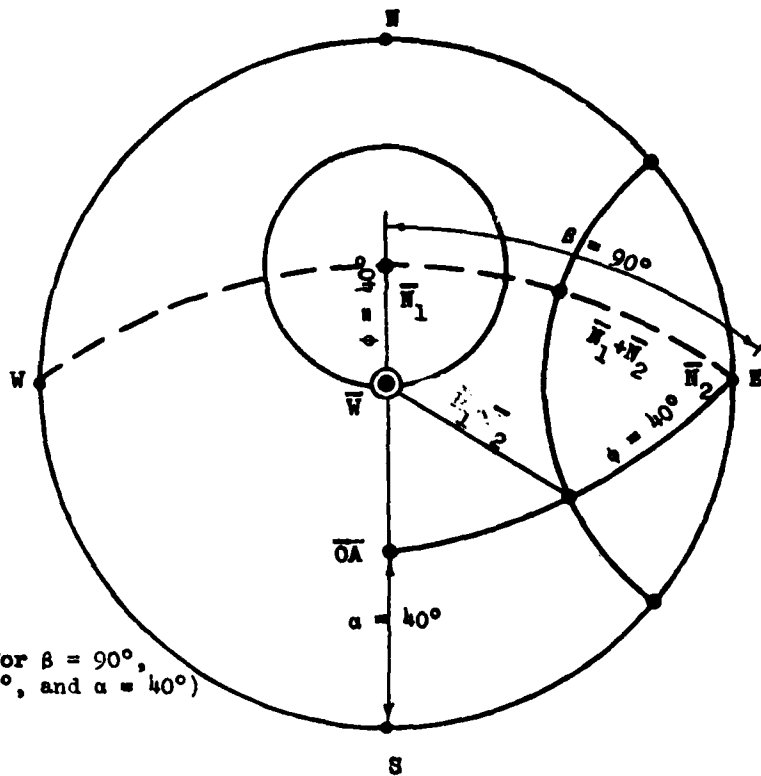
Case 1	$\beta=180^\circ$	$C_1=C_2=0$
Case 2	$C_1=0$	
Case 3	$\beta=0$	
Case 4	$C_1=C_2, \gamma=0$	
Case 5	$C_1 \neq C_2$	

Analysis of each of these five cases by the use of stereonets is illustrated in Figs. 6.3, 6.4, 6.5, 6.6, and 6.7.

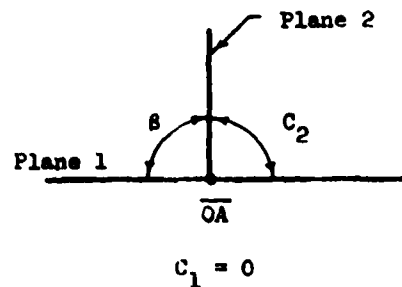
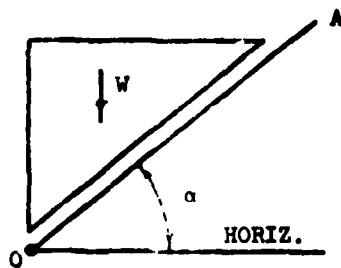
### 6.2 Dynamic Stability

The analysis of rock slopes in a static fashion by considering the inertia force as a static load (Wittke, 1965a) is not considered adequate for assessment of the dynamic behavior of rock slopes. In this report a method was given in sections 3.2.2 and 3.4.2 for calculating the dynamic resistance  $\overline{NW}$  for a rock slope by means of vector analysis. The calculation of the dynamic resistance by means of stereonets is given in section 4.3.4. The dynamic resistance  $\overline{NW}$  should then be used in the dynamic analysis proposed by Newmark (1965), which is explained and illustrated in Chapter 5. From this analysis the dynamic displacement is computed. This displacement should then be compared with the wavelength of the asperities on the failure planes as shown in Fig. 5.6 to determine if the dynamic displacement would be detrimental to the static stability of the slope. The calculation of the dynamic factor of safety using a pseudo static analysis has little meaning.





(shown for  $\beta = 90^\circ$ ,  
 $C_2 = 90^\circ$ , and  $\alpha = 40^\circ$ )



For F.S. = 1,  $\phi_{\text{required}} = \alpha$

FIG. 6.4. WEDGE ACTING UNDER OWN WEIGHT  
 CASE 2:  $C_1 = 0$ ,  $\beta$  and  $C_2 = \text{any value}$   
 (SINGLE PLANE CASE)

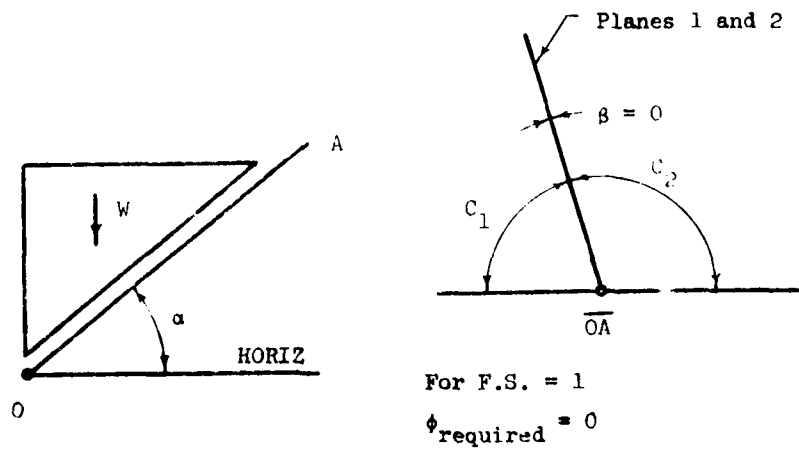
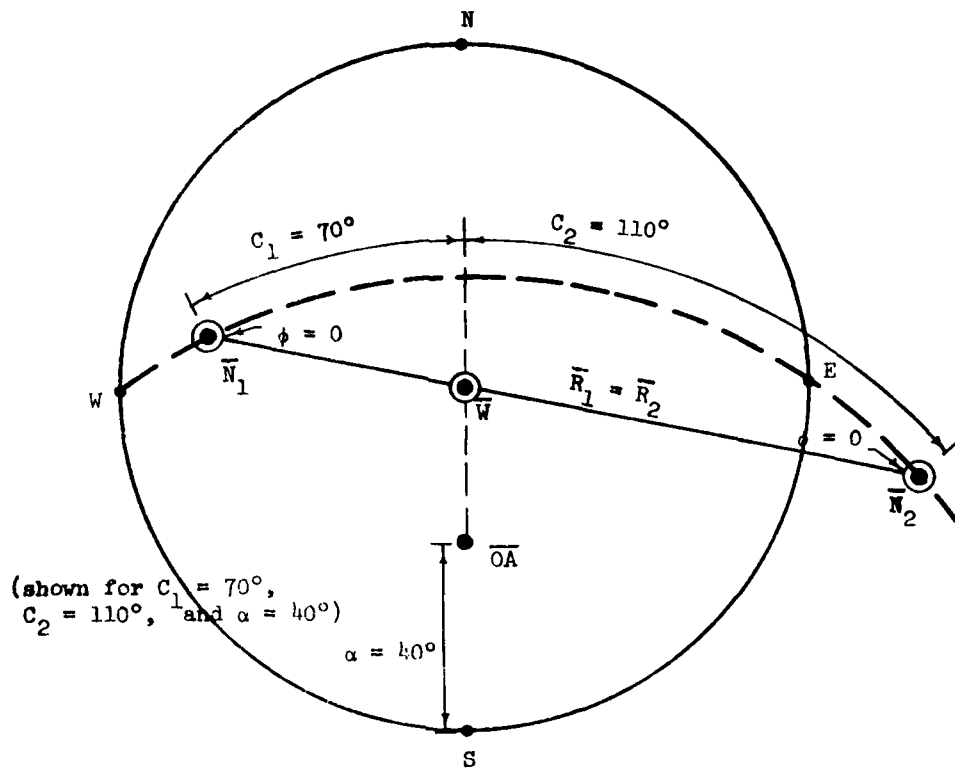
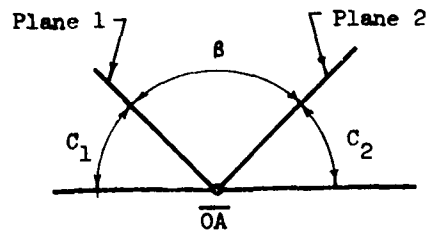
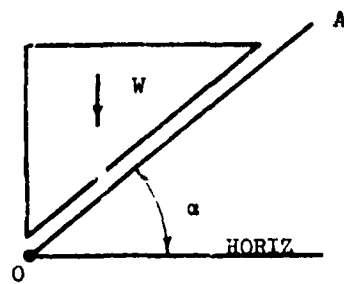
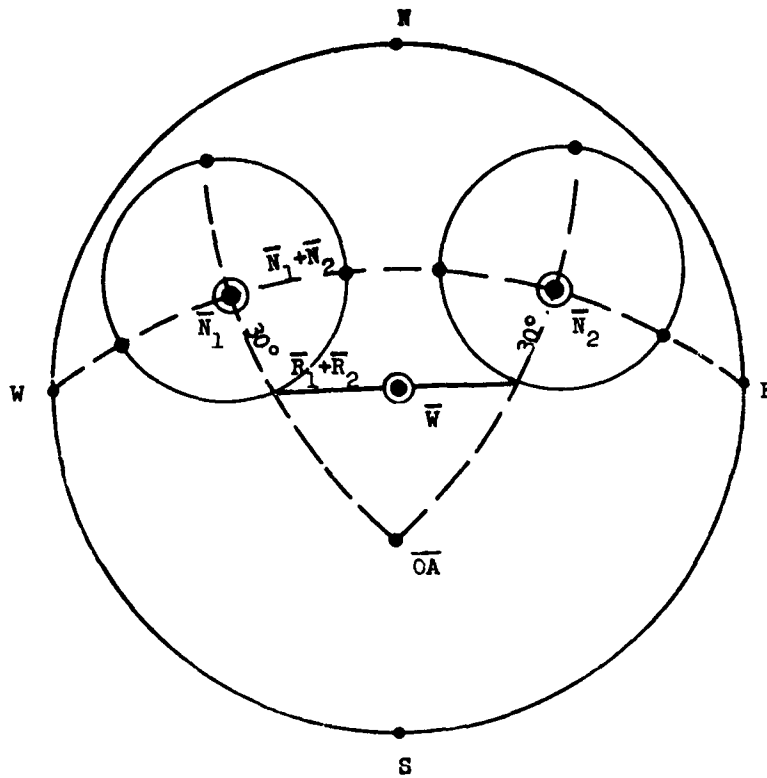


FIG. 6.5. WEDGE ACTING UNDER OWN WEIGHT  
CASE 3:  $\beta = 0$ ; ANY  $C_1, C_2, \alpha$

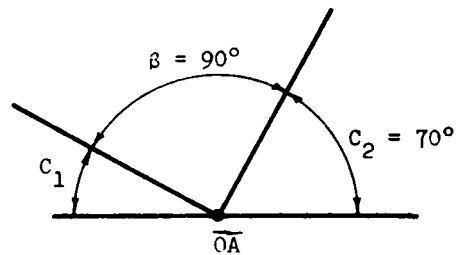
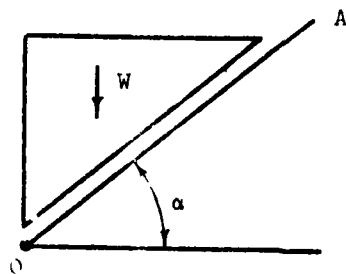
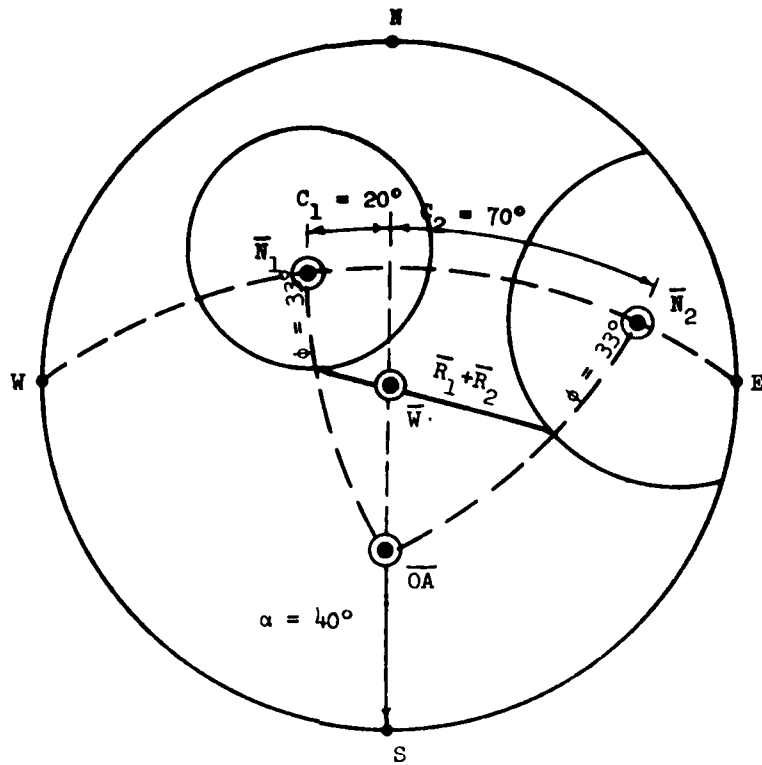




For F.S. = 1 and  $\beta > 0$ :  
 $\phi$  required  $< \alpha$

For F.S. = 1,  $C_1 = C_2 = 45^\circ$ ,  $\alpha = 40^\circ$   
 then  $\phi$  required =  $30^\circ$

FIG. 6.6. WEDGE ACTING UNDER OWN WEIGHT  
 CASE 4:  $C_1 = C_2 \neq 0$ ,  $\beta \neq 0$



For F.S. = 1 and  $\beta$  = same as Case 4:

$\phi_{\text{required}} (\text{Case 4}) < \phi_{\text{required}} (\text{Case 5}) < \alpha$

For F.S. = 1,  $\alpha = 40^\circ$ ,  $\beta = 90^\circ$ ,  $C_1 = 20^\circ$ ,  $C_2 = 70^\circ$  then  $\phi_{\text{required}} = 33^\circ$

FIG. 6.7. WEDGE ACTING UNDER OWN WEIGHT  
CASE 5:  $C_1 \neq C_2$ ,  $\beta \neq 0$

#### REFERENCES

- Goodman, R. E., (1964), "The Resolution of Stresses in Rock Using Stereographic Projection," International Journal of Rock Mechanics and Mining Science, Vol. 1, pp. 93-103.
- Goodman, R. E., and Taylor, R. L., (1967), "Methods of Analysis for Rock Slopes and Abutments: a Review of Recent Developments," Failure and Breakage of Rock, AIME, Chapter 12, pp. 303-320.
- John, Klaus W., (1968), "Graphical Stability Analysis of Slopes in Jointed Rock," Journal of the Soil Mechanics and Foundations Divisions, Proceedings, Vol. 94, SM2, pp. 497-526.
- Londe, Pierre, (1965), "Une Methode D'Analyse a Trois Dimensions De La Stabilité D'une Rive Rocheuse," Annales Des Ponts Et Chaussees, N° 1 De Janvier-Fevrier, pp. 37-60.
- Londe, P., (1968), "Stability of Rock Slopes Application to Dams," (in French), Annales de l'Institut Technique du Batiment et des Travaux Publics, Paris No. 69, Nov., pp. 1615-1638.
- Londe, P., G. Vigier, R. Vormeringer, (1969), "Stability of Rock Slopes, A Three-Dimensional Study," Proceedings, of ASCE, Vol. 95, No. SMI, January, pp. 235-262.
- Newmark, N., (1965) "Effects of Earthquakes on Dams and Embankments," Geotechnique, 15:140-141; 156.
- Wittke, W., (1964), "Ein rechnerischer Weg zur Ermittlung der Standsicherheit von Boschungen in Fels mit durchgehenden, ebenen Absonderungsflächen," Principles in the Field of Geomechanics, Rock Mechanics and Engineering Geology, Supplementum I, 14th Symposium of the Austrian Regional Group (i.f.) of the International Society for Rock Mechanics, Salzburg, 27 und 28 September 1963, pp. 101-129.
- Wittke, W., (1965a), "Verfahren zur Berechnung der Standsicherheit belasteter und unbelasteter Felsboschungen," Rock Mechanics and Engineering Geology Supplementum II, 15th Symposium of the Austrian Regional Group (i.f.) of the International Society for Rock Mechanics, Salzburg, 25 und 25 September 1964, pp. 52-79.
- Wittke, W., (1965b), "Verfahren zur Standischerheitsberechnung starrer, auf ebenen Flächen gelagerter Körper und die Anwendung der Ergebnisse auf die Standischerheitsberechnung von Felsboschungen," Veröffentlichungen, des Institutes für Bodenmechanik und Grundbau der Technischen Hochschule Fridericiana in Karlsruhe, Heft 20.
- Wittke, W., (1966), "Berechnungsmöglichkeiten der Standsicherheit von Boschungen in Fels," Deutsche Gesellschaft für Erd- und Grundbau e.V.

APPENDIX A  
COMPUTER PROGRAMS  
for the  
STABILITY OF ROCK SLOPES

## PROGRAM #1

This program is for the analysis of a rock tetrahedron supported on two planes and acted on by its own weight. The program is coded in FORTRAN IV language. The format and definition of parameters are given below.

### INPUT PARAMETERS

CARD 1 Format (10F7.2)

<u>Parameter</u>	<u>Card Column</u>	<u>Definition of Parameter</u>
BETA 1	1 - 7	Strike of plane 1
BETA 2	8 - 14	Strike of plane 2
GAMMA 1	15-- 21	Dip of plane 1
GAMMA 2	22 - 28	Dip of plane 2
PHI 1	29 - 35	Angle of Shearing Resistance on plane 1
PHI 2	36 42	Angle of Shearing Resistance on plane 2
ALPHA	43 - 49	$\alpha$ , Slope angle as shown in Fig. 3.9
DELTA	50 - 56	$\delta$ , Slope angle as shown in Fig. 3.9
H	57 - 63	Height of slope as shown in Fig. 3.9
Q	64 - 70	Desired factor of safety for design

### OUTPUT PARAMETERS

<u>Parameter</u>	<u>Definition of Parameter</u>
UX(1) UY(1) UZ(1)	x, y, and z components of a unit vector $\bar{U}$ in the direction of the strike of plane 1.
VX(1) VY(1) VZ(1)	x, y, and z components of a unit vector $\bar{V}$ in the direction of the dip of plane 1.
WX(1) WY(1) WZ(1)	x, y, and z components of a unit vector $\bar{W}$ in a direction normal to plane 1.
UX(2) UY(2) UZ(2)	x, y, and z components of a unit vector $\bar{U}$ in the direction of the strike of plane 2.
VX(2) VY(2) VZ(2)	x, y, and z components of a unit vector $\bar{V}$ in the direction of the dip of plane 2.

WX(2)	x, y, and z components of a unit vector $\bar{W}$ in a direction normal to plane 2.
WY(2)	
WZ(2)	
XX	x, y, and z components of a vector $\bar{X}$ directed along the line of intersection of planes 1 and 2.
XY	
XZ	
X	The magnitude of the vector $\bar{X}$ .
FS	Factor of safety.

Definition of Parameters Calculated in Program in Intermediate Steps

ODX	x, y, and z components of line OD, Fig. 3.9
ODY	
ODZ	
OCX	x, y, and z components of line OC, Fig. 3.9
OCY	
OCZ	
OBX	x, y, and z components of line OB, Fig. 3.9
OBY	
OBZ	
OSX	x, y, and z components of line OS, Fig. 3.9
OSY	
OSZ	
RX	x, y, and z components of resultant force action on tetrahedron (Note: since this program is for a slope acted on by its own weight RX and R <sub>i</sub> are always zero and RZ is taken as -1 unit since the magnitude of the weight does not affect the factor of safety.)
RY	
RZ	
EMX	Moment about the line of intersection of planes 1 and 2 of the weight of the tetrahedron applied through the center of gravity of the tetrahedron.
EN(J)	Magnitude of the normal component of the vector $\bar{R}$ on plane J
TX(J)	x, y, and z components of the tangential component of the vector $\bar{R}$ on plane J
TY(J)	
TZ(J)	
T(J)	Magnitude of the tangential component of the vector $\bar{R}$ on plane J
SX1	x, y, and z components of the vector ${}_z\bar{S}_{12}$ shown in Fig. 3.5(b)
SY1	
SZ1	
SX2	x, y, and z components of the vector ${}_z\bar{S}_{12}$ shown in Fig. 3.5(b)
SY2	
SZ2	

COMPUTER PROGRAM #1

```

C   STABILITY ANALYSIS OF ROCK SLOPES
    DIMENSION B(2),C(2),PHI(2),EN(2),UX(2),UY(2),UZ(2),VX(2),VY(2),
    1VZ(2),WX(2),WY(2),WZ(2),TX(2),TY(2),TZ(2),T(2)
    READ (5,11) BETA1,BETA2,GAMMA1,GAMMA2,PHI1,PHI2,ALPHA,DELTA,H,Q
11  FORMAT (10F7.2)
    WRITE (6,12) BETA1,BETA2,GAMMA1,GAMMA2,PHI1,PHI2,ALPHA,DELTA,H,Q
12  FORMAT (1H1,9X,8HBETA1 =,F7.1,8H DEGREES,10X,8HBETA2 =,F7.1,
    18H DEGREES/10X,8HGAMMA1 =,F7.1,8H DEGREES,10X,8HGAMMA2 =,F7.1,
    28H DEGREES/10X,8HPHI1 =,F7.1,8H DEGREES,10X,8HPHI2 =,F7.1,
    38H DEGREES/10X,8HALPHA =,F7.1,8H DEGREES,10X,8HDELTA =,F7.1,
    48H DEGREES/10X,8HEIGHT =,F7.1,4HFEET,14X,8HQ =,F7.2)
    B(1) = BETA1 / (180.0/3.141593)
    B(2) = BETA2 / (180.0/3.141593)
    C(1) = GAMMA1 / (180.0/3.141593)
    C(2) = GAMMA2 / (180.0/3.141593)
    PHI(1) = PHI1 / (180.0/3.141593)
    PHI(2) = PHI2 / (180.0/3.141593)
    A = ALPHA / (180.0/3.141593)
    D = DELTA / (180.0/3.141593)
    DO 101 K=1,2
    UX(K) = COS(B(K))
    UY(K) = SIN(B(K))
    UZ(K) = 0.0
    VX(K) = COS(C(K))*SIN(B(K))
    VY(K) = -COS(C(K))*COS(B(K))
    VZ(K) = -SIN(C(K))
    WX(K) = (UY(K)*VZ(K)) - (UZ(K)*VY(K))
    WY(K) = (UZ(K)*VX(K)) - (UX(K)*VZ(K))
101  WZ(K) = (UX(K)*VY(K)) - (UY(K)*VX(K))
    WRITE (6,13) UX(1),UY(1),UZ(1),VX(1),VY(1),VZ(1),WX(1),WY(1),WZ(1)
13  FORMAT(1H0,9X,4HU1 =,F6.3,1H,,2X,F6.3,1H,,2X,F6.3/
    1      10X,4HV1 =,F6.3,1H,,2X,F6.3,1H,,2X,F6.3/
    2      10X,4HW1 =,F6.3,1H,,2X,F6.3,1H,,2X,F6.3)
    WRITE (6,14) UX(2),UY(2),UZ(2),VX(2),VY(2),VZ(2),WX(2),WY(2),WZ(2)
14  FORMAT(1H0,9X,4HU2 =,F6.3,1H,,2X,F6.3,1H,,2X,F6.3/
    1      10X,4HV2 =,F6.3,1H,,2X,F6.3,1H,,2X,F6.3/
    2      10X,4HW2 =,F6.3,1H,,2X,F6.3,1H,,2X,F6.3)
    XX = (WY(2)*WZ(1) - WZ(2)*WY(1))
    XY = (WZ(2)*WX(1) - WX(2)*WZ(1))
    XZ = (WX(2)*WY(1) - WY(2)*WX(1))
    X = SQRT(XX**2 + XY**2 + XZ**2)
    WRITE (6,15) XX,XY,XZ,X
15  FORMAT(1H0,9X,4HX =,F6.3,1H,,2X,F6.3,1H,,2X,F6.3,5X,8HABS(X) =,
    1F6.3)
    ODX = -(H*COS(C(1))/(SIN(C(1))*SIN(B(1)))) + (H*COS(A)*COS(B(1))/
    1      (SIN(A)*SIN(B(1))))
    ODY = H*COS(A)/SIN(A)
    ODZ = H
    OCX = -(H*COS(C(2))/(SIN(C(2))*SIN(B(2)))) + (H*COS(A)*COS(B(2))/
    1      (SIN(A)*SIN(B(2))))
    OCY = H*COS(A)/SIN(A)
    OCZ = H
  
```

```

AAA =(SIN(A)/COS(A))-(XZ/XY)
BBB =(XZ/XY)-(SIN(D)/COS(D))
FFF=(SIN(D)*COS(A))/(COS(D)*SIN(A))
HH = H*AAA*FFF/BBB
CCC =(H+HH)/XZ
OBX = CCC*XX
OBY = CCC*XY
OBZ = CCC*XZ
OSX =(OBX+OCX+ODX)/4.0
OSY =(OBY+OCY+ODY)/4.0
OSZ =(OBZ+OCZ+ODZ)/4.0
RX = 0.0
RY = 0.0
RZ =-1.0
EMX = XX*(OBY-RZ-OSY*RY)+XY*(OSZ*RX-OSX*RZ)+XZ*(OSX*RY-OSY*RX)
IF (EMX) 102,103,104
104 WRITE(6,105)
105 FORMAT(1H0,9X,29HRESULTANT INTERSECTS PLANE E1)
J = 1
110 EN(J)= RX*WX(J)+RY*WY(J)+RZ*WZ(J)
TX(J)= RX-EN(J)*WX(J)
TY(J)= RY-EN(J)*WY(J)
TZ(J)= RZ-EN(J)*WZ(J)
T(J) = SQRT(TX(J)**2 +TY(J)**2 +TZ(J)**2 )
FS = EN(J)*SIN(PHI(J))/(T(J)*COS(PHI(J)))
IF (FS.LT.Q) GO TO 106
108 WRITE(6,107) FS,J
107 FORMAT(1H0,9X,4HFS =,F5.2,10X,25HSLIDING OCCURS ON PLANE E,1I)
GO TO 200
106 IF(J.EQ.1) GO TO 111
GO TO 112
111 SX1 = (XY*WZ(1)-XZ*WY(1))/X
SY1 = (XZ*WX(1)-XX*WZ(1))/X
SZ1 = (XX*WY(1)-XY*WX(1))/X
DDD1= TX(1)*SX1+TY(1)*SY1+TZ(1)*SZ1
IF(DDD1.LE.0.0) GO TO 108
GO TO 103
102 WRITE (6,109)
109 FORMAT(1H0,9X,29HRESULTANT INTERSECTS PLANE E2)
J = 2
GO TO 110
112 SX2 =-(XY*WZ(2)-XZ*WY(2))/X
SY2 =-(XZ*WX(2)-XX*WZ(2))/X
SZ2 =-(XX*WY(2)-XY*WX(2))/X
DDD2= TX(2)*SX2+TY(2)*SY2+TZ(2)*SZ2
IF (DDD2.LE.0.0) GO TO 108
103 T12 = (RX*XX+RY*XY+RZ*XZ)/X
EN12X= RX-T12*XX/X
EN12Y= RY-T12*XY/X
EN12Z= RZ-T12*XZ/X
EEE =-WX(1)*WY(2)+WY(1)*WX(2)
EEE1 =-EN12X*WY(2)+EN12Y*WX(2)
EEE2 =+WX(1)*EN12Y-WY(1)*EN12X
ENN1 + EEE1/EEE

```



```
ENN2 = EEE2/EEE
FS=((ENN1*SIN(PHI(1))/COS(PHI(1)))+(ENN2*SIN(PHI(2))/COS(PHI(2))))
1/T12
WRITE (6,113) FS
113  FORMAT(1H0,9X,4HFS =,F5.2,10X,4HSLIDING OCCURS ALONG THE LINE OF
2INTERSECTION)
200  STOP
    END
```

```
* DATA
```

## PROGRAM #2

This program is for the analysis of a rock tetrahedron supported by 3 planes and acted on by its own weight, an external force, and porewater forces on each of the three support planes. The program is coded in FORTRAN IV language. The format and definitions of parameters are given below.

### INPUT PARAMETERS

CARD 1   FORMAT (9F5.1)

<u>Parameter</u>	<u>Card Column</u>	<u>Definition of Parameter</u>
BETA 1	1 - 5	Strike of plane 1
BETA 2	6 - 10	Strike of plane 2
BETA 3	11 - 15	Strike of plane 3
GAMMA 1	16 - 20	Dip of plane 1
GAMMA 2	21 - 25	Dip of plane 2
GAMMA 3	26 - 30	Dip of plane 3
PHI 1	31 - 35	Angle of Shearing Resistance on plane 1
PHI 2	36 - 40	Angle of Shearing Resistance on plane 2
PHI 3	41 - 45	Angle of Shearing Resistance on plane 3

CARD 2   FORMAT (7F7.2)

WT	1 - 7	Weight of the rock tetrahedron being analyzed
QX	8 - 14	z, y and z components of a force Q applied to the tetrahedron
QY	15 - 21	
QZ	22 - 28	
UP 1	29 - 35	Magnitude of the porewater force on plane 1
UP 2	36 - 42	Magnitude of the porewater force on plane 2
UP 3	43 - 49	Magnitude of the porewater force on plane 3

### OUTPUT PARAMETERS

<u>Parameter</u>	<u>Definition of Parameter</u>
UX(1)	x, y, and z components of a unit vector in the direction of the strike of plane 1
UY(1)	
UZ(1)	
VX(1)	x, y, and z components of a unit vector in the direction of the dip of plane 1
VY(1)	
VZ(1)	
WX(1)	x, y, and z components of a unit vector in the direction normal to plane 1
WY(1)	
WZ(1)	

UX(2)	x, y, and z components of a unit vector in the direction of
UY(2)	the strike of plane 2
UZ(2)	
VX(2)	x, y, and z components of a unit vector in the direction of
VY(2)	the dip of plane 2
VZ(2)	
WX(2)	x, y, and z components of a unit vector in the direction
WY(2)	normal to plane 2
WZ(2)	
UX(3)	x, y and z components of a unit vector in the direction of
UY(3)	the strike of plane 3
UZ(3 )	
VX(3)	x, y, and z components of a unit vector in the direction
VY(3)	of the dip of plane 3
VZ(3)	
WX(3)	x, y, and z components of a unit vector in the direction
WY(3)	normal to plane 3
WZ(3)	
X12X	x, y, and z components of a vector, $\bar{x}_{12}$ , in the direction
X12Y	of the line of intersection of planes 1 and 2 as shown
X12Z	in Fig. 3.14
X12	the magnitude of the vector $\bar{x}_{12}$
X23X	x, y, and z components of a vector, $\bar{x}_{23}$ , in the direction of
X23Y	the line of intersection of planes 2 and 3 as shown in Fig. 3.14
X23Z	
X23	the magnitude of the vector $\bar{x}_{23}$
X31X	x, y, and z components of a vector, $\bar{x}_{31}$ in the direction of the
X31Y	line of intersection of planes 1 and 3 as shown in Fig. 3.14
X31Z	
X31	the magnitude of the vector $\bar{x}_{31}$
S121X	x, y, and z components of vector ${}_1\bar{s}_{13}$ shown in Fig. 3.14
S121Y	
S121Z	
S122X	x, y, and z components of vector ${}_2\bar{s}_{12}$ shown in Fig. 3.14
S122Y	
S122Z	
S232X	x, y, and z components of vector ${}_2\bar{s}_{23}$ shown in Fig. 3.14
S232Y	
S232Z	

S233X x, y, and z components of vector  ${}_3\bar{S}_{23}$  shown in Fig. 3.14  
S233Y  
S233Z

S313X x, y, and z components of vector  ${}_3\bar{S}_{31}$  shown in Fig. 3.14  
S313Y  
S313Z

S311X x, y, and z components of vector  ${}_1\bar{S}_{31}$  shown in Fig. 3.14  
S311Y  
S311Z

(Sliding tends to occur along  $\bar{X}_{12}$  on planes 1 and 2)

FS Factor of Safety  
EN1 Normal force on plane 1  
EN2 Normal force on plane 2  
T12 Component of disturbing forces parallel to the line of intersection of planes 1 and 2

(Sliding tends to occur along  $\bar{X}_{23}$  on planes 2 and 3)

FS Factor of Safety  
EN2 Normal force on plane 2  
EN3 Normal force on plane 3  
T23 Component of disturbing forces parallel to the line of intersection of planes 2 and 3

(Sliding tends to occur along  $\bar{X}_{31}$  on planes 1 and 3)

FS Factor of Safety  
EN3 Normal force on plane 3  
EN1 Normal force on plane 1  
T31 Component of disturbing forces parallel to the line of intersection of planes 1 and 3

(Sliding tends to occur on plane 1)

FS Factor of Safety  
EN1 Normal force on plane 1  
T1 Tangential force on plane 1

(Sliding tends to occur on plane 2)

FS Factor of Safety  
EN2 Normal force on plane 2  
T2 Tangential force on plane 2

(Sliding tends to occur on plane 3)

FS Factor of safety  
EN3 Normal Force on plane 3  
T3 Tangential force on plane 3

Note: Tests 1 through 12 in program #2 are used to determine the mode of sliding as can be determined from eqs. 3.69, 3.70, 3.71, 3.81, 3.82, 3.83, 3.84, 3.85, 3.86, 3.87, 3.88, 3.89, 3.90, 3.91, 3.92, 3.93, 3.94, 3.95, 3.96, 3.97, and 3.98.

COMPUTER PROGRAM # 2

```

C   STABILITY ANALYSIS OF ROCK SLOPES-THREE INTERSECTING JOINT SETS

   DIMENSION B(3),C(3),GAMMA(3),VX(3),VY(3),VZ(3),UX(3),UY(3),
1  UZ(3),WX(3),WY(3),WZ(3)
   DO 200 IJK=1,2
   READ (5,11) BETA1,BETA2,BETA3,GAMMA(1),GAMMA(2),GAMMA(3),PHI1,
1  PHI2,PHI3,WT,QX,QY,QZ,UP1,UP2,UP3
11  FORMAT (9F5.1/7F7.2)
   WRITE (6,12) BETA1,BETA2,BETA3,GAMMA(1),GAMMA(2),GAMMA(3),PHI1,
1  PHI2,PHI3,WT,QX,QY,QZ,UP1,UP2,UP3
12  FORMAT(1H1,8X,8HBETA1 =,F5.1,5H DEG.,14X,8HBETA2 =,F5.1,5H DEG.,
1  14X,8HBETA3 =,F5.1,5H DEG.,//9X,8HGAMMA1 =,F5.1,5H DEG.,14X,
28HGAMMA2 =,F5.1,5H DEG.,14X,8HGAMMA3 =,F5.1,5H DEG.//9X,8HPHI1 =
3,F5.1,5H DEG.,14X,8HPHI2 =,F5.1,5H DEG.,14X,8HPHI3 =,F5.1,5H D
4EG.//9X,4HWT =,F7.2,5X,4HQX =,F7.2,5X,4HQY =,F7.2,5X,4HQZ =,F7.2,
55X,5HUP1 =,F7.2,5X,5HUP2 =,F7.2,5X,5HUP3 =,F7.2)
   B(1) = BETA1/(180.0/3.141593)
   B(2) = BETA2/(180.0/3.141593)
   B(3) = BETA3/(180.0/3.141593)
   C(1) = GAMMA(1)/(180.0/3.141593)
   C(2) = GAMMA(2)/(180.0/3.141593)
   C(3) = GAMMA(3)/(180.0/3.141593)
   PHI1 = PHI1/(180.0/3.141593)
   PHI2 = PHI2/(180.0/3.141593)
   PHI3 = PHI3/(180.0/3.141593)
   DO 201 K=1,3
   UX(K) = COS(B(K))
   UY(K) = SIN(B(K))
   UZ(K) = 0.0
   VX(K) = COS(C(K))*SIN(B(K))
   VY(K) = -COS(C(K))*COS(B(K))
   VZ(K) = -SIN(C(K))
   WX(K) = (UY(K)*VZ(K))-(UZ(K)*VY(K))
   WY(K) = (UZ(K)*VX(K))-(UX(K)*VZ(K))
   WZ(K) = (UX(K)*VY(K))-(UY(K)*VX(K))
   IF(GAMMA(K).GT.90.0) GO TO 201
   WX(K) = -WX(K)
   WY(K) = -WY(K)
   WZ(K) = -WZ(K)
201 CONTINUE
   WRITE (6,13) UX(1),UY(1),UZ(1),VX(1),VY(1),VZ(1),WX(1),WY(1),WZ(1)
13  FORMAT(1H0,9X,4HU1 =,F6.3,1H,,2X,F6.3,1H,,2X,F6.3/
1  10X,4HV1 =,F6.3,1H,,2X,F6.3,1H,,2X,F6.3/
2  10X,4HW1 =,F6.3,1H,,2X,F6.3,1H,,2X,F6.3)
   WRITE (6,14) UX(2),UY(2),UZ(2),VX(2),VY(2),VZ(2),WX(2),WY(2),WZ(2)
14  FORMAT(1H0,9X,4HU2 =,F6.3,1H,,2X,F6.3,1H,,2X,F6.3/
1  10X,4HV2 =,F6.3,1H,,2X,F6.3,1H,,2X,F6.3/
2  10X,4HW2 =,F6.3,1H,,2X,F6.3,1H,,2X,F6.3)
   WRITE(6,115) UX(3),UY(3),UZ(3),VX(3),VY(3),VZ(3),WX(3),WY(3),WZ(3)
115 FORMAT(1H0,9X,4HU3 =,F6.3,1H,,2X,F6.3,1H,,2X,F6.3/

```

```

1      10X,4HV3 =,F6.3,1H,,2X,F6.3,1H,,2X,F6.3/
2      10X,4HW3 =,F6.3,1H,,2X,F6.3,1H,,2X,F6.3)
W1X = WX(1)
W1Y = WY(1)
W1Z = WZ(1)
W2X = WX(2)
W2Y = WY(2)
W2Z = WZ(2)
W3X = WX(3)
W3Y = WY(3)
W3Z = WZ(3)
X12X=W2Y*W1Z-W2Z*W1Y
X12Y=W2Z*W1X-W2X*W1Z
X12Z=W2X*W1Y-W2Y*W1X
X12=SQRT(X12X**2+X12Y**2+X12Z**2)
X23X=W3Y*W2Z-W3Z*W2Y
X23Y=W3Z*W2X-W3X*W2Z
X23Z=W3X*W2Y-W3Y*W2X
X23 =SQRT(X23X**2+X23Y**2+X23Z**2)
X31X=W1Y*W3Z-W1Z*W3Y
X31Y=W1Z*W3X-W1X*W3Z
X31Z=W1X*W3Y-W1Y*W3X
X31 =SQRT(X31X**2+X31Y**2+X31Z**2)
WRITE(6,15) X12X,X12Y,X12Z,X12,X23X,X23Y,X23Z,X23,X31X,X31Y,X31Z,
1X31
15  FORMAT(1H0,9X,5HX12 =,2(F6.3,1H,,2X),F6.3,5X,10HABS(X12) =,F6.3//
1      10X,5HX23 =,2(F6.3,1H,,2X),F6.3,5X,10HABS(X23) =,F6.3//
2      10X,5HX31 =,2(F6.3,1H,,2X),F6.3,5X,10HABS(X31) =,F6.3)
RX= QX + UP1*W1X + UP2*W2X + UP3*W3X
RY= QY + UP1*W1Y + UP2*W2Y + UP3*W3Y
RZ= QZ + UP1*W1Z + UP2*W2Z + UP3*W3Z + WT
S121X= W1Y*X12Z-W1Z*X12Y
S121Y= W1Z*X12X-W1X*X12Z
S121Z= W1X*X12Y-W1Y*X12X
S122X= X12Y*W2Z-X12Z*W2Y
S122Y= X12Z*W2X-X12X*W2Z
S122Z= X12X*W2Y-X12Y*W2X
S232X= W2Y*X23Z-W2Z*X23Y
S232Y= W2Y*X23X-W2X*X23Z
S232Z= W2X*X23Y-W2Y*X23X
S233X= X23Y*W3Z-X23Z*W3Y
S233Y= X23Z*W3X-X23X*W3Z
S233Z= X23X*W3Y-X23Y*W3X
S313X= W3Y*X31Z-W3Z*X31Y
S313Y= W3Z*X31X-W3X*X31Z
S313Z= W3X*X31Y-W3Y*X31X
S311X= X31Y*W1Z-X31Z*W1Y
S311Y= X31Z*W1X-X31X*W1Z
S311Z= X31X*W1Y-X31Y*W1X
WRITE(6,121) S121X,S121Y,S121Z,S122X,S122Y,S122Z,S232X,S232Y,
1S232Z,S233X,S233Y,S233Z,S313X,S313Y,S313Z,S311X,S311Y,S311Z
121  FORMAT(1H0,9X,5HS121=,2(F6.3,1H,,2X),F6.3,5X,5HS122=,2(F6.3,1H,,
12X),F6.3//10X,5HS232=,2(F6.3,1H,,2X),F6.3,5X,5HS233=,2(F6.3,1H,,
22X),F6.3//10X,5HS313=,2(F6.3,1H,,2X),F6.3,5X,5HS311=,2(F6.3,1H,,

```

```

32X),F6.3)
TEST1 =RX*X12X+RY*X12Y+RZ*X12Z
TEST2 =RX*X23X+RY*X23Y+RZ*X23Z
TEST3 =RX*X31X+RY*X31Y+RZ*X31Z
TEST4 =RX*W1X+RY*W1Y+RZ*W1Z
TEST5 =RX*W2X+RY*W2Y+RZ*W2Z
TEST6 =RX*W3X+RY*W3Y+RZ*W3Z
TEST7 =RX*S121X+RY*S121Y+RZ*S121Z
TEST8 =RX*S122X+RY*S122Y+RZ*S122Z
TEST9 =RX*S232X+RY*S232Y+RZ*S232Z
TEST10=RX*S233X+RY*S233Y+RZ*S233Z
TEST11=RX*S313X+RY*S313Y+RZ*S313Z
TEST12=RX*S311X+RY*S311Y+RZ*S311Z
IF(TEST1.GE.0.0.AND.TEST7.LE.0.0.AND.TEST8.LE.0.0) GO TO 101
IF(TEST2.GE.0.0.AND.TEST9.LE.0.0.AND.TEST10.LE.0.0) GO TO 102
IF(TEST3.GE.0.0.AND.TEST11.LE.0.0.AND.TEST12.LE.0.0) GO TO 103
IF(TEST4.LE.0.0.AND.TEST7.GE.0.0.AND.TEST12.GE.0.0) GO TO 104
IF(TEST5.LE.0.0.AND.TEST8.GE.0.0.AND.TEST9.GE.0.0) GO TO 105
IF(TEST6.LE.0.0.AND.TEST10.GE.0.0.AND.TEST11.GE.0.0) GO TO 106
IF(TEST4.GE.0.0.AND.TEST5.GE.0.0.AND.TEST6.GE.0.0) GO TO 119
101 WRITE(6,107)
107 FORMAT(1H0,9X,50HSLIDING TENDS TO OCCUR ALONG X12 ON PLANES 1 AND
12)
T12 = TEST1/X12
EN12X=RX-T12*X12X/X12
EN12Y=RY-T12*X12Y/X12
EN12Z=RZ-T12*X12Z/X12
EEE =W1X*W2Y-W2X*W1Y
IF (EEE.EQ.0.0) GO TO 122
EEE1=W2X*EN12Y-W2Y*EN12X
EEE2=W1Y*EN12X-W1X*EN12Y
EN1 =EEE1/EEE
EN2 =EEE2/EEE
GO TO 123
122 EEE=W1Y*W2Z-W1Z*W2Y
EEE1=W2Y*EN12Z-W2Z*EN12Y
EEE2=W1Z*EN12Y-W1Y*EN12Z
EN1=EEE1/EEE
EN2=EEE2/EEE
123 FS =((EN1*SIN(PHI1)/COS(PHI1))+(EN2*SIN(PHI2)/COS(PHI2)))/T12
WRITE(6,108) FS,EN1,EN2,T12
108 FORMAT(1H0,9X,4HFS =,F5.2,10X,5HEN1 =,F7.2,5X,5HEN2 =,F7.2,5X,5HT1
12 =,F7.2)
GO TO 200
102 WRITE(6,109)
109 FORMAT(1H0,9X,50HSLIDING TENDS TO OCCUR ALONG X23 ON PLANES 2 AND
13)
T23 = TEST2/X23
EN23X=RX-T23*X23X/X23
EN23Y=RY-T23*X23Y/X23
EN23Z=RZ-T23*X23Z/X23
EEE =W2X*W3Y-W3X*W2Y
IF(EEE.EQ.0.0) GO TO 124
EEE2 =W3X*EN23Y-W3Y*EN23X

```

```

      EEE3 =W2Y*EN23X-W2X*EN23Y
      EN2  =EEE2/EEE
      EN3  =EEE3/EEE
      GO TO 125
124  EEE=W2Y*W3Z-W2Z*W3Y
      EEE2=W3Y*EN23Z-W3Z*EN23Y
      EEE3=W2Z*EN23Y-W2Y*EN23Z
      EN2=EEE2/EEE
      EN3=EEE3/EEE
125  FS  =(((EN2*SIN(PHI2)/COS(PHI2)))+(EN3*SIN(PHI3)/COS(PHI3)))/T23
      WRITE(6,110) FS,EN2,EN3,T23
110  FORMAT(1H0,9X,4HFS =,F5.2,10X,5HEN2 =,F7.2,5X,5HEN3 =,F7.2,5X,5HT2
      T3 =,F7.2)
      GO TO 200
103  WRITE(6,111)
111  FORMAT(1H0,9X,50HSLIDING TENDS TO OCCUR ALONG X31 ON PLANES 3 AND
      11)
      T31 = TEST3/X31
      EN31X=RX-T31*X31X/X31
      EN31Y=RY-T31*X31Y/X31
      EN31Z=RZ-T31*X31Z/X31
      EEE =W3X*W1Y-W1X*W3Y
      IF(EEE.EQ.0.0) GO TO 126
      EEE3 =W1X*EN31Y-W1Y*EN31X
      EEE1 =W3Y*EN31X-W3X*EN31Y
      EN3  =EEE3/EEE
      EN1=EEE1/EEE
      GO TO 127
126  EEE=W3Y*W1Z-W3Z*W1Y
      EEE3=W1Y*EN31Z-W1Z*EN31Y
      EEE1=W3Z*EN31Y-W3Y*EN31Z
      EN3=EEE3/EEE
      EN1=EEE1/EEE
127  FS  =(((EN3*SIN(PHI3)/COS(PHI3)))+(EN1*SIN(PHI1)/COS(PHI1)))/T31
      WRITE(6,112) FS,EN3,EN1,T31
112  FORMAT(1H0,9X,4HFS =,F5.2,10X,5HEN3 =,F7.2,5X,5HEN1 =,F7.2,5X,5HT3
      T1 =,F7.2)
      GO TO 200
104  WRITE(6,113)
113  FORMAT(1H0,9X,33HSLIDING TENDS TO OCCUR ON PLANE 1)
      EN1 = -TEST4
      T1X = RX + EN1*W1X
      T1Y = RY + EN1*W1Y
      T1Z = RZ + EN1*W1Z
      T1 = SQRT(T1X**2+T1Y**2+T1Z**2)
      FS  = EN1*SIN(PHI1)/(COS(PHI1)*T1)
      WRITE(6,114) FS,EN1,T1
114  FORMAT(1H0,9X,4HFS =,F5.2,10X,5HEN1 =,F7.2,5X,5HT1 =,F7.2)
      GO TO 300
105  WRITE(6,215)
215  FORMAT(1H0,9X,33HSLIDING TENDS TO OCCUR ON PLANE 2)
      EN2 = -TEST5
      T2X = RX + EN2*W2X
      T2Y = RY + EN2*W2Y

```



```

T2Z = RZ + EN2*W2Z
T2 = SQRT(T2X**2+T2Y**2+T2Z**2)
FS = EN2*SIN(PHI2)/(COS(PHI2)*T2)
WRITE(6,116) FS,EN2,T2
116  FORMAT(1H0,9X,4HFS =,F5.2,10X,5HEN2 =,F7.2,5X,5HT2 =,F7.2)
GO TO 300
106  WRITE(6,117)
117  FORMAT(1H0,9X,33HSLIDING TENDS TO OCCUR ON PLANE 3)
EN3 = -TEST6
T3X = RX + EN3*W3X
T3Y = RY + EN3*W3Y
T3Z = RZ + EN3*W3Z
T3 = SQRT(T3X**2+T3Y**2+T3Z**2)
FS = EN3*SIN(PHI3)/(COS(PHI3)*T3)
WRITE(6,118) FS,EN3,T3
118  FORMAT(1H0,9X,4HFS =,F5.2,10X,5HEN3 =,F7.2,5X,5HT3 =,F7.2)
GO TO 300
119  WRITE(6,120)
120  FORMAT(1H0,9X,40HROCK WEDGE IS LIFTED OFF THE BASE PLANES)
300  IF(TEST1.LT.0.0.AND.TEST7 .LE.0.0.AND.TEST8 .LE.0.0) GO TO 101
IF(TEST2.LT.0.0.AND.TEST9 .LE.0.0.AND.TEST10.LE.0.0) GO TO 102
IF(TEST3.LT.0.0.AND.TEST11.LE.0.0.AND.TEST12.LE.0.0) GO TO 103
200  CONTINUE
STOP
END

```

\* DATA

In accordance with letter from DAEN-RDC, DAEN-ASI dated 22 July 1977, Subject: Facsimile Catalog Cards for Laboratory Technical Publications, a facsimile catalog card in Library of Congress MARC format is reproduced below.

Hendron, Alfred Joseph

Analytical and graphical methods for the analysis of slopes in rock masses / by A. J. Hendron, Jr., E. J. Cording, and A. K. Aiyer, Department of Civil Engineering, University of Illinois, Urbana, Ill. Vicksburg, Miss. : U. S. Waterways Experiment Station ; Springfield, Va. : available from National Technical Information Service, 1980. xi, 148, 14 p. : ill. ; 27 cm. (Technical report - U. S. Army Engineer Waterways Experiment Station ; GL-80-2) Prepared for U. S. Army Engineer Nuclear Cratering Group, Livermore, Calif., under Contract No. DACW 39-67-C-0097. Reprint of NCG Technical Report No. 36. References: p. 148.

1. Dynamic slope stability. 2. Graphical methods. 3. Rock masses. 4. Rock mechanics. 5. Slope stability. 6. Stereonet. 7. Vector analysis. I. Aiyer, Arunachalam Kulathu, joint author. II. Cording, Edward J., joint author. III. Illinois.

(Continued on next card)

Hendron, Alfred Joseph

Analytical and graphical methods for the analysis of slopes in rock masses ... 1980. (Card 2)

University. Dept. of Civil Engineering. IV. United States. Army Engineer Nuclear Cratering Group. V. Series: United States. Waterways Experiment Station, Vicksburg, Miss. Technical report ; GL-80-2. TA7.W34 no.GL-80-2